AFCRL-62-82

INTERACTION EFFECTS BETWEEN A PLASMA AND A VELOCITY-MODULATED ELECTRON BEAM

By
Gabriel F. Freire

Scientific Report No. 38
Contract AF 19(604)-1930

The research reported in this document has been sponsored by the
Electronics Research Directorate
Air Force Cambridge Research Laboratories
Office of Aerospace Research
United States Air Force
Bedford, Massachusetts

M.L. Report No. 890
February 1962

Microwave Laboratory
W. W. Hansen Laboratories of Physics
Stanford University
Stanford, California

AFCRL-62-82

INTERACTION EFFECTS BETWEEN A PLASMA AND A VELOCITY-MODULATED ELECTRON BEAM

By

Gabriel F. Freire

Scientific Report No. 38
Contract AF 19(604)-1930

M. L. Report No. 890

February 1962

Project 4619
Task 46191

The research reported in this document has been sponsored by the
Electronics Research Directorate
Air Force Cambridge Research Laboratories
Office of Aerospace Research
United States Air Force
Bedford, Massachusetts

Microwave Laboratory
W. W. Hansen Laboratories of Physics
Stanford University
Stanford, California

AFCRL-62-82

SCIENTIFIC REPORT NO. 38

INTERACTION EFFECTS BETWEEN A PLASMA AND A VELOCITY-MODULATED ELECTRON BEAM

By

Gabriel F. Freire

Electronics Research Directorate
Air Force Cambridge Research Laboratories
Office of Aerospace Research (USAF)

CONTRACT AF 19(604)-1930

M. L. Report No. 890
Project 4619
Task 46191

The research reported in this document has been sponsored by The Electronics Research Directorate of the Air Force Cambridge Research Laboratories, Office of Aerospace Research, UNITED STATES AIR FORCE, BEDFORD, MASSACHUSETTS. The publication of this report does not necessarily constitute approval by the Air Force of the findings or conclusions contained herein.

Microwave Laboratory
W. W. Hansen Laboratories of Physics
Stanford University
Stanford, California

ABSTRACT

The interaction between a grid modulated electron beam of finite diameter and a stationary plasma column, in the absence of a magnetic field, was investigated both theoretically and experimentally.

Experiments performed with a beam-plasma tube, with modulation of the electron beam by grids, revealed a maximum interaction when the modulation frequency of the beam was equal to or near the plasma frequency of the plasma. An electronic gain of 7.5 db due to the plasma was observed. The output powers were low with no net gain in any condition, due to the low impedances of the cavities which were used, and to the low beam current available. Nevertheless, it was possible, by driving the beam to saturation power levels, to obtain fundamental components of the beam current such that $I_1/I_0 = 1.5$ near the resonance condition. With only the electron beam on the plasma being off, the saturation output current measured was about $.8\ I_0$. These large saturation currents which were observed may be attributed to the fact that when $\omega < \omega_{pp}$ the plasma behaves like an inductive medium which has a similar effect to the inductively detuned intermediate cavity in a three-cavity klystron.

Second harmonic signals were detected, and a maximum peak of the output signal was observed when the plasma frequency of the plasma was twice the modulation frequency of the beam. Another smaller peak was observed at $f \sim f_p$. The second-harmonic currents were shown to increase approximately by a factor of two, at input saturation powers, when the plasma density was increased from zero to a value such that $f_p \sim 2f$. The theoretical model which was the subject of analysis consisted of a perfectly conducting cylindrical waveguide completely filled by a lossless, uniform plasma. The electron beam was assumed to be modulated by a gridded gap.

Two pairs of field solutions inside the beam region are shown to be possible. One pair of solutions, not excited with a gridless gap modulation, was associated with space-charge density variations inside the beam. The propagation constants of these volume space-charge waves were the same as in the infinite beam plasma system. The other pair of solutions for the electric fields within the beam corresponds to the

condition for which there is no charge accumulation in the beam. These solutions are associated with charge rippling at the beam-plasma interface. The propagation constants of these surface waves depend on the transverse dimensions of the beam and plasma. These surface waves grow exponentially with distance, when $\omega < \omega_{pp}$, at a rate which is smaller than the growth rate of the volume space-charge waves.

It was shown also that, under conditions for existence of growing waves in the system, strong harmonic generation becomes possible as a result of modifications of space-charge forces on the beam, due to the presence of the plasma.

Expressions for the second-harmonic components of the relevant rf quantities in the infinite beam-plasma system were derived, indicating the existence of growing second-harmonics.

ACKNOWLEDGMENTS

I wish to express my gratitude and thankfulness to Dr. M. Chodorow for his continued interest in this project. Without his advice and encouragement the project could not have been successfully completed.

My appreciation goes also to Dr. G. S. Kino for valuable suggestions and for the reading of the manuscript.

Special mention should also be made to E. Steed and D. L. Masterson for their excellent work in building the tube.

In addition, I wish to thank A. Braun, F. Ivanek, and the staff of the Reports Office.

TABLE OF CONTENTS

LIST OF FIGURES

LIST OF SYMBOLS

ξ_b	ac displacement of beam electrons
ξ_p	ac displacement of plasma electrons
$D_b = \epsilon_0 E_b$	displacement field due to beam electrons
E_b	electric field in the beam
$D_p = \epsilon_0 E_p$	displacement field due to plasma electrons
E_p	electric field in the plasma
ω_{pb}	plasma frequency of the electron beam
$\omega = 2\pi f$	angular frequency
$u_0 = \sqrt{2\eta V_0}$	dc beam velocity
$\eta = e/m$	ratio between electron charge and electron mass
V_0	beam voltage
I_0	dc beam current
$\beta_e = \omega/u_0$	beam wave number
$\beta_{pb} = \omega_{pb}/u_0$	beam plasma wave number
ω_{pp}	plasma frequency of the plasma
ρ_{0b}	dc charge density of the beam
ρ_{0p}	dc charge density of the plasma
D_1	displacement field in the beam-plasma system; fundamental component
$h_1 = \dfrac{\beta_{pb}}{\sqrt{1 - \dfrac{\omega_{pp}^2}{\omega^2}}}$	beam-plasma wave number for infinite beam in a plasma
$\alpha = V_1/V_0$	voltage modulation index
V_1	peak rf modulation voltage
a	radius of the electron beam
b	radius of the plasma

v_{b_1}	ac velocity of the beam electrons; fundamental component
v_{p_1}	ac velocity of the plasma electrons; fundamental component
ρ_{b_1}	ac charge density of the electron beam; fundamental component
ρ_{p_1}	ac charge density of the plasma; fundamental component
i_{b_1}	linearized beam current density; fundamental component
i_{p_1}	linearized plasma current density; fundamental component
i_{b_2}	second component of the beam current density
i_{p_2}	second component of the plasma current density
v_{b_2}	second component of the ac beam velocity
v_{p_2}	second component of the ac plasma velocity
D_2	second harmonic component of the displacement fields
$M = (\sin d/2)/(d/2)$	beam coupling coefficient
d	gap distance
$X = \pi N\alpha$	ballistic (no space charge) bunching parameter
$N = Z(f/u_0)$	drift tube length in cycles
z	drift distance
σ_b	surface charge density due to the beam
σ_p	surface charge density due to the plasma

$\epsilon_1 = 1 - \omega_{pp}^2/\omega^2$

$\epsilon_2 = 1 - \omega_{pp}^2/(\partial\omega)^2$

CHAPTER I

INTRODUCTION

The purpose of this study was to investigate the interaction effects between a velocity-modulated electron beam and plasma, effects which result in amplification and harmonic generation. The existence of spatially growing waves was predicted some years ago by Bohm and Gross.[1] Experiments performed in 1958 by Boyd, Gould and Field,[2] and in Russia by Bogdanov[3] et. al., successfully demonstrated the existence of such growing waves. More recently, similar experiments using a thermally generated cesium plasma were reported by Allen and Kino.[4] In these experiments, a velocity-modulated electron beam was allowed to transverse a plasma region, and maximum interaction between the beam and the plasma was obtained at a modulation frequency which was equal to or near to the plasma frequency.

We shall be primarily concerned with the amplification and the associated harmonic generation mechanisms, which we show to be related to the velocity modulation process and subsequent bunching of electrons of the beam, in the plasma medium.

Chapter II is devoted to an analysis which makes use of the Lagrangian approach to determine the beam-plasma interaction mechanism. It is shown that a high harmonic content would be expected to exist in the current in the bunched beam supporting a growing space-charge wave. Only the case of a plasma and electron beam of infinite extent is considered in this chapter.

Chapter III deals with a more practical configuration which consists of an electron beam of finite diameter passing along the axis of a plasma column, with no external dc nagnetic field applied and velocity-modulated by grids.

It is shown in the analysis of this problem that, with modulation by grids, the space-charge waves propagating along the beam increase exponentially with distance at a rate of growth which is higher than the one corresponding to the wave solution in the case of gap or helix modulation. The excitation of the individual space-charge waves by a gridded gap is determined and an expression for the rf beam current at the output grid is derived. These solutions which lead to these high growth rates correspond to the case in which there is a charge bunching within the beam; they are nonsolenoidal and $\rho \neq 0$ inside this region.

When the modulation frequency of the electron beam is above the plasma frequency of the plasma, it is shown in the text that there is no field in the plasma outside the beam corresponding to these nonsolenoidal waves.

When the $\omega < \omega_{pp}$, the propagation constants become complex and the proof given in the text does not apply. It can be shown however by an analagous treatment of Bessel functions of complex argument that the fields of the nonsolenoidal waves vanish in this case also.[5,6]

The method which is used throughout this analysis is the superposition method, in contrast to the Boltzmann approach or the Fourier analysis of density distribution. The reader is referred to Buneman[7] for a discussion of the latter two methods. According to the superposition approach we treat the streams of electrons (beam and plasma) by a perturbation method leading to the Eulerian, small-signal description of motion of electrons.

The term plasma is used in this report to denote an assembly of equal numbers of electrons and positive ions and perhaps neutral molecules. The ions are assumed stationary. Unless otherwise specified, thermal motions and collisions are neglected.

The nonlinear aspects of the beam-plasma interaction problem are investigated in Chapter IV by means of a complete formal derivation of the relevant second harmonic quantities.

The experimental work is described in the final chapter. The purpose of the experiment was to investigate the beam-plasma interaction near the plasma frequency of the plasma, under the conditions of the analysis made in Chapter III, i.e., (a) no magnetic field, and, (b) modulation by grids. Other interesting effects concerned with beam saturation data and second harmonic generation are also reported and discussed.

CHAPTER II

ELECTRON BEAM-PLASMA INTERACTION MECHANISM; LAGRANGIAN APPROACH; HARMONIC GENERATION

2.1 INTRODUCTION

Before undertaking (in the next chapter) the analysis of the interaction of a finite electron beam with a plasma column through which it passes, it is of interest to consider the essential aspects of the beam plasma interaction which are apparent in the simple one-dimensional treatment of the problem.

In this introductory chapter we shall deal then with the ideal situation of a one-dimensional, infinite cross-section beam model and an unbounded cold plasma.

Our analysis shall be restricted to small signals. The possibility of cross-over of beam electrons is excluded, so that a unique velocity vector is associated with any point of the beam at a given time. It is shown that each infinite sheet of electrons constituting the plasma will oscillate about its equilibrium position, provided that the sheet does not cross another sheet in the course of its motion.

It is the purpose of this chapter to investigate, under these circumstances and without going into details, the nature of the space-charge effects of a modulated electron beam drifting along the z-direction through the plasma medium. To study the influence of the plasma upon the space-charge waves on the moving beam, we chose the Lagrangian description where attention is primarily concentrated on the trajectories of individual electrons. It is indicated, in this elementary analysis, that the plasma affects the bunching in the beam in such a way that, under some conditions, growing space-charge waves are supported by the electron beam. Also, under these same conditions, strong harmonic generation might be possible as a result of modifications of space-charge forces on the beam, due to the presence of the plasma.

2.2 EQUATIONS FOR THE UNCOUPLED ELECTRON BEAM AND PLASMA

The system of variables useful in the small signal analysis and suitable for our present purposes is described by Bobroff[8] as the

"polarization system" which in the absence of a dc velocity (as in our case of a stationary plasma) becomes identical to the Lagrangian system.

In this section a brief discussion of the dependent variables which play important roles in the analysis which follows is presented. Reference should be made to the Bobroff paper for further details.

We shall first define the ac position vector or displacement vector. It is known that when modulation is applied to the input gap the electrons constituting the beam are displaced from their dc positions. This displacement will be called the displacement vector and will be denoted by $\vec{\xi}_b$. To first order it is a function of the dc position and also an explicit function of the time. Thus we write

$$\vec{z}_b(z_{0b} , t) = \vec{z}_{0b} + \vec{\xi}_b(z_{0L} , t) \tag{2.1}$$

where z_{0b} denotes the dc position of the beam electrons.

The "polarization" or electric displacement arises from the charge separation caused by the displacement of electrons from their equilibrium positions. For the electron beam, it is defined to first order in terms of the above displacement as

$$\vec{D}_b = - \rho_{0b} \cdot \vec{\xi}_b \tag{2.2}$$

where ρ_{0b} is the dc charge density of the beam. The minus sign in this expression accounts for the fact that we deal with displacements of negatively charged sheets.

The other first-order dependent variable is the ac velocity which is denoted by $\vec{v}_b$.

The Eulerian charge and linearized current density may be expressed, as is shown by Bobroff, in terms of the above variables. The ac charge density of the electron beam is

$$\rho_{b_1} = - \rho_{0b} \cdot \nabla \cdot \vec{\xi}_b \ . \tag{2.3}$$

The linearized current density of the beam is given by the relation

$$\vec{i}_{b_1} = \frac{\partial}{\partial t}(\rho_{0b} \cdot \vec{\xi}_b) + \nabla \times (\rho_{0b}\vec{\xi}_b \times \vec{u}_0) \quad . \tag{2.4}$$

It can be shown (see reference 6) that the following relation holds between $\vec{v}_{b_1}$ and $\vec{\xi}_b$:

$$\left(\frac{\partial}{\partial t} + u_0 \cdot \nabla\right)\vec{\xi}_b = \vec{v}_{b_1} \quad . \tag{2.5}$$

Similarly, the equation of motion for the beam electrons in this system of variables is to first-order:

$$\left(\frac{\partial}{\partial t} + u_0 \cdot \nabla\right)\vec{v}_{b_1} = \frac{\omega_{pb}^2}{\rho_{0b}} \cdot \vec{D}_b \quad , \tag{2.6}$$

where

$$\omega_{pb} \triangleq \sqrt{\frac{\rho_{0b}e}{m\epsilon_0}} \tag{2.7}$$

is the plasma frequency of the electron beam.

It follows from Eqs. (2.2), (2.5) and (2.6) that

$$\left(\frac{\partial}{\partial t} + u_0 \cdot \frac{\partial}{\partial z}\right)^2 \cdot \xi_b = \frac{\omega_{pb}^2}{\rho_{0b}} \cdot D_b = -\omega_{pb}^2 \cdot \xi_b \quad . \tag{2.8}$$

In a frame of reference moving at the dc beam velocity, the quantities ξ_b and D_b obey the following differential equations:

$$\frac{\partial^2 \xi_b}{\partial t'^2} + \omega_{pb}^2 \xi_b = 0$$

$$\frac{\partial^2 D_b}{\partial t'^2} + \omega_{pb}^2 D_b = 0 \quad , \tag{2.9}$$

where t' represents time in the moving system.

The solution of Eq. (2.8), which gives the displacements ξ_b of the beam electrons drifting along the z direction with a dc velocity u_0, is of the form[9]

$$\xi_b(z_0, t) = A \sin(\omega t - \beta_e z_0).\sin\beta_{pb} z_0 \tag{2.10}$$

where

$$A = \frac{u_0 \alpha}{2\omega_{pb}}$$

with

$$\alpha = \frac{V_1}{V_0} = \frac{\text{rf modulation voltage}}{\text{dc beam voltage}},$$

and the z_0 denotes the dc equilibrium position of the beam electrons, and it is assumed that at $t = t_0$ we have

$$\xi_L = 0$$

$$\dot{z} = u_0(1 + \frac{\alpha}{2} \sin\omega t_0) \; ; \; \alpha \ll 1 \quad .$$

It follows similarly that the equation of motion for the plasma electrons is

$$\frac{\partial}{\partial t} v_{p_1} = \frac{\omega_{pp}^2}{\rho_{0p}} D_p \quad , \tag{2.11}$$

where

$$\omega_{pp} \triangleq \sqrt{\frac{\rho_{0p} e}{m\epsilon_0}}$$

designates the plasma frequency of the plasma, and

$$v_{p_1} = \frac{\partial \xi_p}{\partial r} \tag{2.12}$$

is the ac velocity of the plasma electrons.

By combining together Eqs. (2.11) and (2.12), and by using the relation $D_p = - \rho_{Op} \xi_p$, we obtain for the plasma small amplitude equations of simple harmonic motion:

$$\frac{\partial^2 \xi_p}{\partial t^2} + \omega_{pp}^2 \xi_p = 0$$

$$\frac{\partial^2 D_p}{\partial t^2} + \omega_{pp}^2 D_p = 0 \quad . \tag{2.13}$$

These equations represent plasma oscillations which, in the case we are considering (a stationary plasma), do not propagate, since any disturbance would in the absence of collisions or thermal velocities persist indefinitely at the location of the disturbance.

2.3 THE INHOMOGENEOUS DIFFERENTIAL EQUATIONS FOR THE LINEAR INTERACTION OF A BEAM-PLASMA SYSTEM

We have been considering in the previous section the electron beam and the plasma as two independent uncoupled systems. We shall be concerned now with the interaction that takes place between the plasma and the beam when they are coupled together.

We shall restrict ourselves to linear interaction. This means that we shall use only the linearized equations of motion which were derived in section 2.2.

The displacements of the electrons of the beam and plasma are changed by the coupling. These displacements are therefore denoted by ξ_b' and ξ_p' , respectively.

The electric field in the beam-plasma system is

$$E_1 = \frac{D_1}{\epsilon_0}$$

where

$$D_1 = - \rho_{Ob} \xi_b' - \rho_{Op} \xi_p' \quad . \tag{2.14}$$

The equation of motion for the plasma electrons is

$$\frac{\partial^2 \xi_p}{\partial t^2} = \frac{\omega_{pp}^2}{\rho_{0p}} \cdot D_1 \quad . \tag{2.15}$$

For a one-dimensional system, the total longitudinal current (convection plus displacement current) must be zero. It follows that

$$\frac{\partial D_1}{\partial t} = - i_{b_1} - i_{p_1} \quad . \tag{2.16}$$

Substitution of Eq. (2.4) in Eq. (2.16) yields the result

$$\frac{\partial D_1}{\partial t} = - \frac{\partial}{\partial t} (\rho_{0b} \xi_b') - \frac{\partial}{\partial t} (\rho_{0p} \xi_p') \quad , \tag{2.17}$$

since the second term in Eq. (2.4) is zero for the one dimensional beam.

Partial differentiation with respect to time of the above equation gives the following expression:

$$\frac{\partial^2 D_1}{\partial t^2} = - \rho_{0b} \cdot \frac{\partial^2 \xi_b}{\partial t^2} - \rho_{0p} \cdot \frac{\partial^2 \xi_p}{\partial t^2} \quad , \tag{2.18}$$

into which may be substituted Eq. (2.15) to yield the inhomogeneous differential equation for D_1 :

$$\frac{\partial^2 D_1}{\partial t^2} + \omega_{pp}^2 D_1 = - \rho_{0b} \cdot \frac{\partial^2 \xi_b'}{\partial t^2} \quad . \tag{2.19}$$

The equation of motion for the beam electrons is

$$\left(\frac{\partial}{\partial t} + u_0 \frac{\partial}{\partial z} \right)^2 \cdot \xi_b' = \frac{\omega_{pb}^2}{\rho_{0b}} D_1 \quad . \tag{2.20}$$

This equation, together with the preceding one, constitutes a system of equations which may then be solved by assuming that all quantities vary as $\exp(\omega t - \beta z)$. The following dispersion relation is then obtained from Eqs. (2.19) and (2.20):

$$1 - \frac{\omega_{pp}^2}{\omega^2} - \frac{\omega_{pb}^2}{(\omega - u_0\beta)^2} = 0 \quad , \tag{2.21}$$

from which it may be seen that

$$\beta = \beta_e \pm h \quad ,$$

$$h = \frac{\beta_{pb}}{\sqrt{1 - \frac{\omega_{pp}^2}{\omega^2}}} \quad , \tag{2.22}$$

where

$$\beta_e = \frac{\omega}{u_0} \quad , \quad \beta_{pb} = \frac{\omega_{pb}}{u_0} \quad .$$

This equation indicates that, when the electron beam is modulated at a frequency ω above the plasma frequency of the plasma ω_{pp}, there are two propagating waves that can be excited: one with a phase velocity greater than u_0, and the other with a phase velocity less than u_0. When $\omega < \omega_{pp}$, the denominator of the right hand side of Eq. (2.22) is negative, β becomes complex and two waves are found: one growing with distance, and the other decreasing with distance. By introducing Eq. (2.14) into Eq. (2.19), and writing $\rho_{0b}/\rho_{0p} = (\omega_{pb}/\omega_{pp})^2$, the following differential equation for the displacements of the electrons constituting the plasma is obtained:

$$\frac{\partial^2 \xi_p'}{\partial t^2} + \omega_{pp}^2 \xi_p' = - \omega_{pb}^2 \xi_b' \quad . \tag{2.23}$$

The right-hand side of this equation can be written in terms of the beam current density, yielding

$$\frac{\partial^2 \xi_p'}{\partial t^2} + \omega_{pp}^2 \xi_p' = - \frac{j\eta}{\omega\epsilon_0} \cdot i_{b_1} \quad .$$

Instead of free, undamped oscillations of the plasma electrons as given by Eq. (2.13) in the presence of the electron beam, we now have forced oscillations in the plasma with the driving force being due to the ac modulated beam.

By assuming as before that the displacements of the plasma electrons varies as $e^{j\omega t}$, it will be seen that

$$\xi_p' = \frac{\omega_{pb}^2}{\omega^2 - \omega_{pp}^2} \cdot \xi_b' \quad . \tag{2.24}$$

This equation established the relation between the steady-state displacements of the electrons which constitute, respectively, the electron beam and the plasma.

From Eqs. (2.14) and (2.24) it is seen that the electric field originating from this displacement of charges is

$$D_1 = - \rho_{0b} \cdot \xi_b' - \rho_{0p} \xi_p' = \frac{- \rho_{0b}}{\left(1 - \frac{\omega_{pp}^2}{\omega^2}\right)} \cdot \xi_b' \quad . \tag{2.25}$$

The resulting force on a beam electron due to this displacement field is

$$F = \frac{e}{\epsilon_0} D_1 = \frac{- e\rho_{0b}}{\epsilon_0\left(1 - \frac{\omega_{pp}^2}{\omega^2}\right)} \cdot \xi_b' \quad . \tag{2.26}$$

On examination of this equation, it may be seen that (F/ξ_b') reverses sign as the frequency is changed from $\omega > \omega_{pp}$ to $\omega < \omega_{pp}$.

Consequently the displacement field bunches the beam when $\omega < \omega_{pp}$, instead of debunching it as it would be if there were no plasma present or if $\omega > \omega_{pp}$. We should expect that because of this tight bunching of the beam electrons, there would be a high harmonic content in the resulting current.

Equation (2.26) can also be written in the following form:

$$F = m \frac{\partial^2 \xi'_b}{\partial t^2} = - \frac{e}{\epsilon_0} \frac{\rho_{0b}}{\left(1 - \frac{\omega_{pp}^2}{\omega^2}\right)} \cdot \xi'_b \quad , \tag{2.27}$$

with the result that

$$\frac{\partial^2 \xi'_b}{\partial t'^2} = - \frac{\omega_{pb}^2}{\left(1 - \frac{\omega_{pp}^2}{\omega^2}\right)} \cdot \xi'_b \quad , \tag{2.28}$$

in a coordinate system moving with the beam.

Comparing the above expression with Eq. (2.9), which was derived in the absence of plasma, gives a simple interpretation to the effects that the plasma has upon the motion of the beam electrons. We interpret the presence of plasma as having the effect of changing the plasma frequency of the electron beam from its value ω_{pb}, in the absence of plasma, to the effective value

$$\omega_{qb} = \frac{\omega_{pb}}{\sqrt{1 - \frac{\omega_{pp}^2}{\omega^2}}} \quad . \tag{2.29}$$

In a system of reference stationary with respect to the beam, Eq. (2.28) becomes

$$\left(\frac{\partial}{\partial t} + u_0 \frac{\partial}{\partial z}\right)^2 \cdot D_1 = - \frac{\omega_{pb}^2}{1 - \frac{\omega_{pp}^2}{\omega^2}} \cdot D_1 \quad . \tag{2.30}$$

After expanding the left hand side of the above differential equation, we find that

$$\frac{\partial^2 D_1}{\partial z^2} + \frac{2}{u_0}\frac{\partial^2 D_1}{\partial t \partial z} + \frac{1}{u_0^2}\frac{\partial^2 D_1}{\partial t^2} = -\frac{\beta_{pb}^2}{1 - \frac{\omega_{pp}^2}{\omega^2}} \cdot D_1 \quad . \tag{2.31}$$

This second-order homogeneous differential equation will be derived again, in Chapter IV, by using the Eulerian approach, as an introduction to the nonlinear analysis which will be developed in that Chapter.

2.4 ELECTRON CROSSOVER; NONLINEARITY

The fact that the amplitude of ξ_p', in Eq. (2.24) for example, becomes infinite for $\omega = \omega_{pp}$ illustrates the phenomenon of resonance. Care should be taken, however, in discussing the implications of this condition, since our linear differential equations hold only for small oscillations of electrons within the framework of the small-signal theory of space-charge debunching forces.

As pointed out before, when the modulating frequency f is below f_p and approaches f_p, there exist strong space-charge forces on the beam electrons in such a direction to reinforce the bunching process set up in the beam by velocity modulation.

Under this condition, the phenomenon of electron crossover would be expected to occur. It is known from the study of the bunching motion in klystron theory that crossover of electrons exists whenever the following inequality holds:[10]

$$1 + \frac{\partial \xi}{\partial z_0} < 0 \quad . \tag{2.32}$$

The displacements of the plasma electrons were shown to be related to the beam electron displacements according to the equation

$$\xi_p' = \frac{\omega_{pb}^2}{\omega^2 - \omega_{pp}^2} \cdot \xi_b' \quad .$$

It follows then that

$$\frac{\partial \xi_p'}{\partial z} = \frac{\omega_{pb}^2}{\omega^2\left(1 - \frac{\omega_{pp}^2}{\omega^2}\right)} \cdot \frac{\partial \xi_b'}{\partial z} = \left(\frac{h}{\beta_e}\right)^2 \cdot \frac{\partial \xi_b'}{\partial z} \quad . \tag{2.33}$$

By assuming, as is usual, that

$$\frac{h}{\beta_e} < 1 \quad , \tag{2.34}$$

we have, from Eq. (2.33) and the crossover criterion [Eq. (2.32)] the following result:

$$\left|\frac{\partial \xi_b'}{\partial z}\right| > \left|\frac{\partial \xi_p'}{\partial z}\right| \quad ,$$

indicating that the beam electrons cross over before such a phenomenon occurs for the plasma electrons.

The relationship between the ac charge densities of the electron beam and plasma may be easily derived. We know that

$$\begin{aligned} \rho_{b_1} &= -\rho_{0b} \frac{\partial \xi_b'}{\partial z} \\ \rho_{p_1} &= -\rho_{0p} \frac{\partial \xi_p'}{\partial z} \quad . \end{aligned} \tag{2.35a}$$

The following equation is then obtained, with the help of Eq. (2.33):

$$\rho_{p_1} = \rho_{b_1} \frac{\omega_{pp}^2}{\omega^2 - \omega_{pp}^2} \quad . \tag{2.35b}$$

This equation can be written in the following form:

$$\rho_{p_1} = \rho_{b_1} \left(\frac{h}{\beta_e}\right)^2 \cdot \left(\frac{\omega_{pp}}{\omega_{pb}}\right)^2 \quad .$$

By using some typical experimental figures it may be seen that

$$\left(\frac{\omega_{pp}}{\omega_{pb}}\right)^2 \gg 1 \quad .$$

In our experiment it will be shown that this quantity is of the order of 10^{+4} . Therefore, we may have

$$\left|\rho_{p_1}\right| > \left|\rho_{b_1}\right| \quad .$$

Furthermore, the same equation (2.24) may be used to derive a relation between the plasma velocity and the ac beam velocity. We obtain

$$v_{p_1} = \frac{\partial \xi_p'}{\partial r} = \left(\frac{h}{\beta_e}\right)^2 \cdot \frac{\partial \xi_b'}{\partial t} \quad .$$

We know however that

$$+ \frac{\partial \xi_b'}{\partial t} = v_{b_1} + u_0 \left(\frac{\rho_{b_1}}{\rho_{0b}}\right) \quad .$$

It results in the following expression for the plasma velocity in terms of the ac charge density and ac velocity of the electron beam:

$$v_{p_1} = +\left(\frac{h}{\beta_e}\right)^2 \left\{v_{b_1} + u_0 \left(\frac{\rho_{b_1}}{\rho_{0b}}\right)\right\} \quad .$$

It is apparent then that we may have

$$\left|v_{p_1}\right| < \left|v_{b_1}\right| \quad .$$

These inequalities for relative magnitudes of charge densities and velocities do not determine the relative magnitudes of $\rho_{p,1}v_{p,1}$ and $\rho_{b,1}v_{b,1}$. However a more careful consideration of common values of $(h/\beta_e)^2$ and $(\omega_{pp}/\omega)^2$ would indicate that in the interesting range of behavior one would usually have

$$\left|\rho_{p_1}v_{p_1}\right| > \left|\rho_{b_1}v_{b_1}\right| .$$

This means that second-order nonlinear effects may become first more important in the plasma. In a nonlinear analysis to be carried out in Chapter IV, the nonlinear term $(\rho_{b,1}v_{p,1})$ which enters in the definition of the second-order plasma current density may be considered a more relevant term than the corresponding second-order term $(\rho_{b,1}v_{b,1})$ in the expression for the beam current density.

CHAPTER III

INTERACTION OF A GRID-MODULATED ELECTRON BEAM WITH A PLASMA (NO EXTERNAL MAGNETIC FIELD)

3.1 INTRODUCTION

This chapter is concerned with an analysis of the interaction of an electron beam of finite radius with a plasma. More specifically, as shown in Fig. 1, we consider a perfectly conducting cylindrical waveguide of diameter 2b completely filled with an ideal electron plasma. An electron beam of diameter $2a(a < b)$ drifts with a constant uniform velocity $u_0(u_0 \ll c)$ through this plasma column after being velocity-modulated by ideal grids. Identical output grids are used as parts of an external cavity where the demodulation process takes place. It is assumed that there is no dc magnetic field applied and the electron beam is focused by positive ions.

The problem is to obtain solutions for the space-charge waves in this system, to combine these solutions to match the boundary conditions at the input, and to derive expressions for the rf beam current at the output grids. Feenberg[6] developed the theory of small signal bunching in a beam of finite cross-section in a drift tube, with positive ion focusing and zero dc magnetic field. The following analysis, where modulation is assumed to be by grids, is based on Feenberg's work which is modified to take into account the presence of plasma in the drift space.

It will be shown that the plasma has the effect of changing the expressions for the field quantities in such a way that, under certain conditions, waves increasing exponentially with distance become possible. Moreover, with modulation by grids, volume space-charge waves involving charge density variations are shown to be possible solutions of the problem. It is important to note that their growth rate is greater than the corresponding growth rate for the wave solutions in the case of modulation of the electron beam by a gap or a helix.

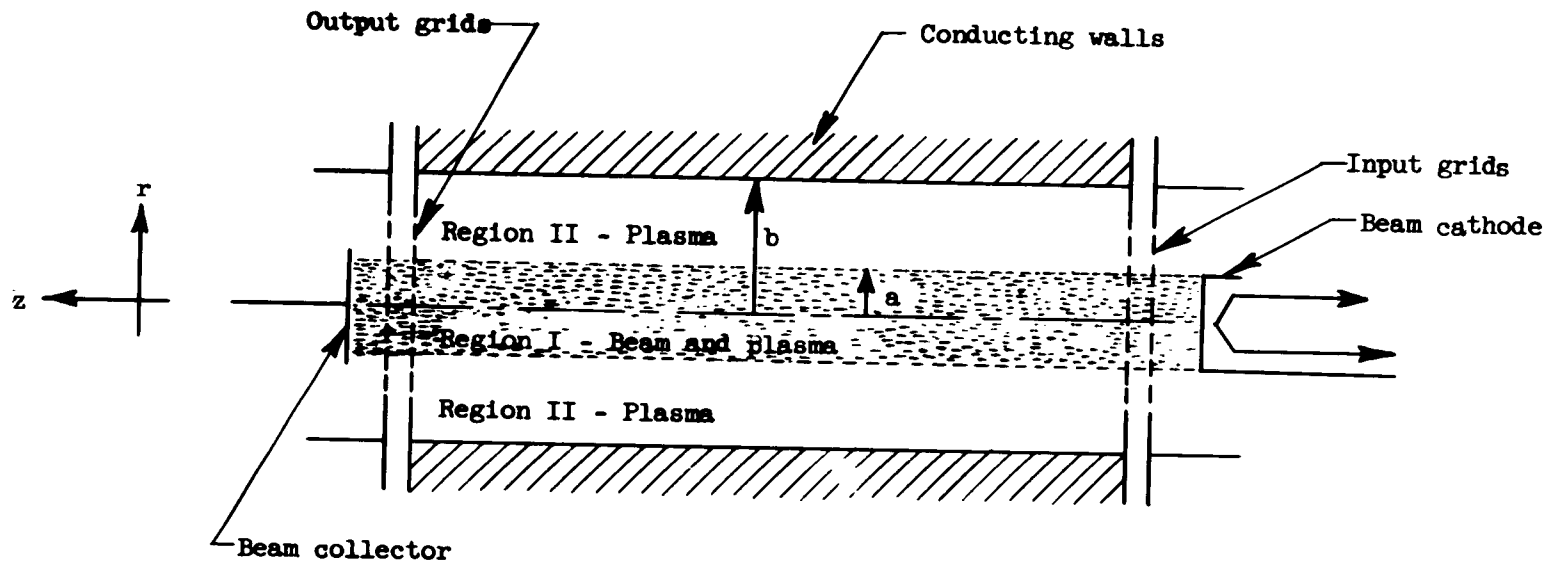

Fig. 1--Schematic of a grid-gap modulated beam in a plasma column. Theoretical model.

3.2 GENERAL ASSUMPTIONS; INHOMOGENEOUS WAVE EQUATION

To study the propagation of waves in this system, Maxwell's equations

$$\nabla \times \vec{E} = - \frac{\partial \vec{B}}{\partial t} \tag{3.1}$$

$$\nabla \times \vec{H} = \vec{i} + \frac{\partial \vec{D}}{\partial t} \tag{3.2}$$

$$\nabla . \vec{D} = \rho \tag{3.3}$$

$$\nabla . \vec{B} = 0 \tag{3.4}$$

will be used. The convection current density, $\vec{i} = \rho \vec{v}$, is assumed to be due to only the electrons, of the beam and/or of the plasma. It is assumed that all quantities have an average value plus a small harmonic time dependent perturbation:

$$F(r , \theta , z , t) = F_0(r , \theta , z) + F_1(r , \theta , z)e^{j\omega t} , \tag{3.5}$$

and the perturbations are wave-like in nature, so that $F_1(r , \theta , z)$ has the form

$$F_1(r , \theta , z) = F_1(r , \theta)e^{-j\beta z} , \tag{3.6}$$

where β is the propagation constant along the axis of symmetry of the system. We can write Maxwell's equations for the ac quantities in terms of the spatial coordinates as

$$\nabla \times \vec{E}_1 = - j\omega \vec{B}_1 \tag{3.7}$$

$$\nabla \times \vec{H}_1 = \vec{i}_1 + j\omega \epsilon_0 \vec{E}_1 \tag{3.8}$$

$$\nabla . \vec{E}_1 = \frac{\rho_1}{\epsilon_0} \tag{3.9}$$

$$\nabla . \vec{B}_1 = 0 , \tag{3.10}$$

where $\vec{E}_1 = \vec{E}_1(r, \theta, z)$, $\rho_1 = \rho_1(r, \theta, z)$, etc. If we now take the curl of Eq. (3.1) and substitute in Eq. (3.2), we find that

$$\nabla \times \nabla \times \vec{E}_1 = k^2 \vec{E}_1 - j\omega\mu_0 \vec{I}_1 \quad ,$$

where $k = \frac{\omega}{c}$. Using a vector identity and Eq. (3.9)

$$\nabla \times \nabla \times \vec{E}_1 = -\nabla^2 \vec{E}_1 + \nabla(\nabla \cdot \vec{E}_1)$$

$$= -\nabla^2 \vec{E}_1 + \frac{\nabla \rho_1}{\epsilon_0}$$

yields the inhomogeneous wave equation for E_1 , which is

$$\nabla^2 \vec{E}_1 + k^2 \vec{E}_1 = \frac{\nabla \rho_1}{\epsilon_0} + j\omega\mu_0 \vec{I}_1 \quad . \tag{3.11}$$

This equation can also be written in the form

$$\nabla_\perp^2 \vec{E}_1 - (\beta^2 - k^2)\vec{E}_1 = \frac{\nabla \rho_1}{\epsilon_0} + j\omega\mu_0 \vec{I}_1 \tag{3.12}$$

where the symbol $\nabla_\perp^2$ denotes the transverse Laplacian. For cylindrical coordinates, $\nabla_\perp^2$ may be written as

$$\nabla_\perp^2 \triangleq \frac{1}{r}\frac{\partial}{\partial r}\left(r \frac{\partial}{\partial r}\right) + \frac{1}{r^2}\frac{\partial^2}{\partial \theta^2} \quad . \tag{3.13}$$

It follows similarly that

$$\nabla_\perp^2 \vec{B}_1 - (\beta^2 - k^2)\vec{B}_1 = 0 \quad . \tag{3.14}$$

If we make the slow-wave approximation $(k^2 \ll \beta^2)$, the differential equations satisfied by E_z and B_z are, respectively,

$$\nabla_\perp^2 E_z - \beta^2 E_z = -j \frac{\beta}{\epsilon_0} \rho_1 + j\omega\mu_0 i_z \tag{3.15}$$

and

$$\nabla_{\perp}^2 B_z - \beta^2 B_z = 0 \quad . \tag{3.16}$$

The continuity equation is

$$\nabla . \vec{i} + \frac{\partial \rho}{\partial t} = 0 \quad . \tag{3.17}$$

In cylindrical coordinates, Eq. (3.17) may be written as

$$\frac{1}{r} \frac{\partial}{\partial r} (r i_r) - j\beta i_z = - j\omega\rho \quad . \tag{3.18}$$

This equation is used to express the volume charge density ρ in terms of the components of the current density, i.e.,

$$\rho = - \frac{1}{j\omega} \left[\frac{1}{r} \frac{d}{dr} (r i_r) - j\beta i_z \right] \quad . \tag{3.19}$$

Then Eq. (3.19) may be substituted into the wave equation [Eq. (3.15)], so that the inhomogeneous term in the equation becomes a function only of the current density:

$$\nabla_{\perp}^2 E_z - \beta^2 E_z = \frac{\beta}{\omega\epsilon_0} \frac{1}{r} \frac{d}{dr} (r i_r) - j \frac{\beta^2}{\omega\epsilon_0} i_z \quad . \tag{3.20}$$

If we restrict ourselves to circularly symmetrical solutions, i.e., $(\partial/\partial\theta \equiv 0)$, Eq. (3.20) becomes

$$\frac{1}{r} \frac{d}{dr} \left(r \frac{dE_z}{dr} \right) - \beta^2 E_z = \frac{\beta}{\omega\epsilon_0} \frac{1}{r} \frac{d}{dr} (r i_r) - j \frac{\beta^2}{\omega\epsilon_0} i_z \quad . \tag{3.21}$$

This cylindrical wave equation is to be solved, in the two regions of interest of the system as shown in Fig. 1:

a. Region I - $(0 \leq r \leq a)$ is the electron beam-plasma region, defined to the limits of the edge of the beam. In this region we find

$$\begin{aligned} i_{z_I} &= i_{zb_I} + i_{zp_I} \\ i_{r_I} &= i_{rb_I} + i_{rp_I} \end{aligned} \quad . \tag{3.22}$$

b. Region II - $(a \leq r \leq b)$ is outside the beam region, where only plasma is present, and

$$i_{z_{II}} = i_{zp_{II}}$$

$$i_{r_{II}} = i_{rp_{II}} \quad . \tag{3.23}$$

3.3 ELECTRON BEAM-PLASMA INTERACTION REGION

Consider the beam-plasma region (Region I), $(0 \leq r \leq a)$. Under the small-signal assumption, the axial and radial components of the linearized beam current densities are, respectively,

$$i_{zb} = \rho_b \cdot u_0 + \rho_{0b} \cdot v_{zb} \tag{3.24}$$

$$i_{rb} = \rho_{0b} \cdot v_{rb} \quad . \tag{3.25}$$

The equations of motion for the electrons in the beam lead to the following expressions for the beam velocity components:

$$v_{zb} = \frac{-j\eta}{(\omega - u_0\beta)} E_{z_I} \tag{3.26}$$

$$v_{rb} = \frac{-j\eta}{(\omega - u_0\beta)} E_{r_I} \quad , \tag{3.27}$$

where $\eta \triangleq e/m$ and the index (I) denotes the region which is being considered. From the continuity equation, applied to the electron beam, we find that

$$\rho_b = -\frac{1}{j\omega}\left(\frac{1}{r}\frac{d}{dr}(ri_{rb}) - j\beta i_{zb}\right) \tag{3.28}$$

which, by using the previous equations for the current densities and ac velocities, assumes the following form:

$$\rho_b = \frac{\epsilon_0 \omega_{pb}^2}{(\omega - u_0\beta)^2} \cdot \frac{1}{r}\frac{d}{dr}\left(rE_{r_I}\right) - j\beta\epsilon_0 \frac{\omega_{pb}^2}{(\omega - u_0\beta)^2} \cdot E_{z_I} \quad , \tag{3.29}$$

where

$$\omega_{pb} \triangleq \sqrt{\frac{\rho_{0b}\eta}{\epsilon_0}} \tag{3.30}$$

is the plasma frequency of the beam. We know, however, that with the slow-wave approximation the radial component of the electric field, as derived from Maxwell's equation, is

$$E_r = \frac{j}{\beta} \cdot \frac{\partial E_z}{\partial r} \quad .$$

It follows that

$$\rho_b = \frac{j\epsilon_0}{\beta} \cdot \frac{\omega_{pb}^2}{(\omega - u_0\beta)^2} \cdot \frac{1}{r}\frac{\partial}{\partial r}\left(\frac{r\partial E_{z_I}}{\partial r}\right) - j\beta\epsilon_0 \frac{\omega_{pb}^2}{(\omega - u_0\beta)^2} E_{z_I} \quad .$$

By substituting the above equation into Eq. (3.24) and using (3.26) we obtain the result

$$i_{zb} = \frac{j\epsilon_0 u_0}{\beta} \frac{\omega_{pb}^2}{(\omega - u_0\beta)^2} \cdot \frac{1}{r}\frac{\partial}{\partial r}\left(\frac{r\partial E_{z_I}}{\partial r}\right) - j\omega\epsilon_0 \frac{\omega_{pb}^2}{(\omega - u_0\beta)^2} E_{z_I} \quad . \tag{3.31}$$

The radial component of the beam current density is

$$i_{rb} = \rho_{0b} v_{rb} = \frac{\epsilon_0}{\beta} \frac{\omega_{pb}^2}{(\omega - u_0\beta)} \cdot \frac{\partial E_{z_I}}{\partial r} \quad . \tag{3.32}$$

For the plasma electrons in the same region $(0 \leq r \leq a)$, the current density components are

$$i_{zp_I} = \rho_{0p} v_{zp_I} = - j\omega\epsilon_0 \frac{\omega_{pp}^2}{\omega^2} \cdot E_{z_I} \quad , \tag{3.33}$$

and

$$i_{rp_I} = \rho_{0p} v_{rp_I} = \frac{\omega\epsilon_0}{\beta} \cdot \frac{\omega_{pp}^2}{\omega^2} \cdot \frac{\partial E_{z_I}}{\partial r} \quad , \tag{3.34}$$

where

$$\omega_{pp} \triangleq \sqrt{\frac{\rho_{0p}\eta}{\epsilon_0}} \tag{3.35}$$

is the plasma frequency of the plasma. In this region I, the total longitudinal and transverse current densities are, respectively,

$$i_{z_I} = i_{zb} + i_{zp_I} \tag{3.36}$$

and

$$i_{r_I} = i_{rb} + i_{rp_I} \quad . \tag{3.37}$$

Therefore, by using the expressions above, derived for the current densities, we have

$$i_{z_I} = - j\omega\epsilon_0 \left\{ \frac{\omega_{pb}^2}{(\omega - u_0\beta)^2} + \frac{\omega_{pp}^2}{\omega^2} \right\} E_{z_I} + j\epsilon_0 \frac{u_0}{\beta} \frac{\omega_{pb}^2}{(\omega - u_0\beta)^2} \cdot \frac{1}{r} \frac{\partial}{\partial r} \left(\frac{r \partial E_{z_I}}{\partial r} \right) \tag{3.38}$$

and

$$i_{r_I} = \frac{\epsilon_0}{\beta} \left\{ \frac{\omega_{pb}^2}{\omega - u_0\beta} + \frac{\omega_{pp}^2}{\omega} \right\} \cdot \frac{\partial E_{z_I}}{\partial r} \quad . \tag{3.39}$$

By substituting these last two equations into the wave equation [Eq. (3.2)], we obtain

$$\left(1 - \frac{\omega_{pb}^2}{(\omega - u_0\beta)^2} - \frac{\omega_{pp}^2}{\omega^2} \right) \cdot \nabla^2 E_{z_I} = 0 \quad . \tag{3.40}$$

We conclude, then, that there are two possibilities for the fields, in the beam-plasma region, namely:

$$\nabla^2 E_{z_I} = 0 \tag{3.41}$$

$$1 - \frac{\omega_{pb}^2}{(\omega - u_0\beta)^2} - \frac{\omega_{pp}^2}{\omega^2} = 0 \quad . \tag{3.42}$$

Consider now the Region II ($a \leq r \leq b$) .

In this region, there is only plasma and for the two components of the current density we write

$$\begin{aligned} i_{z_{II}} &= i_{zp_{II}} \\ i_{r_{II}} &= i_{rp_{II}} \end{aligned} \quad . \tag{3.43}$$

In this case it may be seen that the wave equation [Eq. (3.21)], assumes the following form:

$$\left(1 - \frac{\omega_{pp}^2}{\omega^2}\right)\left[\frac{1}{r}\frac{\partial}{\partial r}\left(r\frac{\partial E_{z_{II}}}{\partial r}\right) - \beta^2 E_{z_{II}}\right] = 0 \quad , \qquad (3.44)$$

which, for $\omega \neq \omega_{pp}$, is reduced to

$$\nabla^2 E_{z_{II}} = 0 \quad . \qquad (3.45)$$

3.4 BOUNDARY CONDITIONS AT THE EDGE OF THE BEAM

We calculate the charge perturbation at the surface of the electron beam, due to the radial motions of electrons of the beam as well as of the plasma. The ripple at the boundary of the electron beam-plasma is approximated, by the method introduced by Hahn,[5] by a sheet of ac surface charge at the same boundary the electron beam has in the absence of ac excitation.

The net surface charge density, at r = a, results from contributions due to radial motions of electrons coming from region I (beam and plasma), and also of electrons coming from region II (plasma only).

The surface charge densities are calculated from the small radial displacements of electrons at $r = a$. The continuity equation is applied in a small element of volume on the dc boundary of the beam. The equivalent surface charge density which is due to radial displacements of electrons of the beam turns out to be

$$\sigma_b = \rho_{0b} \frac{v_{rb}}{j(\omega - u_0\beta)}\bigg|_{r=a} = \frac{i_{rb}}{j(\omega - u_0\beta)}\bigg|_{r=a} \quad . \qquad (3.46)$$

Upon substituting in this equation the expression derived before for the radial component of the beam current density (Eq. 3.32), we obtain

$$\sigma_b = -j\frac{\epsilon_0}{\beta} \cdot \frac{\omega_{pb}^2}{(\omega - u_0\beta)^2} \cdot \frac{\partial E_{z_I}}{\partial r}\bigg|_{r=a} \quad . \qquad (3.47)$$

In a similar way, the surface charge density at $r = a$ resulting from plasma electrons coming from region I is calculated in terms of the electric field, yielding the equation

$$\sigma_{p_I} = \frac{i_{rp_I}}{j\omega}\bigg|_{r=a} = -j\,\frac{\epsilon_0}{\beta}\left(\frac{\omega_{pp}^2}{\omega^2}\right)\frac{\partial E_{z_I}}{\partial r}\bigg|_{r=a} . \qquad (3.48)$$

Finally, the surface charge density at $r = a$ due to plasma electrons coming from region II is

$$\sigma_{p_{II}} = \frac{i_{rp_{II}}}{j\omega}\bigg|_{r=a} = -j\,\frac{\epsilon_0}{\beta}\left(\frac{\omega_{pp}^2}{\omega^2}\right)\frac{\partial E_{z_{II}}}{\partial r}\bigg|_{r=a} . \qquad (3.49)$$

We know that at $r = a$ the normal component of the electric field, (i.e., the radial component of $\vec{E}$) is discontinuous by the amount of the total equivalent surface charge density associated with the perturbation. We have

$$E_{r_{II}} - E_{r_I} = \frac{1}{\epsilon_0}\left(\sigma_b + \sigma_{p_I} - \sigma_{p_{II}}\right) . \qquad (3.50)$$

The other boundary condition, at $r = a$, states the continuity of the longitudinal electric field, namely

$$E_{z_I} = E_{z_{II}} \quad , \quad \text{at} \quad r = a . \qquad (3.51)$$

With the help of the expressions for the equivalent surface charge densities, as presented above, these two boundary conditions lead to the following equation:

$$\left(1 - \frac{\omega_{pp}^2}{\omega^2}\right)\frac{\partial E_{z_{II}}}{\partial r}\bigg|_{r=a} = \left(1 - \frac{\omega_{pb}^2}{(\omega - u_0\beta)^2} - \frac{\omega_{pp}^2}{\omega^2}\right)\frac{\partial E_{z_I}}{\partial r}\bigg|_{r=a} . \qquad (3.52)$$

It should be pointed out here that the analysis made so far applies each set of field solutions in the beam region, namely

a. the solutions deriving from Eq. (3.42), rewritten below:

$$1 - \frac{\omega_{pb}^2}{(\omega - u_0\beta)^2} - \frac{\omega_{pp}^2}{\omega^2} = 0 \quad ,$$

and

b. solutions which result from

$$\nabla^2 E_{z_I} = 0 \quad .$$

3.5 NONSOLENOIDAL FLOW EQUATIONS

Let us consider now the case (a) where the longitudinal propagation constants β for the fields in region I are the solutions of Eq. (3.42), that is

$$\beta_{1,2} = \beta_e \pm h \tag{3.53}$$

where $\beta_e = \omega/u_0$ is the beam wave number and h is defined as given by

$$h = \frac{\omega_{pb}}{u_0\sqrt{1 - \frac{\omega_{pp}^2}{\omega^2}}} \quad . \tag{3.54}$$

The pair of waves corresponding to these propagation constants is referred to as the nonsolenoidal mode. The electric field inside the beam region (region I) has nonvanishing divergence. Consequently the propagation of this pair of space-charge waves is associated with a charge bunching ($\rho \neq 0$) within the beam. The propagation constants are the same as in the case of an infinite cross-section beam-plasma, and are therefore independent of the finite geometry of the system.

Inside the electron beam, we have

$$\rho_{b_I} \neq 0 \ , \quad \rho_{p_I} \neq 0 \quad . \tag{3.55}$$

Assume that the modulation frequency of the beam ω is different from the plasma frequency of the plasma ω_{pp} . $(\omega \neq \omega_{pp})$. It follows then, from Eq. (3.52), that the following boundary condition exists at $r = a$:

$$\left.\frac{\partial E_{z_{II}}}{\partial r}\right|_{r = a} = 0 \quad , \quad (\omega \neq \omega_{pp}) \quad . \tag{3.56}$$

We have, therefore, in the outside beam region (region II), the longitudinal fields satisfying the differential equation

$$\nabla^2 E_{z_{II}} = 0 \quad , \quad (a \leq r \leq b)$$

and the boundary conditions:

$$\begin{aligned} E_{z_{II}}(b) &= 0 \\ \left.\frac{\partial E_{z_{II}}}{\partial r}\right|_{r = a} &= 0 \quad . \end{aligned} \tag{3.57}$$

The solution of the differential equation, for $a \leq r \leq b$, is written

$$E_{z_{II}}(r) = A_2 I_0(\beta r) + B_2 K_0(\beta r) \quad , \tag{3.58}$$

where A_2 and B_2 are constants to be determined with the aid of the prescribed boundary conditions. We have

$$\left.\frac{\partial E_{z_{II}}}{\partial r}\right|_{r = a} = \beta\left(A_2 I_1(\beta a) - B_2 K_1(\beta a)\right) = 0 \tag{3.59a}$$

and

$$E_{z_{II}}\Big|_{r=b} = A_2 I_0(\beta b) + B_2 K_0(\beta b) = 0 \quad , \tag{3.59b}$$

for each $\beta(\beta_1$ and $\beta_2)$. We have to solve then, for $\beta \neq 0$, this system of linear homogeneous equations for the unknowns A_2 and B_2, respectively. It is well known that this system has a nontrivial solution $(A_2 \neq 0 , B_2 \neq 0)$ if the determinant of the coefficients is zero. This means that we should have

$$\Delta = I_1(\beta a)K_0(\beta b) + I_0(\beta b)K_1(\beta a) = 0 \quad . \tag{3.60}$$

However for real values of $\beta(\beta \neq 0)$, this determinant does not vanish. It follows then that $A_2 = 0 , B_2 = 0$. This result implies that there is no field in the plasma region outside the electron beam. The solution in region II is

$$\overset{+}{E}_{II}^{(1,2)} = 0 \quad , \tag{3.61a}$$

corresponding to the nonsolenoidal fields inside the beam. From the boundary condition at $r = a$, as expressed by Eq. (3.51), it follows that

$$E_{z_I}(a) = 0 \quad . \tag{3.61b}$$

It had been shown in the preceding lines that when $\omega > \omega_{pp}$, these nonsolenoidal modes do not have fields external to the beam region. Therefore they cannot couple to the fields of an external structure. However if this structure penetrates into the beam by means of an obstruction as in the case of grids, which will concern us, these solutions become possible solutions for the problem. For the case $\omega < \omega_{pp}$, β will have complex values; but a similar consideration of (3.60) for this case indicates no solutions and therefore requires $A = B = 0$ and Eqs. (3.61a) and (3.61b) also apply.

3.6 NONSOLENOIDAL AND NONGROWING WAVE SOLUTIONS

Under the assumption that the modulation frequency of the grid-modulated beam is always above the plasma frequency of the plasma, we have seen in the previous section that:

a. There are two possible propagating waves that can be excited, one with a phase velocity faster than u_0, and the other with a phase velocity slower than u_0.

b. There is no field in the plasma region outside the beam. The analysis which follows in this section will consider only this pair of nonsolenoidal solutions. The treatment will be nonrelativistic, and this means that the forces on the beam electrons caused by the beam magnetic fields may be neglected and that the electric field of the electron beam may be expressed as the gradient of a scalar potential satisfying Poisson's equation. This type of description for the space-charge field is sometimes called the quasi-static approximation.

Inside the beam-plasma region, which has been denoted as region I, we have

$$v_I(r,z) = \left(v_I^{(1)}(r)e^{-j\beta z} + v_I^{(2)}(r)e^{j\beta z}\right) \cdot e^{j(\omega t - \beta_e z)}, \quad (3.62)$$

where $v_I(r,z)$ is the electric potential defined in this region, and the superscripts (1) and (2) indicate, respectively, the correspondence with each nonsolenoidal propagating wave described in Eq. (3.42).

The longitudinal and radial components of the electron beam velocity are, respectively,

$$v_{zb}(r,z) = \left(v_{zb}^{(1)}(r) \cdot e^{-j\beta z} + v_{zb}^{(2)}(r)e^{j\beta z}\right) e^{j(\omega t - \beta_e z)}$$

and

$$v_{rb}(r,z) = \left(v_{rb}^{(1)}(r)e^{-j\beta z} + v_{rb}^{(2)}(r)e^{j\beta z}\right) \cdot e^{j(\omega t - \beta_e z)}.$$

Similar expressions hold for the plasma electrons velocity components v_{zp} and v_{rp}, respectively.

The equation of motion for the electrons in the beam, along the z-direction, is

$$\left(\frac{\partial}{\partial r} + u_0 \frac{\partial}{\partial z}\right) v_{zb} = - \frac{e}{m} \frac{\partial}{\partial z} V_I \quad ,$$

from which the longitudinal velocity components are obtained in terms of the potential:

$$\frac{v^{(1)}_{zb_I}}{u_0} = - \left(1 + \frac{\beta e}{h}\right) \frac{V_I^{(1)}}{2V_0}$$

and

$$\frac{v^{(2)}_{zb_I}}{u_0} = - \left(1 - \frac{\beta e}{h}\right) \cdot \frac{V_I^{(2)}}{2V_0} \quad . \tag{3.63}$$

The radial velocity components are derived from the equation of transverse motion, resulting in the following expressions:

$$\frac{v^{(1)}_{rb_I}}{u_0} = \frac{1}{jh} \cdot \frac{d}{dr} \left(\frac{V_I^{(1)}}{2V_0}\right)$$

$$\frac{v^{(2)}_{rb_I}}{u_0} = - \frac{1}{jh} \frac{d}{dr} \cdot \left(\frac{V_I^{(2)}}{2V_0}\right) \quad . \tag{3.64}$$

For the plasma electrons, in this same region ($0 \leq r \leq a$), we find that the longitudinal velocity components are

$$\frac{v^{(1)}_{zp_I}}{u_0} = \left(1 + \frac{h}{\beta e}\right) \frac{V_I^{(1)}}{2V_0}$$

$$\frac{v^{(2)}_{zp_I}}{u_0} = \left(1 - \frac{h}{\beta e}\right) \frac{V_I^{(2)}}{2V_0} \quad , \tag{3.65}$$

and the radial velocity components are

$$\frac{v_{rp_I}^{(1)}}{u_0} = \frac{j}{\beta_e} \cdot \frac{d}{dr}\left(\frac{V_I^{(1)}}{2V_0}\right)$$

$$\frac{v_{rp_I}^{(2)}}{u_0} = \frac{j}{\beta_e} \cdot \frac{d}{dr}\left(\frac{V_I^{(2)}}{2V_0}\right) . \qquad (3.66)$$

By using the above expressions, and suppressing, for convenience, the phase factor $e^{j(\omega t - \beta_e z)}$, we may write, for the electron beam velocity components,

$$\frac{v_{zb}}{u_0} = -\cos(hz)\left[\frac{V_I^{(1)} + V_I^{(2)}}{2V_0} + \left(\frac{\beta_e}{h}\right)\left(\frac{V_I^{(1)} - V_I^{(2)}}{2V_0}\right)\right]$$

$$+ j \sin(hz)\left[\frac{V_I^{(1)} - V_I^{(2)}}{2V_0} + \left(\frac{\beta_e}{h}\right)\left(\frac{V_I^{(1)} + V_I^{(2)}}{2V_0}\right)\right]$$

and

$$\frac{v_{rb}}{u_0} = -\frac{j}{h}\cos(hz)\left[\frac{d}{dr}\left(\frac{V_I^{(1)} - V_I^{(2)}}{2V_0}\right)\right] - \frac{1}{h}\sin(hz)\left[\frac{d}{dr}\left(\frac{V_I^{(1)} + V_I^{(2)}}{2V_0}\right)\right] .$$

The corresponding velocity components, for the plasma electrons, in the same region I, are given by

$$\frac{v_{zp}}{u_0} = \cos(hz)\left[\frac{V_I^{(1)} + V_I^{(2)}}{2V_0} + \left(\frac{h}{\beta_e}\right)\left(\frac{V_I^{(1)} - V_I^{(2)}}{2V_0}\right)\right]$$

$$- j \sin(hz)\left[\frac{V_I^{(1)} - V_I^{(2)}}{2V_0} + \left(\frac{h}{\beta_e}\right)\left(\frac{V_I^{(1)} + V_I^{(2)}}{2V_0}\right)\right]$$

and

$$\frac{v_{rp}}{u_0} = \frac{j}{\beta_e} \cdot \cos(hz)\left[\frac{d}{dr} \cdot \left(\frac{V_I^{(1)} + V_I^{(2)}}{2V_0}\right)\right] + \frac{1}{\beta_e} \sin(hz)\left[\frac{d}{dr}\left(\frac{V_I^{(1)} - V_I^{(2)}}{2V_0}\right)\right] .$$

It had been shown in the preceding section that, in region II ($a \leq r \leq b$), we must have Laplace's equations satisfied:

$$\nabla^2 V_{II}^{(1)} = \nabla^2 V_{II}^{(2)} = 0 \qquad (3.67)$$

by the trivial solutions:

$$V_{II}^{(1)}(r) = 0 \quad , \quad V_{II}^{(2)}(r) = 0 \quad . \qquad (3.68)$$

From the continuity of the potentials, at the boundary of the two regions I and II, the following conditions result, for the potentials, in the region I at $r = a$:

$$V_I^{(1)}(a) = V_I^{(2)}(a) = 0 \quad . \qquad (3.69)$$

The surface charge densities, at $r = a$, are now calculated for the nonsolenoidal solutions. The contribution to the total surface charge density, at $r = a$, due to the radial motion of the electrons of the beam is given by

$$\frac{\sigma_b}{\rho_{0b}} = \frac{\sigma_b^{(1)}}{\rho_{0b}} \cdot e^{-jhz} + \frac{\sigma_b^{(2)}}{\rho_{0b}} \cdot e^{jhz} \quad , \qquad (3.70)$$

where, for simplicity, we again omitted the phase-factor $e^{j(\omega t - \beta_e z)}$.
We have

$$\frac{\sigma_b^{(1)}}{\rho_{0b}} = - \left.\frac{v_{rb}^{(1)}}{jhu_0}\right|_{r = a} = \frac{1}{h^2} \cdot \frac{d}{dr}\left(\frac{V_I^{(1)}}{2V_0}\right)_{r = a} ,$$

and

$$\frac{\sigma_b^{(2)}}{\rho_{0b}} = \frac{v_{rb}^{(2)}}{jhu_0}\bigg|_{r=a} = \frac{1}{h^2}\cdot\frac{d}{dr}\left(\frac{V_I^{(2)}}{2V_0}\right)_{r=a} , \qquad (3.71)$$

expressions which follow from equations (3.64).

The contribution to the total ac surface charge density, at $r = a$, which is due to the plasma electrons coming from region I, is written

$$\frac{\sigma_p}{\rho_{0p}} = \frac{\sigma_p^{(1)}}{\rho_{0p}} e^{-jhz} + \frac{\sigma_p^{(2)}}{\rho_{0p}} e^{jhz} ,$$

where

$$\frac{\sigma_p^{(1)}}{\rho_{0p}} = \frac{v_{rp_I}^{(1)}}{j\omega}\bigg|_{r=a} = \frac{1}{\beta_e^2}\cdot\frac{d}{dr}\left(\frac{V_I^{(1)}}{2V_0}\right)_{r=a}$$

and

$$\frac{\sigma_p^{(2)}}{\rho_{0p}} = \frac{v_{rp_I}^{(2)}}{j\omega}\bigg|_{r=a} = \frac{1}{\beta_e^2}\cdot\frac{d}{dr}\left(\frac{V_I^{(2)}}{2V_0}\right)_{r=a} . \qquad (3.72)$$

3.7 SOLENOIDAL FLOW; APPROXIMATE SOLUTIONS

For the second possibility given by (3.40) we assume, alternatively, that Eq. (3.41) is satisfied in the beam-plasma region. The field solutions are therefore to be derived from the Laplacian of the longitudinal electric field

$$\nabla^2 E_{z_I} = 0 . \qquad (3.73)$$

If, however, we refer to Eq. (3.21) and write the right-hand side of this equation in terms of the charge density with the help of the continuity equation, we have

$$\nabla^2 E_{z_I} = \frac{1}{r}\frac{\partial}{\partial r}\left(r\frac{\partial E_{z_I}}{\partial r}\right) - \beta^2 E_{z_I} = -j\frac{\beta}{\epsilon_0}\rho_I . \qquad (3.74)$$

It follows then, from Eq. (3.73), that we must have

$$\rho_I = 0, (\rho_{b_I} = 0 \ , \ \rho_{p_I} = 0) \quad , \tag{3.75}$$

and, consequently

$$\text{div} \ . \ \vec{E}_I = 0 \quad . \tag{3.76}$$

We refer to these modes as solenoidal modes in contrast to the other solutions considered before - nonsolenoidal solutions - where the fields have nonvanishing divergence.

In this solenoidal case, where the divergence of the electric field is zero everywhere within region I, there is no ac volume charge density inside the beam. These solutions correspond to space-charge wave propagation involving a rippling at the surface of the electron beam.

The fields produced by these modes are caused entirely by the bulging and contracting of the surface separating regions I and II.

In solving the differential equation

$$\nabla^2 E_{z_I} = 0 \quad , \quad (0 \leq r \leq a)$$

we assume solutions of the form

$$E_{z_I}(r) = A_1 I_0(\beta r) \quad , \tag{3.78}$$

where a second solution, which is not finite at the origin, has been omitted.

In region II ($a \leq r \leq b$) , we also have

$$\nabla^2 E_{z_{II}} = 0 \quad , \tag{3.79}$$

and the solution of this equation satisfying the prescribed boundary condition at $r = b$, is

$$E_{z_{II}}(r) = A_2[I_0(\beta r)K_0(\beta b) - I_0(\beta b)K_0(\beta r)] \quad , \tag{3.80}$$

for $a \leq r \leq b$.

By using Eq. (3.52) with the above expressions for the fields in the two regions, the following determinantal equation is obtained:

$$\left(1 - \frac{\omega_{pb}^2}{(\omega - u_0\beta)^2} - \frac{\omega_{pp}^2}{\omega^2}\right) \frac{I_1(\beta a)}{I_0(\beta a)}$$

$$= \left(1 - \frac{\omega_{pp}^2}{\omega^2}\right) \left\{ \frac{I_1(\beta a)K_0(\beta b) + I_0(\beta b)K_1(\beta a)}{I_0(\beta a)K_0(\beta b) - I_0(\beta b)K_0(\beta a)} \right\}$$

from which we get

$$\beta = \beta_e \pm \frac{\beta_{pb}}{\sqrt{1 - \frac{\omega_{pp}^2}{\omega^2}}} \cdot \left\{ \frac{I_1(\beta a)}{I_0(\beta b)} \cdot \frac{I_0(\beta b)K_0(\beta a) - I_0(\beta a)K_0(\beta b)}{I_1(\beta a)K_0(\beta a) + I_0(\beta a)K_1(\beta a)} \right\}^{\frac{1}{2}} . \quad (3.81)$$

With the aid of the Wronskian relation,

$$I_1(\beta a)K_0(\beta a) + I_0(\beta a)K_1(\beta a) = \frac{1}{\beta a} ,$$

we write

$$\beta = \beta_e \pm \frac{\beta_{pb}}{\sqrt{1 - \frac{\omega_{pp}^2}{\omega^2}}} \left\{ (\beta a) \frac{I_1(\beta a)}{I_0(\beta b)} \cdot [I_0(\beta b)K_0(\beta a) - I_0(\beta a)K_0(\beta b)] \right\}^{\frac{1}{2}} . \quad (3.82)$$

By making the identifications

$$F(\beta) = \left\{ (\beta a) \frac{I_1(\beta a)}{I_0(\beta b)} [I_0(\beta b)K_0(\beta a) - I_0(\beta a)K_0(\beta b)] \right\}^{\frac{1}{2}} \quad (3.83)$$

and

$$h = \frac{\beta_{pb}}{\sqrt{1 - \frac{\omega_{pp}^2}{\omega^2}}} , \quad (3.84)$$

we may write

$$\beta = \beta_e \pm hF(\beta) \quad . \tag{3.85}$$

This determinantal equation is a rather involved equation to be solved for β . Instead of trying to solve it in the most general case, we proceed by making simplifying assumptions, which are shown below to be valid, under a practical point of view.

To begin with, we assume that $\omega > \omega_{pp}$, which means that we shall be concerned with real values for β .

We denote the propagation constants for this pair of solenoidal waves by

$$\beta_3 = \beta_e + hF_3(\beta_3) = \beta_e + \Delta_3 \tag{3.86}$$

and

$$\beta_4 = \beta_e - hF_4(\beta_4) = \beta_e - \Delta_4 \quad ,$$

where, by definition

$$\Delta_3 = hF_3 = hF(\beta_3)$$

and

$$\Delta_4 = hF_4 = hF(\beta_4) \quad .$$

We assume further that

$$\frac{\Delta_{3,4}}{\beta_e} < 1 \quad . \tag{3.87}$$

The degree to which such approximation can be applied can be estimated by using some typical figures. In the experiment to be described in a subsequent chapter, we have

$$\frac{\beta_{pb}}{\beta_e} \simeq 0.02 \quad .$$

We should have then, apart from the factor F, the following inequality

$$\left(\frac{\beta_{pb}}{\beta_e}\right)^2 < 1 - \frac{\omega_{pp}^2}{\omega^2} \quad ,$$

which leads to the conclusion that this condition is indeed fulfilled for values of ω very near ω_{pp} ($\omega_{pp} \sim 99\% \, \omega$) .
With this approximation, we have for a first-order solution

$$\Delta_3 = \Delta_4 \simeq \Delta \quad , \tag{3.88}$$

where Δ is defined as being given by

$$\Delta = hF(\beta_e) \quad . \tag{3.89}$$

Figure 2 shows $F(\beta_e)$, which is always less than unity, as a function of $(\beta_e a)$ and b/a . This factor $F(\beta_e)$ is the usual "plasma frequency reduction factor" which takes into account effects of space-charge on bunching in klystrons.[11] The curves in Fig. 2 were taken from Feenberg's paper (ref. 6).

Under this first order approximation, we are allowed to write

$$\begin{aligned} \beta_3 &= \beta_e + hF(\beta_e) = \beta_e + \Delta \\ \beta_4 &= \beta_e - hF(\beta_e) = \beta_e - \Delta \quad . \end{aligned} \tag{3.90}$$

As a next approximation, we make

$$\begin{aligned} \beta_3 &= \beta_e + hF(\beta_e + \Delta) = \beta_e + \Delta' \\ \beta_4 &= \beta_e - hF(\beta_e - \Delta) = \beta_e - \Delta'' \quad . \end{aligned} \tag{3.91}$$

It follows that

$$\Delta' = hF(\beta_e + \Delta) = h\left\{F(\beta_e) + \Delta \frac{\partial}{\partial \beta_e} \cdot F(\beta_e)\right\} = hF(\beta_e) + h^2 . F(\beta_e) \cdot \frac{\partial}{\partial \beta_e} F(\beta_e) \quad ,$$

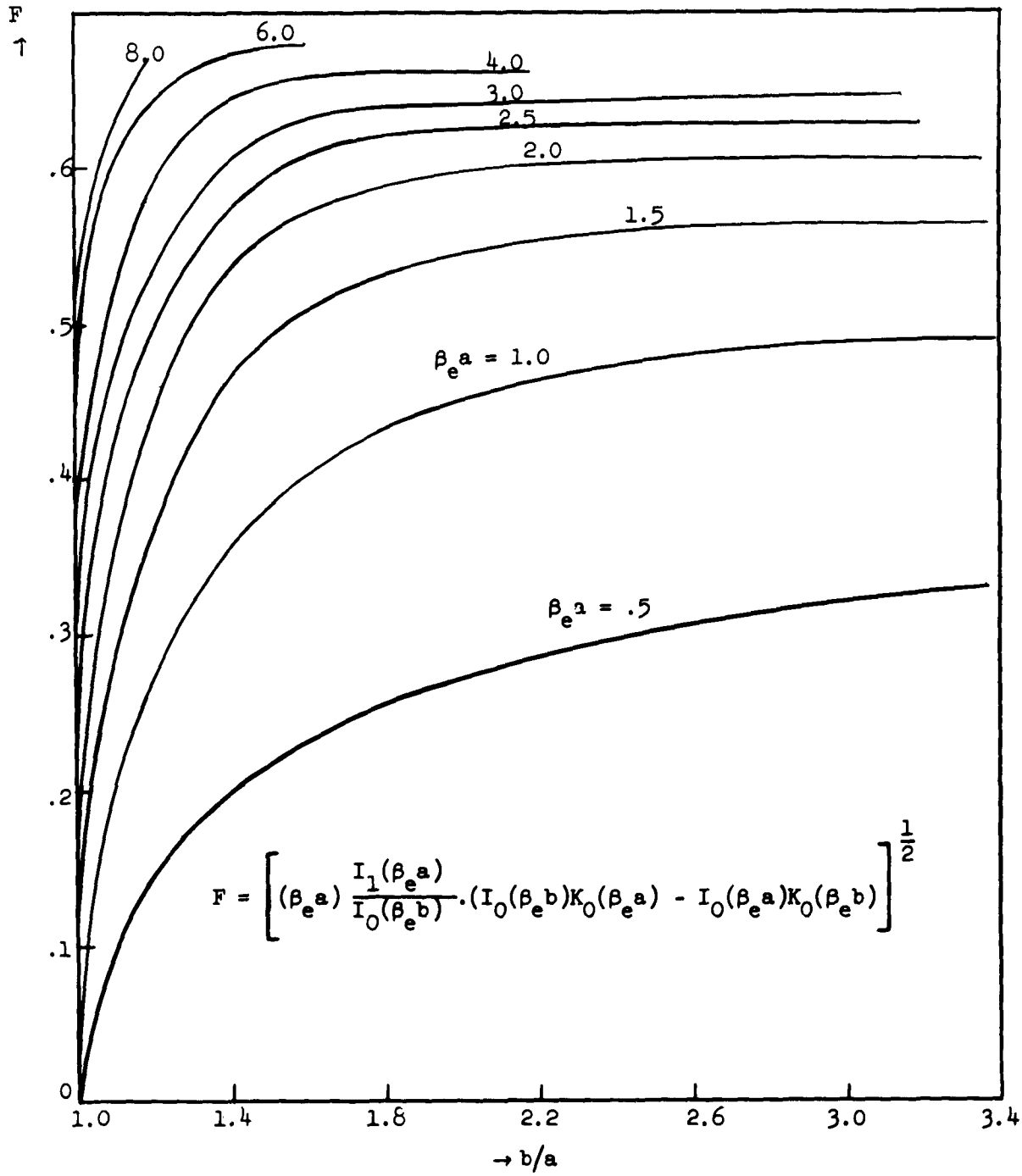

Fig. 2--Plot of the reduction factor F for different values of $\beta_e a$ (taken from Feenberg's work).

or

$$\Delta' - \Delta = h^2 F(\beta_e) \cdot \frac{\partial}{\partial \beta_e} F(\beta_e) \quad , \tag{3.92}$$

and similarly

$$\Delta'' - \Delta = - h^2 F(\beta_e) \frac{\partial}{\partial \beta_e} F(\beta_e) \quad .$$

We have, then,

$$\beta_3 = \beta_e + \Delta' = \beta_e + hF(\beta_e) + h^2 F(\beta_e) \cdot \frac{\partial}{\partial \beta_e} F(\beta_e) \quad , \tag{3.93}$$

and

$$\beta_4 = \beta_e - \Delta'' = \beta_e - hF(\beta_e) + h^2 F(\beta_e) \cdot \frac{\partial}{\partial \beta_e} F(\beta_e) \quad , \tag{3.94}$$

from which we identify

$$\Delta_3 = hF_3 = hF(\beta_e) + h^2 \cdot F(\beta_e) \cdot \frac{\partial}{\partial \beta_e} F(\beta_e)$$

and

$$\Delta_4 = hF_4 = hF(\beta_e) - h^2 F(\beta_e) \cdot \frac{\partial}{\partial \beta_e} F(\beta_e)$$

resulting in

$$\delta = \Delta_3 - \Delta_4 = 2h^2 F(\beta_e) \cdot \frac{\partial}{\partial \beta_e} F(\beta_e) \tag{3.95}$$

or

$$\frac{\delta}{h^2} = \frac{\Delta_3 - \Delta_4}{h^2} = 2F(\beta_e) \cdot \frac{\partial}{\partial \beta_e} F(\beta_e) \quad .$$

By putting

$$F^2(\beta_e) = G(\beta_e) \quad ,$$

we have

$$\frac{\delta}{h^2 a} = \frac{\Delta_3 - \Delta_4}{h^2 a} = \frac{\partial G}{\partial(\beta_e a)} \quad . \tag{3.96}$$

Figure 3 shows $\partial G/\partial(\beta_e a)$ as a function of $(\beta_e a)$ and b/a. These curves were adapted from the curves presented by Feenberg.

3.8 MATCHING INPUT BOUNDARY CONDITIONS WITH THE SPACE-CHARGE WAVES

In matching the input conditions with the space-charge waves discussed in (3.6) and (3.7), it is convenient to express the fields for the solenoidal modes as the gradients of potentials $V_I(r,z)$ and $V_{II}(r,z)$ that fulfill Laplace's equations, respectively, inside and outside of the electron beam. This is valid for nonrelativistic velocities.

To determine the solutions of $\nabla^2 V_I = 0$ in region I, as the solutions appropriate to the solenoidal case, where the propagation constants $\beta_{3,4}$ have the approximate expressions derived before, we assume

$$V_I^{(3)}(r) = A_3 I_0(\beta_3 r)$$

$$V_I^{(4)}(r) = A_4 I_0(\beta_4 r) \quad . \tag{3.97}$$

Outside the beam region, we have

$$\nabla^2 V_{II} = 0 \quad , \tag{3.98}$$

the solutions of which must satisfy the following boundary conditions:

$$V_{II}^{(3)}(b) = V_{II}^{(4)}(b) = 0 \tag{3.99}$$

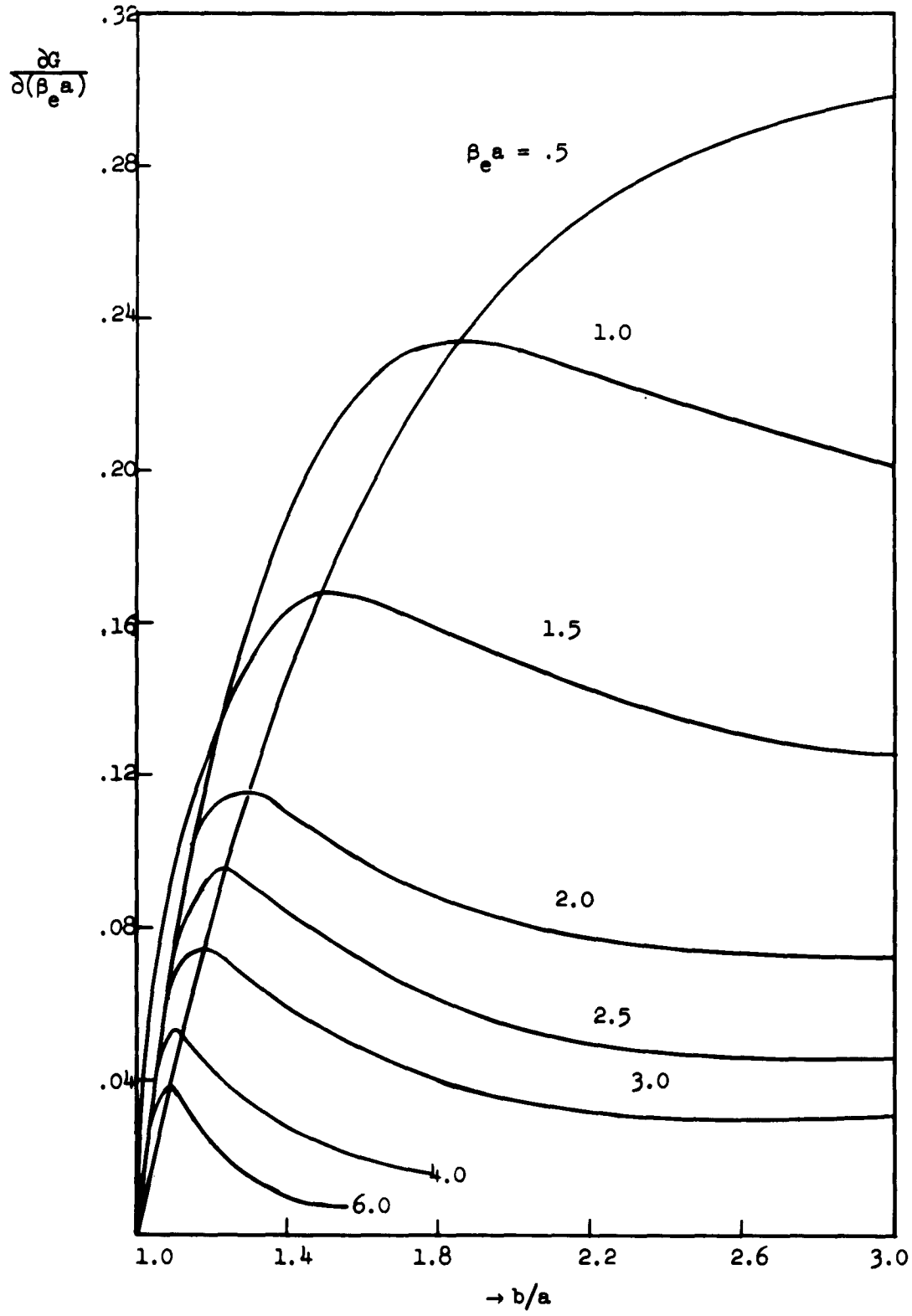

Fig. 3--Plot of $\partial G/\partial(\beta_e a) = \delta a/(ha)^2$ versus b/a, for several values of $\beta_e a$ (Feenberg).

and

$$V_{II}^{(3)}(a) = V_I^{(3)}(a)$$

$$V_{II}^{(4)}(a) = V_I^{(4)}(a) \quad . \tag{3.100}$$

The solutions, in the region II, then, are

$$V_{II}^{(3)}(r) = B_3[I_0(\beta_3 r)K_0(\beta_3 b) - I_0(\beta_3 b)K_0(\beta_3 r)]$$

$$V_{II}^{(4)}(r) = B_4[I_0(\beta_4 r) \cdot K_0(\beta_4 b) - I_0(\beta_4 b)K_0(\beta_4 r)] \quad , \tag{3.101}$$

where the constants B_3 and B_4 must be determined in order that the prescribed boundary conditions at $r = a$, are fulfilled. With the help of these conditions, and Eqs. (3.100), we obtain

$$A_3 = \frac{B_3}{I_0(\beta_3 a)} [I_0(\beta_3 a)K_0(\beta_3 b) - I_0(\beta_3 b)K_0(\beta_3 a)]$$

and

$$A_4 = \frac{B_4}{I_0(\beta_4 a)} [I_0(\beta_4 a) \cdot K_0(\beta_4 b) - I_0(\beta_4 b)K_0(\beta_4 a)] \quad . \tag{3.102}$$

Additional relations among the constants arise from one of the conditions at the input plane $(z = 0)$. We should have $V_{II}(r) = \text{const.} = 0$, for $a \leq r \leq b$. This imposes the condition that

$$V_{II}(a) = 0 \quad . \tag{3.103}$$

That is,

$$V_{II}^{(3)}(a) + V_{II}^{(4)}(a) = 0 \quad , \tag{3.103b}$$

since the nonsolenoidal fields within the beam do not have fields in region II. This equation together with Eqs. (3.97) yields the following relation between the coefficients A_3 and A_4 :

$$A_3 I_0(\beta_3 a) = - A_4 I_0(\beta_4 a) \quad .$$

Note that condition (3.103) results in $V_{II}^{(2)} = 0$ for $a \leq r \leq b$ only within the approximation that $\beta_3 \approx \beta_4$ or $\beta_e/h \gg 1$. The solenoidal potentials may then be written in terms of one of the coefficients A_3 or A_4 :

$$V_I^{(3)}(r) = - A_4 I_0(\beta_4 a) \cdot \frac{I_0(\beta_3 r)}{I_0(\beta_3 a)}$$

$$V_I^{(4)}(r) = A_4 I_0(\beta_4 a) \cdot \frac{I_0(\beta_4 r)}{J_0(\beta_4 a)} \quad . \qquad (3.104)$$

The nonsolenoidal field solutions which have the same propagation constants as in an infinite system are allowed to have an arbitrary transverse dependence.

We proceed by applying the remaining input boundary conditions to the two pair of waves which are excited in the gridded gap. The radial variation for the solenoidal modes, as shown above, is completely specified from the solution of the Bessel differential equation [Eq. (3.73)] inside the beam.

The boundary conditions to be satisfied at the input plane will impose then a <u>particular transverse</u> dependence on the nonsolenoidal modes. This dependence is not the most general radial variation which could be prescribed for these nonsolenoidal field components. Feenberg shows that this general solution includes terms which are negligible under approximations previously made in deriving the propagation constants [terms of order $(\beta_q/\beta_e)^2$ and higher order].

However, all that is really required is to show that the radial variation used here for these waves, together with the solenoidal waves, fulfill the boundary conditions of the problem.

In the remainder of this section this relation between the two pair of modes is determined.

At the input plane $(z = 0)$, by assuming ideal grids, we must have the following condition inside the beam region:

$$V_I(r) = 0 \quad , \quad \text{at} \quad z = 0 \quad .$$

This means that

$$\sum_{n=1}^{4} V_I^{(n)}(r) = 0 \quad . \tag{3.105}$$

By applying Eqs. (3.104), it follows that

$$V_I^{(1)} + V_I^{(2)} = - A_4 I_0(\beta_4 a) \left(\frac{I_0(\beta_4 r)}{I_0(\beta_4 a)} - \frac{I_0(\beta_3 r)}{I_0(\beta_3 a)} \right) \quad . \tag{3.106}$$

The input longitudinal velocity of the electron beam is a specified quantity. Let $v_{zb} = v_0$ at $z = 0$. Therefore we may write

$$\frac{v_0}{u_0} = \frac{\alpha M}{2} = \frac{1}{u_0} \sum_{n=1}^{4} v_{zb}^{(n)}(r) \quad , \tag{3.107}$$

where u_0 is the dc beam velocity, $M = (\sin d/2)/(d/2)$ is the beam coupling coefficient, and α is the voltage modulation index $(\alpha = V_1/V_0)$.

By using Eqs. (3.63) and the similar ones for the solenoidal components $v_{zb}^{(3)}$ and $v_{zb}^{(4)}$ of the beam longitudinal velocity, we obtain the following equation:

$$\frac{v_0}{u_0} = \frac{\alpha M}{2} = - \left(\frac{V_I^{(1)} + V_I^{(2)}}{2V_0} \right) - \left(\frac{V_I^{(3)} + V_I^{(4)}}{2V_0} \right) - \left(\frac{\beta_e}{h} \right)$$

$$\cdot \left[\left(\frac{V_I^{(1)} - V_I^{(2)}}{2V_0} \right) - \left(\frac{V_I^{(3)} - V_I^{(4)}}{2V_0} \right) \right] \quad .$$

This equation together with Eq. (3.106) yields

$$\frac{V_I^{(1)} - V_I^{(2)}}{2V_0} = -\frac{\alpha h M}{2\beta_e} + A_4 \frac{I_0(\beta_4 a)}{2V_0} \cdot \left(\frac{1}{F_4} \cdot \frac{I_0(\beta_4 r)}{I_0(\beta_4 a)} + \frac{1}{F_3} \cdot \frac{I_0(\beta_3 r)}{I_0(\beta_3 a)} \right) . \tag{3.108}$$

But, from the continuity of E_z at $r = a$ and the fact that $E_z = 0$ for $r > a$ for the nonsolenoidal waves,

$$V_I^{(1)}(a) = V_I^{(2)}(a) = 0 \quad ,$$

and it follows that

$$A_4 = \frac{1}{I_0(\beta_4 a)} \cdot \frac{\frac{\alpha h}{\beta_e} M V_0}{\left(\frac{1}{F_3} + \frac{1}{F_4} \right)} \quad ,$$

and

$$A_3 = -\frac{1}{I_0(\beta_3 a)} \cdot \frac{\frac{\alpha h}{\beta_e} M V_0}{\left(\frac{1}{F_3} + \frac{1}{F_4} \right)} . \tag{3.109}$$

We have, then, the solenoidal components of the electric potential in the beam region given by the following expressions:

$$V_I^{(3)}(r) = A_3 I_0(\beta_3 r) = \frac{-\alpha M V_0}{\left(\frac{1}{F_3} + \frac{1}{F_4} \right)} \left(\frac{h}{\beta_e} \right) \cdot \frac{I_0(\beta_3 r)}{I_0(\beta_3 a)}$$

and

$$V_I^{(4)}(r) = A_4 I_0(\beta_4 r) = \frac{\alpha M V_0}{\left(\frac{1}{F_3} + \frac{1}{F_4} \right)} \cdot \left(\frac{h}{\beta_e} \right) \cdot \frac{I_0(\beta_4 r)}{I_0(\beta_4 a)} . \tag{3.110}$$

The other input boundary condition to be satisfied is

$$v_{rb} = 0 \quad , \quad \text{at} \quad z = 0 \quad .$$

Using Eqs. (3.64) and similar ones for $v_{rb}^{(3)}$ and $v_{rb}^{(4)}$, the following equation results:

$$\frac{d}{dr}\left(\frac{V_I^{(1)} - V_I^{(2)}}{2V_0}\right) + \frac{1}{F_3} \cdot \frac{d}{dr}\left(\frac{V_I^{(3)}}{2V_0}\right) - \frac{1}{F_4} \cdot \frac{d}{dr}\left(\frac{V_I^{(4)}}{2V_0}\right) = 0 \quad ,$$

which can be written

$$\frac{d}{dr}\left(\frac{V_I^{(1)} - V_I^{(2)}}{2V_0}\right) = \frac{\alpha M}{2}\left(\frac{h}{\beta_e}\right)\left\{\frac{\beta_3}{\beta_e\left(1 + \frac{F_3}{F_4}\right)} \cdot \frac{I_1(\beta_3 r)}{I_0(\beta_3 a)} + \frac{\beta_4}{\beta_e\left(1 + \frac{F_4}{F_3}\right)} \cdot \frac{I_1(\beta_4 r)}{I_0(\beta_4 a)}\right\}$$

where we have used Eqs. (3.109).

The condition on the longitudinal current density of the electron beam at the entrance plane $z = 0$ is stated as follows:

$$i_{zb}(r) = 0 \quad , \tag{3.111}$$

or

$$\sum_{k=1}^{k=4} i_{zb}^{(k)}(r) = 0 \quad .$$

We know, however, that

$$\begin{aligned} i_{zb}^{(1)} &= \left(\rho_b^{(1)} \cdot u_0\right) + \left(\rho_{0b} \cdot v_{zb}^{(1)}\right) \\ i_{zb}^{(2)} &= \left(\rho_b^{(2)} \cdot u_0\right) + \left(\rho_{0b} \cdot v_{zb}^{(2)}\right) \\ i_{zb}^{(3)} &= \rho_{0b} \cdot v_{zb}^{(3)} \\ i_{zb}^{(4)} &= \rho_{0b} \cdot v_{zb}^{(4)} \quad , \end{aligned} \tag{3.112}$$

therefore,

$$\frac{\rho_b^{(1)} + \rho_b^{(2)}}{\rho_{0b}} = - \frac{v_0}{u_0} = - \frac{\alpha M}{2} \quad . \tag{3.113}$$

Moreover, the volume charge densities associated with the nonsolenoidal fields can be calculated, in terms of the corresponding potentials, by applying the continuity equation at $z = 0$. We have

$$\frac{\partial}{\partial z} \, i_{zb} = - j\omega\rho_b \quad , \quad \text{at} \quad z = 0 \quad .$$

Then we find

$$(h + \beta_e) \, i_{zb}^{(1)} = \omega\rho_b^{(1)}$$

$$- (h - \beta_e) \, i_{zb}^{(2)} = \omega\rho_b^{(2)} \quad .$$

By using Eqs. (3.112) for $i_{zb}^{(1)}$ and $i_{zb}^{(2)}$, and substituting in the above equations, we have

$$\frac{\rho_b^{(1)}}{\rho_{0b}} = - \left(1 + \frac{\beta_e}{h}\right) \frac{v_{zb}^{(1)}}{u_0}$$

and

$$\frac{\rho_b^{(1)}}{\rho_{0b}} = - \left(1 - \frac{\beta_e}{h}\right) \frac{v_{zb}^{(2)}}{u_0} \quad .$$

By making use of Eqs. (3.63) we can express $\rho_b^{(1)}$ and $\rho_b^{(2)}$ in terms of the potentials $V_I^{(1)}$ and $V_I^{(2)}$, respectively, yielding

$$\frac{\rho_b^{(1)}}{\rho_{0b}} = \left(1 + \frac{\beta_e}{h}\right)^2 \frac{V_I^{(1)}}{2V_0} \quad ,$$

and

$$\frac{\rho_b^{(2)}}{\rho_{0b}} = \left(1 - \frac{\beta_e}{h}\right)^2 \cdot \frac{V_I^{(2)}}{2V_0} \quad . \tag{3.114}$$

3.9 APPROXIMATE SOLUTIONS FOR THE SPACE-CHARGE WAVES; VOLUME AND SURFACE CURRENTS

In this section we restrict ourselves to the approximations for the propagation constants of the space-charge wave modes, as indicated in Section 3.7.

We assume then that the following inequalities remain valid:

a. $\omega > \omega_{pp}$

b. $\dfrac{h}{\beta_e} < 1 \quad$ where $\quad h = \dfrac{\beta_{pb}}{\sqrt{1 - \dfrac{\omega_{pp}^2}{\omega^2}}}$

c. $\dfrac{\Delta_{(3,4)}}{\beta_e} < 1 \quad$ where $\quad \Delta_{3,4} = \dfrac{\beta_{pb} F_{3,4}}{\sqrt{1 - \dfrac{\omega_{pp}^2}{\omega^2}}}$. (3.115)

Under these approximations, we have

$$\beta_1 \simeq \beta_2 = \beta_e$$

$$\beta_{3,4} = \beta_e \pm hF(\beta_e) = \beta_e \pm \Delta \quad , \tag{3.116}$$

and we can expand the functions $I_0(\beta_3 r)/I_0(\beta_3 a)$ and $I_0(\beta_4 r)/I_0(\beta_4 a)$, respectively, in power series in Δ, to obtain

$$\frac{I_0(\beta_4 r)}{I_0(\beta_4 a)} - \frac{I_0(\beta_3 r)}{I_0(\beta_3 a)} = -2\Delta \cdot \frac{\partial}{\partial \beta_e}\left(\frac{I_0(\beta_e r)}{I_0(\beta_e a)}\right) - \frac{\Delta^3}{3}\frac{\partial^3}{\partial \beta_e^3}\left(\frac{I_0(\beta_e r)}{I_0(\beta_e a)}\right) + \cdots$$

and

$$\frac{1}{F}\left(\frac{I_0(\beta_4 r)}{I_0(\beta_4 a)} + \frac{I_0(\beta_3 r)}{I_0(\beta_3 a)}\right) = \frac{2h}{\Delta}\left(\frac{I_0(\beta_e r)}{I_0(\beta_e a)}\right) + h\Delta \cdot \frac{\partial^2}{\partial \beta_e^2}\left(\frac{I_0(\beta_e r)}{I_0(\beta_e a)}\right) + \cdots$$

Substituting these two expansions in Eqs. (3.106) and (3.108), respectively, results in the following expressions:

$$\frac{V_I^{(1)} + V_I^{(2)}}{2V_0} = \frac{\alpha M}{2}\left(\frac{\Delta}{\beta_e}\right)^2 \left\{ \beta_e \frac{\partial}{\partial \beta_e}\left(\frac{I_0(\beta_e r)}{I_0(\beta_e a)}\right) + O\left(\frac{\Delta}{\beta_e}\right)^2 \right\} \quad (3.117)$$

and

$$\frac{V_I^{(1)} - V_I^{(2)}}{2V_0} = -\frac{\alpha M}{2}\left(\frac{h}{\beta_e}\right)\left\{1 - \frac{I_0(\beta_e r)}{I_0(\beta_e a)} + O\left(\frac{\Delta}{\beta_e}\right)^2\right\} . \quad (3.118)$$

Putting these expressions into Eq. (3.14) yields

$$\frac{\rho_b^{(1)} - \rho_b^{(2)}}{\rho_{0b}} = -\frac{\alpha M}{2}\left(\frac{\beta_e}{h}\right)\left\{1 - \frac{I_0(\beta_e r)}{I_0(\beta_e a)} + O\left(\frac{\Delta}{\beta_e}\right)^2\right\} \quad (3.119)$$

and, as it has been shown before,

$$\frac{\rho_b^{(1)} + \rho_b^{(2)}}{\rho_{0b}} = -\frac{\alpha M}{2} .$$

The nonsolenoidal components of the ac beam velocity are, then, calculated.

a. The longitudinal velocity components are

$$\frac{v_{zb}^{(1)} + v_{zb}^{(2)}}{u_0} = \frac{\alpha M}{2}\left\{1 - \frac{I_0(\beta_e r)}{I_0(\beta_e a)} + O\left(\frac{\Delta}{\beta_e}\right)^2\right\}$$

and

$$\frac{v_{zb}^{(1)} - v_{zb}^{(2)}}{u_0} = -\frac{\alpha M}{2}\left(\frac{\beta_e}{h}\right)\left(\frac{\Delta}{h}\right)^2 \cdot \left\{ \beta_e \cdot \frac{\partial}{\partial \beta_e}\left(\frac{I_0(\beta_e r)}{I_0(\beta_e a)}\right) + O\left(\frac{\Delta}{\beta_e}\right)^2 \right\} \quad (3.120)$$

b. The radial components are

$$\frac{v_{rb}^{(1)} + v_{rb}^{(2)}}{u_0} = \frac{\alpha M}{2j}\left\{\frac{I_1(\beta_e r)}{I_0(\beta_e a)} + O\left(\frac{\Delta^2}{\beta_e^2}\right)\right\}$$

and

$$\frac{v_{rb}^{(1)} - v_{rb}^{(2)}}{u_0} = \frac{\alpha M}{2j}\left(\frac{\beta_e}{h}\right)\left(\frac{\Delta}{\beta_e}\right)^2\left\{\beta_e \cdot \frac{\partial}{\partial\beta_e}\frac{I_1(\beta_e r)}{I_0(\beta_e a)} + O\left(\frac{\Delta}{\beta_e}\right)^2\right\} . \quad (3.121)$$

In this same region, the nonsolenoidal components of the plasma velocity are calculated, yielding the following expressions:

$$\left.\begin{aligned}
\frac{v_{zp_I}^{(1)} + v_{zp_I}^{(2)}}{u_0} &= -\frac{\alpha h M}{2\beta_e}\left(1 - \frac{I_0(\beta_e r)}{I_0(\beta_e a)} + O\left(\frac{\Delta}{\beta_e}\right)^2\right) \\
\frac{v_{zp_I}^{(1)} - v_{zp_I}^{(2)}}{u_0} &= \frac{\alpha M}{2}\left(\frac{\Delta}{\beta_e}\right)^2\left\{\beta_e \frac{\partial}{\partial\beta_e}\left(\frac{I_0(\beta_e r)}{I_0(\beta_e a)}\right) + O\left(\frac{\Delta}{\beta_e}\right)^2\right\} \\
\frac{v_{rp_I}^{(1)} + v_{rp_I}^{(2)}}{u_0} &= -\frac{\alpha M}{2j}\left(\frac{\Delta}{\beta_e}\right)^2\left\{\beta_e \frac{\partial}{\partial\beta_e}\left(\frac{I_1(\beta_e r)}{I_0(\beta_e a)}\right) + O\left(\frac{\Delta}{\beta_e}\right)^2\right\} \\
\frac{v_{rp_I}^{(1)} - v_{rp_I}^{(2)}}{u_0} &= \frac{\alpha M}{2j}\left(\frac{h}{\beta_e}\right)\left\{\frac{I_1(\beta_e r)}{I_0(\beta_e a)} + O\left(\frac{\Delta}{\beta_e}\right)^2\right\} .
\end{aligned}\right\} \quad (3.122)$$

Appendix B contains the derivation of the total volume current. The results are presented below. The electron beam volume current, at $z = L$ (output gap), is given by

$$\frac{I_{vb}}{I_0} = \frac{\alpha M^2}{2}\left\{j\left(\frac{\beta_e}{h}\right)\sin(hL) + \left[e^{-j\frac{\delta}{2}L} \cdot \cos(hL) - \cos(hL)\right] \cdot \frac{2I_1(\beta_e a)}{(\beta_e a)I_0(\beta_e a)} + \ldots\right\}$$

(3.123)

Figure (4) is a plot of $2I_1(\beta_e a)/(\beta_e a)I_0(\beta_e a)$ versus $(\beta_e a)$, taken from Feenberg's work.[6]

The plasma volume current at a distance z from the input gap is given by the following expression:

$$\frac{I_{rp}}{I_0} = \frac{-\alpha M^2}{2}\left(\frac{\omega_{pp}}{\omega_{pb}}\right)^2 \left\{ \frac{h}{\beta_e}\left(1 - \frac{2I_1(\beta_e a)}{(\beta_e a)I_0(\beta_e a)}\right).\cos(hz) - j\left(\frac{\Delta}{\beta_e}\right) \right.$$

$$\left. e^{-j\frac{\delta}{2}z} \cdot \frac{2I_1(\beta_e a)}{(\beta_e a)I_0(\beta_e a)} \sin(\Delta z) + \ldots \right\} . \qquad (3.124)$$

It may be seen from the above expression that the amplitude of the volume plasma current is considerably larger than the beam current, due to the presence of the factor $(\omega_{pp}/\omega_{pb})^2 \gg 1$. The surface currents are calculated in Appendix C. The total surface current at $z = L$ (output gap) turns out to be given by the expression

$$\frac{I_{sb}}{I_0} = \frac{\alpha M^2}{2}\left\{ j\beta_e \cdot \frac{2I_1(\beta_e a)}{(\beta_e a)I_0(\beta_e a)} \cdot \left[\frac{\sin(\Delta L)}{\Delta} e^{-j\frac{\delta}{2}L} - \frac{\sin(hL)}{h}\right] \right.$$

$$\left. + \frac{\partial}{\partial\beta_e}\left(\frac{2I_1(\beta_e a)}{I_0(\beta_e a)}\right)\left[\left(\frac{\Delta}{h}\right)^2 \cdot \left(\cos(hL) - 1\right) + \left(1 - e^{-j\frac{\delta}{2}L}\cos\Delta L\right)\right] \right\} + \ldots \qquad (3.125)$$

Finally the total current, at the output grids $(z = L)$, will be given by

$$\frac{I}{I_0} = \frac{I_{vb}}{I_0} + \frac{I_{sb}}{I_0} = \frac{\alpha M^2}{2}\left\{ j\beta_e e^{-j\frac{\delta}{2}L} \frac{\sin(\Delta L)}{\Delta} \cdot \frac{2I_1(\beta_e a)}{(\beta_e a)I_0(\beta_e a)} \right.$$

$$+ j\beta_e \frac{\sin(hL)}{h}\left[1 - \frac{2I_1(\beta_e a)}{(\beta_e a)I_0(\beta_e a)}\right] + \left[e^{-j\frac{\delta}{2}L}\cos(\Delta L) - \cos(hL)\right]$$

$$\left. \cdot \frac{2I_1(\beta_e a)}{(\beta_e a)I_0(\beta_e a)} + \ldots \right\} . \qquad (3.126)$$

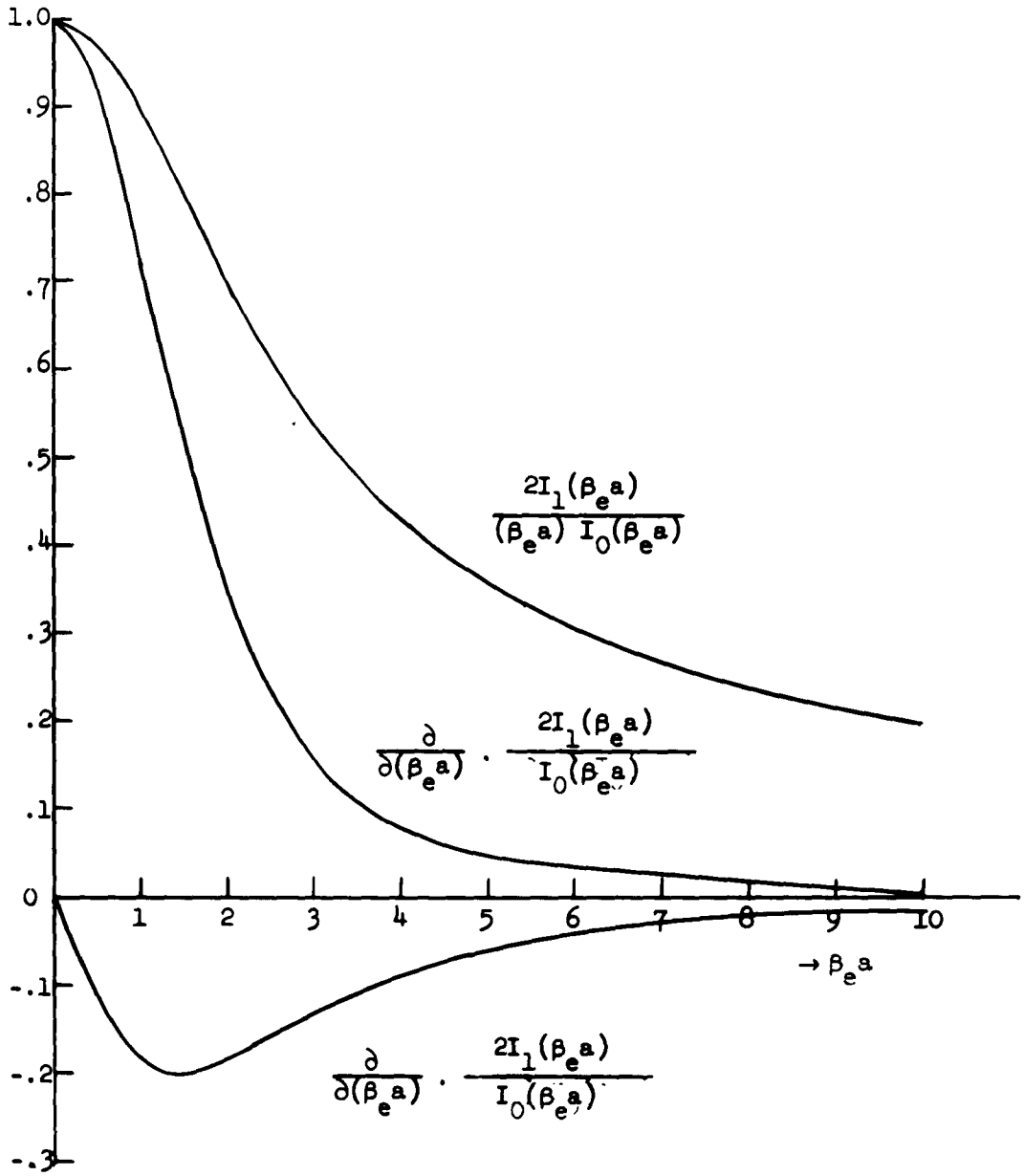

Fig. 4--Coefficients which appear in the expression for the rf current, as a function of $(\beta_e a)$ (Feenberg).

This equation constitutes the formal solution to the problem of finding the driving current at the output grids. For large values of $\beta_e a (\beta_e a > \infty)$ this equation is reduced to the expression for the total current corresponding to the infinite cross-section plasma-electron beam, which is

$$\left(\frac{I}{I_0}\right)_{\beta_e a \to \infty} = \frac{\alpha M^2}{2} \cdot j\beta_e \frac{\sin(hL)}{h} e^{j(\omega t - \beta_e z)} . \qquad (3.127)$$

As pointed out by Feenberg, it may be seen, from the expressions for the volume and surface currents, respectively, and with the aid of Figs. (2) and (4), that the first term in Eq. (3.126) may exceed the second by a factor of ten. The total surface current may then contribute significantly to the total current in the output gap. However, it will be shown in the following sections that, when $\omega < \omega_{pp}$ and growing waves are then present in the system, the rates of growth of the waves--having volume current (nonsolenoidal)--are larger than the growth rates of the solenoidal waves.

3.10 GROWING WAVE CASE

For the case in which the beam modulation frequency is below the plasma frequency of the plasma, it was shown that the propagation constants become complex, indicating a growth in amplitude for the space-charge waves.

We have, for $\omega < \omega_{pp}$,

$$\beta_{1,2} = \beta_e \pm j \frac{\beta_{pb}}{\sqrt{\frac{\omega_{pp}^2}{\omega^2} - 1}} = \beta_e \pm jh'$$

and (3.128)

$$\beta_{3,4} = \beta_e \pm j \frac{F\beta_{pb}}{\sqrt{\frac{\omega_{pp}^2}{\omega^2} - 1}} = \beta_e \pm j\Delta' .$$

If we again confine ourselves to the range of validity of the inequalities

$$\frac{h'}{\beta_e} < 1 \quad , \quad \frac{\Delta'}{\beta_e} < 1 \quad ,$$

the analysis made in the preceding section holds. The potential solutions in region II outside the beam are then given only by the solenoidal components:

$$V_{II}(r,z) = \left(V_{II}^{(3)}(r) e^{-j\Delta' z} + V_{II}^{(4)}(r) \cdot e^{j\Delta' z} \right) \cdot e^{j(\omega t - \beta_e z)}$$

where, from Eqs. (3.101) and (3.109), we have

$$V_{II}^{(3)}(r) = -j \frac{\alpha h' M V_0}{\beta_e \left(\frac{1}{F_3} + \frac{1}{F_4} \right)} \cdot \frac{I_0(\beta_3 r)K_0(\beta_3 b) - I_0(\beta_3 b)K_0(\beta_3 r)}{I_0(\beta_3 a)K_0(\beta_3 b) - I_0(\beta_3 b)K_0(\beta_3 a)} \quad ,$$

and

$$V_{II}^{(4)}(r) = j \frac{\alpha h' M V_0}{\beta_e \left(\frac{1}{F_3} + \frac{1}{F_4} \right)} \cdot \frac{I_0(\beta_4 r)K_0(\beta_4 b) - I_0(\beta_4 b)K_0(\beta_4 r)}{I_0(\beta_4 a)K_0(\beta_4 b) - I_0(\beta_4 b)K_0(\beta_4 a)} \quad . \tag{3.129}$$

The arguments of the modified Bessel functions in the above expressions are complex quantities.

The particular case for which $\omega = \omega_{pp}$ corresponds to a rather peculiar situation at which the above analysis does not hold. The fields in the plasma region outside the beam do not satisfy Eq. (3.45). This means that the expressions for the electric potentials in this region as given by Eqs. (3.129) are no longer true, since they are not derivable from Laplace's equation.

Moreover, at $\omega = \omega_{pp}$ the condition for the fields on the boundaries of the electron beam, as expressed by Eq. (3.52), breaks down; the matching problem becomes unspecified.

These objections may be somewhat academic since the whole theory is based on a mathematical model of surface currents which would not apply if infinities occur in the equation. More serious however is the situation for ω near ω_{pp} when quantities become large even though not infinite and the approximation $h/\beta_e < 1$ seems invalid. In this case, which is discussed in more detail in the next chapter, it can be shown that thermal velocities in the plasma modify the theory in such a way that the approximation $h/\beta_e < 1$ is still valid.

3.11 CONCLUSIONS

It is of value to summarize the results of this chapter for the finite electron beam. For the general case of an electron beam going through a plasma with no magnetic field, the space-charge waves are of two kinds. One set is called the solenoidal; it has no space-charge density within the volume of the beam but does have a rippled beam surface which constitutes a surface current. The other set is called nonsolenoidal; these solutions have both a volume charge density and a surface ripple. The second set is characterized by having no electric field exterior to the electron beam, and the charge distribution in the interior may have an arbitrary dependence on the transverse co-ordinates. All these results are entirely analogous to results obtained for an electron beam in the absence of a plasma (and no magnetic field). The major difference, if a plasma is present, is that all the propagation constants are modified by the equivalent dielectric constant representing the characteristics of the plasma. The most significant result is that, at frequencies below ω_{pp}, the space-charge waves which can exist are growing waves. This is true of both the solenoidal and nonsolenoidal waves. With grid modulation, both kinds of waves are excited, will exist in the beam, and will contribute to the current in the electron beam at the output gap. This is contrary to the case of a gridless gap where only the solenoidal solutions are produced. Another significant result of this calculation is that the growing waves excited by grid modulation which are nonsolenoidal have a greater growth rate than the solenoidal waves and therefore in any amplification process will predominate.

CHAPTER IV

HARMONIC GENERATION IN A VELOCITY-MODULATED ELECTRON BEAM IN A PLASMA MEDIUM

4.1 INTRODUCTION

In this chapter we shall use the Eulerian approach to derive the nonlinear space-charge wave equation for the second harmonic field component. The solution of this nonlinear differential equation is obtained and conditions for second harmonic growing waves are investigated. General expressions for the second harmonic quantities are derived, and some of the implications of the resultant formulas are discussed.

Paschke[12] developed a nonlinear space-charge wave theory for the special case of a drifting velocity-modulated beam. This theory was approached by successive perturbations, beginning with the linearized solution.

The purpose of this chapter is, by using Paschke's technique, to derive solutions for the infinite beam drifting in an infinite cross-section plasma. Unfortunately, this method of successive approximations became extremely lengthy, for higher harmonics, so that we shall restrict ourselves to second harmonics.

The analysis which follows is based essentially on the following assumptions:

a. An input signal of low power modulates the beam. The beam electron velocities as well as the plasma electron velocities remain single-valued, i.e., no overtaking of beam or plasma electrons occurs.

b. Infinite magnetic field is applied along the direction of motion of the electrons, which is taken as the z-axis. Therefore, there is no transverse motion of electrons.

c. The velocity-modulated electron beam is of infinite extent and has a dc velocity along z.

d. The plasma ions are stationary, i.e., are of infinite mass. Thermal motions and collision effects are neglected.

We assume also that all ac quantities vary as

$$\phi(z,t) = \sum_{n=1}^{\infty} \phi_n(h_n z) e^{nj(\omega t - \beta_e z)} , \qquad (4.1)$$

where $\beta_e \triangleq \omega/\mu_0$ is the beam electronic wave number and h_n denotes the electron beam-plasma wave number characteristic of the n^{th} harmonic.

We shall consider, in the above equation, the case where the fundamental and the second harmonic components ($n = 1,2$, respectively) are the relevant ones, and thus neglect the contributions from the higher harmonics. We may, therefore, write

$$\phi(z,t) = \phi_1(h_1 z)e^{j(\omega t-\beta_e z)} + \phi_2(h_2 z)e^{2j(\omega t-\beta_e z)} ,$$

where $h_1 \triangleq \omega_{pb}/\mu_0\sqrt{\epsilon_1}$ and $\epsilon_1 \triangleq 1 - \omega_{pp}^2/\omega^2$, are defined for the first order variables ($n = 1$), and

$$h_2 \triangleq \frac{\omega_{pb}}{\mu_0\sqrt{\epsilon_2}} , \qquad \epsilon_2 = 1 - \frac{\omega_{pp}^2}{(2\omega)^2} \tag{4.2}$$

are related to the second order components ($n = 2$). The corresponding complex conjugate of $\phi(z,t)$ is written

$$\phi^*(z,t) = \phi_1^*(h_1 z)e^{-j(\omega t-\beta_e z)} + \phi_2^*(h_2 z)e^{-2j(\omega t-\beta_e z)} , \tag{4.3}$$

and we shall denote, for convenience, the sum and the difference of ϕ with its complex conjugate ϕ^*, respectively, by the superscripts (+) and (-).

4.2 LINEARIZED THEORY; FUNDAMENTAL COMPONENTS

By means of Eq. (4.1), the first order ac variables are first of all defined. The second order variables are assumed negligible. Linearized equations will result and the well known results of the linear space-charge wave theory are obtained. For the sake of completeness, we shall derive in this section the second order differential equation for the fundamental component of the electric field. In the following section the second harmonic components are considered:

a. Continuity equation applied to the electron beam:

$$\frac{\partial}{\partial z} i_{b_1}^+ = -\frac{\partial}{\partial t} \rho_{b_1}^+ , \tag{4.4}$$

where the linearized beam current density is defined as

$$i_{b_1}^{+} = u_0 \rho_{b_1}^{+} + \rho_{0b} v_{b_1}^{+} \quad . \tag{4.5}$$

b. Force equation applied to the electron beam:

$$\frac{\partial}{\partial t} v_{b_1}^{+} + u_0 \frac{\partial}{\partial_z} v_{b_1}^{+} = \frac{\omega_{pb}^{2}}{\rho_{0b}} D_1^{+} \quad , \tag{4.6}$$

where

$$D_1^{+} = \epsilon_0 E_1^{+} \quad .$$

c. The corresponding equations for the plasma electrons are, respectively,

$$\frac{\partial}{\partial z} i_{p_1}^{+} = - \frac{\partial}{\partial t} \rho_{p_1}^{+} \tag{4.7}$$

where the linearized plasma current density is defined as

$$i_{p_1}^{+} = \rho_{0p} v_{p_1}^{+} \quad , \tag{4.8}$$

and

$$\frac{\partial}{\partial t} v_{p_1}^{+} = \frac{\omega_{pp}^{2}}{\rho_{0p}} D_1^{+} \quad . \tag{4.9}$$

Poisson's equation reads

$$\frac{\partial}{\partial z} D_1^{+} = \rho_{b_1}^{+} + \rho_{p_1}^{+} \quad . \tag{4.10}$$

The velocity of the plasma electrons is obtained from Eq. (4.9) as

$$v_{p_1}^{+} = - j \frac{\omega_{pp}^{2}}{\omega \rho_{0p}} D_1^{-} \quad . \tag{4.11}$$

The plasma current density is, therefore, by using Eq. (4.8),

$$i_{p_1}^{+} = - j \frac{\omega_{pp}^{2}}{\omega} D_1^{-} \quad . \tag{4.12}$$

With Eqs. (4.7) and (4.10) combined together, the result is

$$\frac{\partial^2}{\partial t \partial z} D_1^{+} + \frac{\partial}{\partial z} i_{p_1}^{+} = \frac{\partial}{\partial t} \rho_{b_1}^{+} \quad ,$$

from which, after replacing $\partial/\partial t$ by $j\omega$, we obtain the following expression for the electron beam charge density in terms of the electric field:

$$\rho_{b_1}^{+} = \epsilon_1 \frac{\partial}{\partial z} D_1^{+} \quad . \tag{4.13}$$

The plasma charge density is found from Poisson's equation and the above equation for $\rho_{b_1}^{+}$ to be

$$\rho_{p_1}^{+} = (1 - \epsilon_1) \frac{\partial}{\partial z} D_1^{+} \quad . \tag{4.14}$$

The continuity equation for the electron beam, together with Eq. (4.13), yields

$$\frac{\partial}{\partial z} v_{b_1}^{+} = - j \frac{\omega \epsilon_1}{\rho_{0b}} \cdot \frac{\partial}{\partial z} D_1^{-} - \frac{u_0 \epsilon_1}{\rho_{0b}} \cdot \frac{\partial^2}{\partial z^2} D_1^{+} \quad ,$$

which is substituted into the equation of motion, to give the beam ac velocity in terms of the field:

$$v_{b_1}^{+} = - j \frac{\epsilon_1 u_0^{2}}{\omega \rho_{0b}} \cdot \frac{\partial^2}{\partial z^2} D_1^{-} + \frac{\epsilon_1 u_0}{\rho_{0b}} \frac{\partial}{\partial z} D_1^{+} - j \frac{\omega_{pb}^{2}}{\omega \rho_{0b}} D_1^{-} \quad . \tag{4.15}$$

With the help of Eqs. (4.13) and (4.15), the electron beam current density is seen to be

$$i_{b_1}^{+} = - j \frac{\epsilon_1 u_0^2}{\omega} \cdot \frac{\partial^2}{\partial z^2} D_1^{-} + 2u_0 \epsilon_1 \frac{\partial}{\partial z} D_1^{+} - j \frac{\omega_{pb}^2}{\omega} D_1^{-} \quad . \tag{4.16}$$

It is known, however, that in this one-dimensional problem the total current (convection plus displacement current) must be zero:

$$i_{b_1}^{+} + i_{p_1}^{+} = - \frac{\partial D_1^{+}}{\partial t} = - j\omega D_1^{-} \quad . \tag{4.17}$$

It follows, then, from Eqs. (4.16), (4.17) and (4.12) that

$$\frac{\partial^2 D_1^{-}}{\partial z^2} + \frac{2}{u_0} \cdot \frac{\partial^2}{\partial t \partial z} D_1^{-} + (h_1^2 - \beta_e^2) D_1^{-} = 0 \quad . \tag{4.18}$$

The solution of the homogeneous differential equation corresponding to the case of an infinite beam in a drift space has been derived by several authors (see, for example, A. H. W. Beck[13]). For the electron beam in a plasma, the solution of the differential equation (4.18) which corresponds to the pair of space-charge waves with propagation constants $\beta = \beta_e \pm h_1$, is

$$D_1 = \epsilon_0 E_1 = \frac{\epsilon_0 u_0^2 h_1}{\eta} \left\{ j \frac{\omega_{pb}}{\omega} \cdot \frac{i_{b_1}(0)}{i_0} \cdot \cos h_1 z + \frac{v_{b_1}(0)}{u_0} \cdot \sin h_1 z \right\} e^{j(\omega t - \beta_e z)} , \tag{4.19}$$

where $\eta \triangleq e/m$, and $i_{b_1}(0)$ and $V_{b_1}(0)$ are, respectively, the beam current density and the beam velocity, at the input gridded gap $(z = 0)$.

The electron beam velocity and current density may be shown to be, respectively,

$$v_{b_1} = u_0 \cdot \left\{ \frac{v_{b_1}(0)}{u_0} \cdot \cos h_1 z - j \frac{\omega_{pb}}{\omega\sqrt{\epsilon_1}} \left(\frac{i_{b_1}(0)}{i_0} \right) \cdot \sin h_1 z \right\} e^{j(\omega t - \beta_e z)} , \quad (4.20)$$

$$i_{b_1} = i_0 \cdot \left\{ \frac{i_{b_1}(0)}{i_0} \cdot \cos h_1 z - j \frac{\omega\sqrt{\epsilon_1}}{\omega_{pb}} \sin h_1 z \right\} e^{j(\omega t - \beta_e z)} . \quad (4.21)$$

The boundary conditions to be satisfied at the input gap are

$$\begin{aligned} i_{b_1}(0) &= 0 \\ v_{b_1}(0) &= v_1 = u_0 \alpha \frac{M}{2} \\ D_1(0) &= 0 \end{aligned} , \quad (4.22)$$

where $\alpha \triangleq V_1/V_0$ is the depth of modulation, and M denotes the gap coupling coefficient.

Under these boundary conditions the expression for D_1 is reduced to

$$D_1(z,t) = \frac{i_0}{\omega_{pb}\sqrt{\epsilon_1}} \left(\frac{\alpha M}{2} \right) \cdot \sin h_1 z \cdot e^{j(\omega t - \beta_e z)} ,$$

from which we have

$$D_1^+(z,t) = D_1 + D_1^* = \frac{2 i_0}{\omega_{pb}\sqrt{\epsilon_1}} \left(\frac{\alpha M}{2} \right) \cdot \sin h_1 z \cdot \cos(\omega t - \beta_e z)$$

and (4.23)

$$D_1^-(z,t) = D_1 - D_1^* = 2j \frac{i_0}{\omega_{pb}\sqrt{\epsilon_1}} \left(\frac{\alpha M}{2} \right) \cdot \sin h_1 z \cdot \sin(\omega t - \beta_e z) .$$

The electron beam velocity and current density become, respectively,

$$v_{b_1} = u_0 \frac{\alpha M}{2} \cdot \cos h_1 z \cdot e^{j(\omega t - \beta_e z)} \tag{4.24}$$

and

$$i_{b_1} = j \frac{\omega i_0 \sqrt{\epsilon_1}}{\omega_{pb}} \left(\frac{\alpha M}{2} \right) \sin h_1 z \cdot e^{j(\omega t - \beta_e z)} \quad . \tag{4.25}$$

4.3 FIELD SOLUTIONS FOR THE SECOND HARMONIC COMPONENTS; GROWING WAVE SOLUTIONS

In this section, we shall include the second order terms, in the form of Eq. (4.1), in the expressions for the ac quantities.

These second order variables are solved in terms of the fundamental components which were determined in the previous section.

We start by defining the second harmonic components of the electron beam and plasma current densities, which are, respectively,

$$i^+_{b_2} = u_0 \rho^+_{b_2} + \rho_{0b} v^+_{b_2} + \frac{1}{2} \rho^+_{b_1} v^+_{b_1} \quad , \tag{4.26}$$

and

$$i^+_{p_2} = \rho_{0p} v^+_{p_2} + \frac{1}{2} \rho^+_{p_1} v^+_{p_1} \quad . \tag{4.27}$$

For the electron beam, the continuity and force equations are, respectively,

$$\frac{\partial}{\partial z} i^+_{b_2} = - \frac{\partial}{\partial t} \rho^+_{b_2} \tag{4.28}$$

and

$$\frac{\partial}{\partial t} v^+_{b_2} + u_0 \frac{\partial}{\partial z} v^+_{b_2} + \frac{1}{2} v^+_{b_1} \cdot \frac{\partial}{\partial z} v^+_{b_1} = \frac{\omega_{pb}^2}{\rho_{0b}} D^+_2 \quad . \tag{4.29}$$

The corresponding equations for the plasma electrons are

$$\frac{\partial}{\partial z} i^+_{p_2} = - \frac{\partial}{\partial t} \rho^+_{p_2} \quad , \tag{4.30}$$

and

$$\frac{\partial}{\partial t} v_{p_2}^{+} + \frac{1}{2} v_{p_1}^{+} \cdot \frac{\partial}{\partial z} v_{p_1}^{+} = \frac{\omega_{pp}^{2}}{\rho_{0p}} D_2^{+} \quad . \tag{4.31}$$

Poisson's Equation applied for the second harmonic components is

$$\frac{\partial}{\partial z} D_2^{+} = \rho_{b_2}^{+} + \rho_{p_2}^{+} \quad . \tag{4.32}$$

Take the partial time derivative of the above equation and use Eq. (4.30) to obtain

$$\frac{\partial}{\partial t} \rho_{b_2}^{+} = \frac{\partial}{\partial z} \cdot \left(\frac{\partial}{\partial t} D_2^{+} + \rho_{0p} v_{p_2}^{+} + \frac{1}{2} \rho_{p_1}^{+} v_{p_1}^{+} \right) \quad . \tag{4.33}$$

After eliminating $v_{p_2}^{+}$ from Eqs. (4.31) and (4.33) we find that

$$\rho_{b_2}^{+} = \epsilon_2 \cdot \frac{\partial}{\partial z} D_2^{+} - \frac{1}{4\omega^2} \cdot \frac{\partial}{\partial z} \left[\frac{\partial}{\partial t} \left(\frac{1}{2} \rho_{p_1}^{+} v_{p_1}^{+} \right) - \frac{\rho_{0p}}{2} v_{p_1}^{+} \frac{\partial}{\partial z} v_{p_1}^{+} \right] \quad . \tag{4.34}$$

The continuity equation and equation of motion for the electron beam are combined together with the partial time derivative of Eq. (4.26) to obtain the result

$$\frac{\partial}{\partial t} i_{b_2}^{+} = \omega_{pb}^{2} D_2^{+} + u_0 \; 2 \frac{\partial}{\partial t} + u_0 \frac{\partial}{\partial z} \; \rho_{b_2}^{+}$$

$$+ \left(\frac{\partial}{\partial t} + u_0 \frac{\partial}{\partial z} \right) \left(\frac{1}{2} \rho_{b_1}^{+} v_{b_1}^{+} \right) - \frac{\rho_{0b}}{2} v_{b_1}^{+} \cdot \frac{\partial}{\partial z} v_{b_1}^{+} \quad , \tag{4.35}$$

which, for convenience, is written in the following form:

$$\frac{\partial}{\partial t} i_{b_2}^{+} = \left(\frac{\partial}{\partial t} i_{b_2}^{+} \right)_{(I)} + \left(\frac{\partial}{\partial t} i_{b_2}^{+} \right)_{(II)} \quad ,$$

where

$$\left(\frac{\partial}{\partial t}\, i^{+}_{b_2}\right)_{(I)} = \left(\frac{\partial}{\partial t} + u_0 \frac{\partial}{\partial z}\right)\left(\frac{1}{2}\, \rho^{+}_{b_1} v^{+}_{b_1}\right) - \frac{\rho_{0b}}{2}\, v^{+}_{b_1} \frac{\partial}{\partial z}\, v^{+}_{b_1}$$

and

$$\left(\frac{\partial}{\partial t}\, i^{+}_{b_2}\right)_{(II)} = \omega^2_{pb}\, D^{+}_2 + u_0 \left(2\, \frac{\partial}{\partial t} + u_0 \frac{\partial}{\partial z}\right) \cdot \rho^{+}_{b_2} \quad .$$

It is shown in Appendix D that

$$\left(\frac{\partial}{\partial t}\, i^{+}_{b_2}\right)_{(I)} = -\frac{\epsilon_1{}^2 u_0{}^2}{\rho_{0b}} \Bigg\{ -\frac{3}{2}\, h_1{}^2 D^{+}_i \frac{\partial D^{+}_1}{\partial z} + j\beta_e \left(D^{-}_1 \frac{\partial^2 D^{+}_1}{\partial z^2} - \frac{\partial D^{-}_1}{\partial z} \frac{\partial D^{+}_1}{\partial z}\right) + \beta_e{}^2 \left(D^{+}_1 \frac{\partial D^{+}_1}{\partial z} - D^{-}_1 \frac{\partial D^{-}_1}{\partial z}\right) \Bigg\} \quad , (4.36)$$

and

$$\left(\frac{\partial}{\partial t}\, i^{+}_{b_2}\right)_{(II)} = \omega^2_{pb} D^{+}_2 + u_0 \epsilon_2 \frac{\partial}{\partial z} \cdot \left(\frac{\partial}{\partial t} + u_0 \frac{\partial}{\partial z}\right) D^{+}_2$$

$$- \left(\frac{\omega_{pp}}{\omega}\right)^4 \frac{u_0{}^2}{4\rho_{0p}} \Bigg\{ j\beta_e \left[-3\, \frac{\partial D^{+}_1}{\partial z} \frac{\partial D^{-}_1}{\partial z} + 2 D^{+}_1 \frac{\partial^2 D^{-}_1}{\partial z^2} + D^{-}_1 \frac{\partial^2 D^{+}_1}{\partial z^2} \right]$$

$$+ 2(\beta_e{}^2 - h_1{}^2) \left(D^{+}_1 \frac{\partial D^{-}_1}{\partial z} + 2 D^{-}_1 \frac{\partial D^{-}_1}{\partial z} \right) \Bigg\} \quad . \qquad (4.37)$$

We know also from Eq. (4.27) that

$$\frac{\partial}{\partial t}\, i^{+}_{p_2} = \rho_{0p} \frac{\partial}{\partial t}\, v^{+}_{p_2} + \frac{\partial}{\partial t} \left(\frac{1}{2}\, \rho^{+}_{p_1} v^{+}_{p_1}\right) \quad , \qquad (4.38)$$

where from Eq. (4.31) we have

$$\rho_{0p} \frac{\partial}{\partial} v^{+}_{p_2} = \omega^2_{pp} D^{+}_2 + \frac{\omega^4_{pp}}{2\omega^2 \rho_{0p}} D^{-}_1 \frac{\partial}{\partial z} D^{-}_1 \quad . \tag{4.39}$$

Together Eqs. (4.14) and (4.11) yield the expression

$$\frac{\partial}{\partial} \left(\frac{1}{2} \rho^{+}_{p_1} v^{+}_{p_1} \right) = \frac{\omega^4_{pp}}{2\omega^2 \rho_{0p}} \left(D^{+}_1 \frac{\partial}{\partial z} D^{+}_1 + D^{-}_1 \frac{\partial}{\partial z} D^{-}_1 \right) \quad . \tag{4.40}$$

By substituting Eqs. (4.39) and (4.40) into (4.38) we find that

$$\frac{\partial}{\partial} i^{+}_{p_2} = \omega^2_{pp} D^{+}_2 + \frac{\omega^4_{pp}}{2\rho_{0p}\omega^2} \left(D^{+}_1 \frac{\partial}{\partial z} D^{+}_1 + 2D^{-}_1 \frac{\partial}{\partial z} D^{-}_1 \right) \quad . \tag{4.41}$$

From the condition that the total second harmonic current (convection and displacement current) is zero, it follows that

$$\frac{1}{u_0^2} \frac{\partial}{\partial} \left(i^{+}_{b_2} + i^{+}_{p_2} \right) = 4\beta_e^2 D^{+}_2 \quad . \tag{4.42}$$

Substituting in the above expression the expressions derived before for $(\partial/\partial t) i^{+}_{b_2}$ [Eqs. (4.36) and (4.37)] and for $(\partial/\partial t) i^{+}_{p_2}$ [Eq. (4.41)], we obtain the following inhomogeneous differential equation for the second harmonic electric field:

$$\begin{aligned} \frac{\partial^2 D^{+}_2}{\partial z^2} + \frac{2}{u_0} \frac{\partial^2}{\partial t \partial z} D^{+}_2 + (h_2^2 - 4\beta_e^2) D^{+}_2 = & -\frac{3}{2} \frac{\omega^2_{pb}}{i_0 u_0} \left(\frac{\epsilon_1}{\epsilon_2} \right) (1 + \tfrac{\mu}{3}) D^{+}_1 \frac{\partial}{\partial z} D^{+}_1 \\ & + \frac{\omega^2 \epsilon_1^2}{i_0 u_0 \epsilon_2} \left(D^{+}_1 \frac{\partial}{\partial z} D^{+}_1 - D^{-}_1 \frac{\partial}{\partial z} D^{-}_1 \right) - \frac{\omega^2_{pb}}{2 i_0 u_0} \left(\frac{\epsilon_1}{\epsilon_2} \right) \mu \cdot D^{-}_1 \frac{\partial}{\partial z} D^{-}_1 \\ & + j \frac{\omega \epsilon_1^2}{i_0 \epsilon_2} (1 + \tfrac{\mu}{4}) \left(D^{-}_1 \frac{\partial^2 D^{+}_1}{\partial z^2} - \frac{\partial D^{-}_1}{\partial z} \cdot \frac{\partial D^{+}_1}{\partial z} \right) + j \frac{\omega \epsilon_1^2}{i_0 \epsilon_2} \left(\frac{\mu}{2} \right) \left(D^{+}_1 \frac{\partial^2 D^{-}_1}{\partial z^2} - \frac{\partial D^{-}_1}{\partial z} \frac{\partial D^{+}_1}{\partial z} \right) , \end{aligned} \tag{4.43}$$

where the parameter μ is defined to be

$$\mu \triangleq \frac{\omega_{pp}^2 \omega_{pb}^2}{\omega^4 \cdot \epsilon_1^2} \quad . \tag{4.44}$$

For the case in which there is no plasma ($\omega_{pp} = 0$, $\epsilon_1 = 1$, $\mu = 0$) the inhomogeneous term is simplified, and we have instead of Eq. (4.43) the following differential equation:

$$\frac{\partial^2 D_2^+}{\partial z^2} + \frac{2}{u_0} \frac{\partial^2 D_2^+}{\partial t \partial z} + (\beta_{pb}^2 - 4\beta_e^2) D_2^+ = - \frac{3\omega_{pb}^2}{2i_0 u_0} D_1^+ \cdot \frac{\partial D_1^+}{\partial z}$$

$$+ \frac{\omega^2}{i_0 u_0} \left(D_1^+ \frac{\partial D_1^+}{\partial z} - D_1^- \frac{\partial D_1^-}{\partial z} \right) + j \frac{\omega}{i_0} \left(D_1^- \frac{\partial^2 D_1^+}{\partial z^2} - \frac{\partial D_1^+}{\partial z} \cdot \frac{\partial D_1^-}{\partial z} \right) \quad , \tag{4.45}$$

which is the differential equation obtained by Paschke.[12]

The nonlinear equation [Eq. (4.43)] can now be solved for the second harmonic field by substituting the solutions for the first-order terms into its right-hand side. To solve this inhomogeneous differential equation, we write first the solution of the associated homogeneous equation:

$$D_2^+(z,t) = \left(A_2 e^{jh_2 z} + B_2 e^{-jh_2 z} \right) e^{2j(\omega t - \beta_e z)}$$

$$+ \left(A_2^* e^{-jh_2 z} + B_2^* e^{jh_2 z} \right) \cdot e^{-2j(\omega t - \beta_e z)} \quad .$$

The solution of Eq. (4.43) is then given by the above complementary function added to a particular integral. Appendix E contains the derivation of this particular solution to Eq. (4.43).

With the condition that, at $z = 0$, there is no second harmonic component of the electric field, the following expression is obtained for $D_2^+(z,t)$:

$$D_2^+(z,t) = \frac{i_0\omega}{2\omega_{pb}^2}\left(\frac{\alpha M}{2}\right)^2 \cdot \left\{\left[(1+\mu) - \frac{3(1+\frac{2\mu}{3})}{4\xi^2-1}\cdot\cos 2h_1 z + \frac{4(1-\xi^2)+\mu(3-4\xi^2)}{4\xi^2-1}\cos h_2 z\right]\cdot \sin 2(\omega t-\beta_e z) + 3\left(\frac{h_1}{\beta_e}\right)\frac{(1+\frac{2\mu}{3})}{4\xi^2-1}\sin h_2 z\cdot\cos 2(\omega t-\beta_e z)\right\} \quad , \tag{4.46}$$

where

$$\xi \triangleq \frac{h_1}{h_2} = \sqrt{\frac{\epsilon_2}{\epsilon_1}} \quad .$$

This equation can be conveniently expressed in terms of ϵ_1 instead of the dimensionless parameter ξ , with the help of the following relations:

$$\epsilon_1 = \frac{3}{4\xi^2-1} \quad ; \quad \epsilon_1 - 1 = \frac{4(1-\xi^2)}{4\xi^2-1} \quad . \tag{4.47}$$

The result is

$$E_2(z,t) = \frac{i_0\omega}{\epsilon_0\omega_{pb}^2}\left(\frac{\alpha M}{4}\right)^2 \left\{\left[(1+\mu) - \epsilon_1(1+\frac{2\mu}{3})\cos\frac{2\beta_{pb}}{\sqrt{\epsilon_1}}z - \left(1+\mu-\epsilon_1(1+\frac{2\mu}{3})\right)\cdot\cos\frac{\beta_{pb}}{\sqrt{\epsilon_2}}z\right]\sin 2(\omega t-\beta_e z)\right\} \quad , \tag{4.48}$$

where the term proportional to h_1/β_e was neglected, under the assumption that $h_1/\beta_e < 1$.

The definitions of ϵ_1 and ϵ_2 have been given before and are repeated here for convenience:

$$\epsilon_1 = 1 - \frac{\omega_{pp}^2}{\omega^2} \quad , \qquad \epsilon_2 = 1 - \frac{\omega_{pp}^2}{(2\omega)^2} \quad . \tag{4.49}$$

These expressions can be considered as expressions for the dielectric constants exhibited by the plasma, at excitation frequencies ω and 2ω , respectively. Indeed, it can be shown that, for a infinite plasma, Maxwell's equations can be written in a similar form to that applicable in free space, but with a dielectric constant given by ϵ_1 or ϵ_2 , if we assume, respectively, time-dependence for the rf quantities of the form $e^{j\omega t}$ or $e^{2j\omega t}$.

The solution derived above for the second-harmonic fields presents some interesting features which will be the subject of discussion below. By comparing this equation with the corresponding solution derived by Paschke, in the absence of plasma, one can see that the presence of plasma introduces a significant change in the harmonic amplitudes.

The parameters μ and ξ which appear in Eq. (4.46) and which have been defined previously as being given respectively by

$$\mu = \frac{\omega_{pp}^2 \cdot \omega_{pb}^2}{\omega^4 \cdot \epsilon_1^2}$$

$$\xi = \sqrt{\frac{\epsilon_2}{\epsilon_1}} \quad ,$$

indicate the presence of plasma. The particular values $\mu = 0$, $\xi = 1$ express the absence of plasma in the drifting region of the infinite beam. In this case Paschke's results apply. When the electron beam is modulated at exactly the plasma frequency (i.e., $\omega = \omega_{pp}$) , then we find

$$\mu = \infty \quad , \quad \xi = \infty \quad .$$

The resonance at $\omega_{pp}/2$ is attained when $\xi = 0$ and $\mu = 4/3(\omega_{pp}^2) \cdot \omega_{pb}^2$.

Suppose now that the beam modulation frequency ω is gradually changed from the condition $\omega > \omega_{pp}$ to $\omega < \omega_{pp}/2$. We shall discuss the implications in the second harmonic equation, when we consider each one of the following conditions:

$$(i) \quad \omega > \omega_{pp}$$

$$(ii) \quad \omega_{pp} > \omega > \omega_{pp}/2$$

$$(iii) \quad \omega_{pp}/2 > \omega \quad .$$

Consider first (i); $\omega > \omega_{pp}$. In order to compare our expression for the second harmonic field with that of Paschke we write below the corresponding equation derived by Paschke for a velocity-modulated beam of finite size, with no plasma:

$$D_2 = -i_0 \frac{\omega}{\omega_{pb}^2 \cdot p^2(2\omega)} \left(\frac{\alpha M}{4}\right)^2 \left[1 - \frac{3}{4\xi^2 - 1} \cos 2\beta_{pb} p(\omega) z \right.$$

$$\left. + \frac{4(1 - \xi^2)}{4\xi^2 - 1} \cos \beta_{pb} p(2\omega) z \right] \cdot \sin 2(\omega t - \beta_e z) \quad , \qquad (4.50)$$

where, in this case, the dimensionless parameter ξ denotes the ratio between the plasma frequency reduction factors for the finite beam at the fundamental and second-harmonic components, respectively. That is, Paschke's parameter ξ is $\xi = p(\omega)/p(2\omega)$. If the following correspondences are then established,

$$p(\omega) \rightarrow \frac{1}{\sqrt{\epsilon_1}}$$

$$p(2\omega) \rightarrow \frac{1}{\sqrt{\epsilon_2}} \quad ,$$

we should have our case of an infinite beam in an infinite plasma, the parameter ξ being given by $\sqrt{\epsilon_2/\epsilon_1}$, as it had been defined before. It is evident that in the one-dimensional, no plasma case ($\omega_{pp} = 0$), we have $\xi = 1$, as stated previously.

Consider now case (ii); $\omega_{pp} > \omega > \omega_{pp}/2$. When the above condition is satisfied, it may be seen, from Eqs. (4.48) and (4.49) that ϵ_1 becomes negative and, consequently, the argument of the cosine function involving $\sqrt{\epsilon_1}$ becomes imaginary. A dependence on z by means of a hyperbolic cosine will result, and this means that a growth with distance occurs for the second harmonic fields.

The growth of the fundamental amplitude which exists for the condition $\omega < \omega_{pp}$, becomes, in this case, responsible for excitation of growing second harmonic fields. If the beam modulation frequency is reduced to a value such that $\omega_{pp}/2 > \omega$, not only is ϵ_1 a negative quantity but ϵ_2 also becomes negative.

It follows that both cosine functions in Eq. (4.48) become hyperbolic functions, thus indicating growth with distance. These increasing amplitudes of the second harmonic waves derive, in this case, from nonlinearity due to the growing fundamental waves $(\omega < \omega_{pp})$ and also from interaction with plasma at a subharmonic of the plasma frequency $(\omega_{pp}/2)$.

a. Second Harmonic Currents

To calculate the second harmonic plasma current density we use Eq. (4.41) to obtain

$$i_{p_2}^{+} = (\epsilon_2 - 1)\frac{\partial D_2^{+}}{\partial t} - \frac{3}{8}\frac{\mu\epsilon_1^{2}}{\rho_{0b}} \cdot \left(D_1^{-}\frac{\partial}{\partial z}D_1^{+} + D_1^{+}\frac{\partial}{\partial z}D_1^{-}\right) \quad , \quad (4.51)$$

which with the help of Eqs. (4.23) becomes

$$i_{p_2}^{+} = (\epsilon_2 - 1)\frac{\partial D_2^{+}}{\partial t} - \frac{3}{4}\frac{i_0}{\omega\epsilon_1}\left(\frac{\omega_{pp}}{\omega}\right)^2\left(\frac{\alpha M}{2}\right)^2$$

$$\cdot \left[2\sin^2 h_1 z \sin 2(\omega t - \beta_e z) + \left(\frac{h_1}{\beta_e}\right)\sin 2h_1 z \cdot \cos 2(\omega t - \beta_e z)\right] \quad . \quad (4.52)$$

The second harmonic electron beam current density is derived from the equation, $i_{b_2}^+ + i_{p_2}^+ = -\partial D_2^+/\partial t$, where use is made of the expression for the plasma current density [Eq. (4.52)]. By neglecting the term proportional to h_1/β_e , we have

$$i_{b_2}^+ = -\epsilon_2 \frac{\partial D_2^+}{\partial t} + \frac{3i_0}{2\omega\epsilon_1}\left(\frac{\omega_{pp}}{\omega}\right)^2\left(\frac{\alpha M}{2}\right)^2 \cdot \sin^2 h_1 z \cdot \sin 2(\omega t - \beta_e z) \quad , (4.53)$$

or, in a more explicit form, with the help of Eq. (4.46) we find

$$i_{b_2}^+ = -i_0 \frac{\omega^2}{\omega_{pb}^2} \cdot \epsilon_2 \left(\frac{\alpha M}{2}\right)^2 \cdot \left\{ 1 + \mu - \epsilon_1\left(1 + \frac{2\mu}{3}\right) \cos \frac{2\beta_{pb}}{\sqrt{\epsilon_1}} z \right.$$

$$\left. - \left(1 + \mu - \epsilon_1\left(1 + \frac{2\mu}{3}\right)\right) \cos \frac{\beta_{pb}}{\sqrt{\epsilon_2}} z \right\} \cdot \cos 2(\omega t - \beta_e z) \quad , \quad (4.54)$$

from which an expression for $\mathrm{Re}\left(i_{b_2}\right) = i_{b_2}^+/2$ could be easily written.

b. Second Harmonic Velocities

The electron beam second harmonic velocity, as derived from

$$v_{b_2}^+ = \frac{1}{\rho_{0b}}\left(i_{b_2}^+ - u_0\rho_{b_2}^+ - \frac{1}{2}v_{b_2}^+\rho_{b_1}^+\right) \quad ,$$

is given by the following expression (see Appendix F for details in the derivation):

$$v_{b_2}^+ = -2u_0 \frac{\omega\sqrt{\epsilon_2}}{\omega_{pb}}\left(\frac{\alpha M}{4}\right)^2 \cdot \left\{ \left[\frac{6\xi\left(1 + \frac{2\mu}{3}\right)}{4\xi^2 - 1} - \frac{1}{\xi}\right] \cdot \sin 2h_1 z \cdot \sin 2(\omega t - \beta_e z) \right.$$

$$- \frac{4(1 - \xi^2) + \mu(3 - 4\xi^2)}{4\xi^2 - 1} \cdot \sin h_2 z \cdot \sin 2(\omega t - \beta_e z)$$

$$\left. + \frac{3}{2}\frac{\mu}{\xi} \sin 2h_1 z \cdot \cos 2(\omega t - \beta_e z) \right\} \quad ,$$

where terms proportional to (h_1/β_e) and (h_2/β_e) have been omitted. This is consistent with the assumption that second-harmonic velocities are not excited at $z = 0$, as it may be seen in the complete expression for $v_{b_2}^+$, in Appendix F.

CHAPTER V

EXPERIMENTS

5.1 DESCRIPTION OF THE EXPERIMENTS

a. The Beam-Plasma Tube

An electron beam-plasma experiment in zero magnetic field was performed with a tube which had some features similar to the tubes described by Boyd.[14] The essential difference, however, lies in the fact that we used grids for modulation of the electron beam in an attempt to investigate the volume space-charge waves and to study the behavior of the beam in the plasma under saturation conditions. A schematic of the experimental tube is shown in Fig. 5, and a photograph of it is also included (Fig. 6). The electron beam gun employs a 0.120" diameter planar oxide coated cathode button from a 2K28 Raytheon klystron. This cathode is surrounded by a heat shield that supports the accelerating grid. The beam is velocity modulated by grids which were taken from these same gridded klystrons. Identical grids were used in the output section of the tube. The distance between the input and output grids is approximately 10 cm. This region consists of a 12 mm o.d. nonex glass tube. Beyond the output grids there is a beam collector.

A helix was embedded in this section of the glass tube (0.383" i.d.) by winding 0.010" diameter tungsten wire. The helix, which is nonsynchronous over the range of operating beam velocities, acts as an electrostatic shield for the beam, thus avoiding glass charging difficulties and permitting cavity measurements of plasma density. Experiments were made earlier with a similar tube, one with this section of glass coated on the inside with a conducting surface (stannous oxide).[1] Although gain was observed with this coated tube, measurements of plasma density by cavity perturbation techniques were found to be unreliable due to the high screening effect exhibited by the coating surface. No magnetic field was used.

---

[1] It was because of this geometry that the calculations in Chapter III assumed a metallic boundary outside the plasma. It is not obvious that this is correct for the stannous oxide film. However, as is shown in Appendix A, the nature of the waves is not markedly altered by the assumption of a dielectric boundary; for the nonsolenoidal waves not at all, and for the solenoidal waves only in a change in plasma reduction factors.

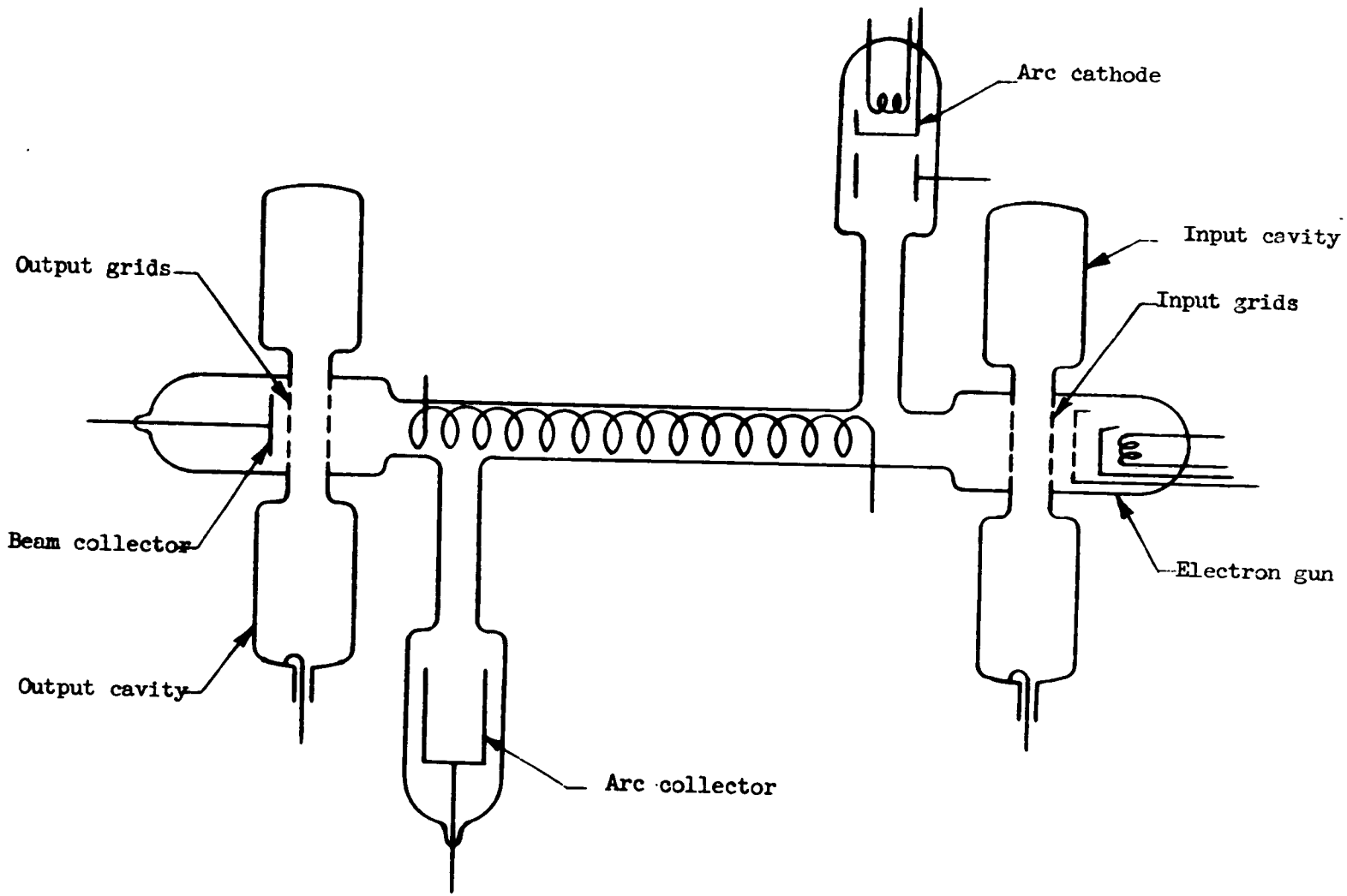

Fig. 5--Schematic of the experimental tube

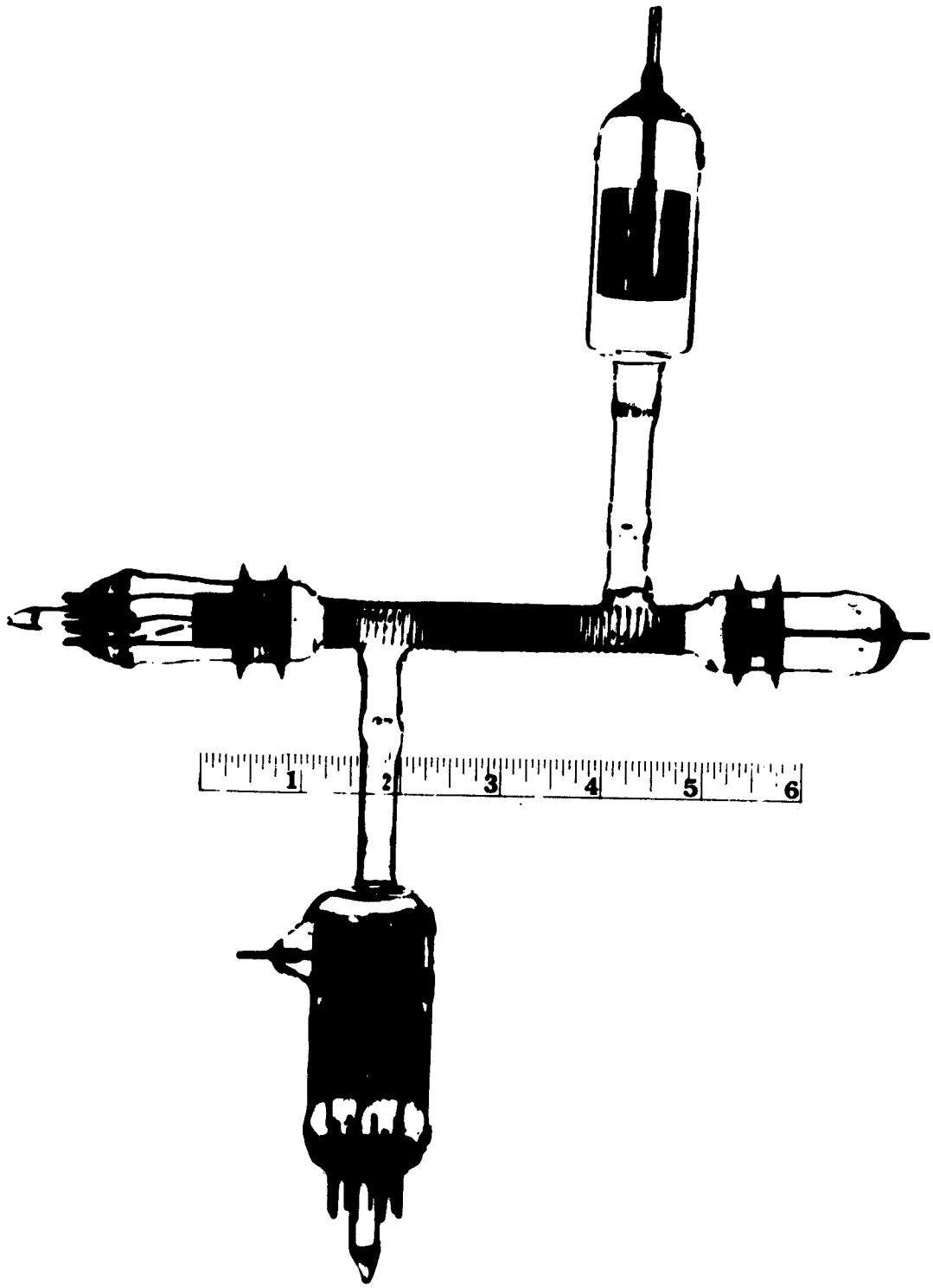

Fig. 6--Photograph of the tube.

b. Experimental Procedure

The operating frequency was selected to be in the 3000 Mc/s region, usually 2890 Mc/s. The pair of cavities used in the tube were split cavities designed for operation in the 10 cm range with the commercial gridded klystrons, from which the grids used were taken. Tuning was accomplished by tuning screws along the periphery of this reentrant cavity.

To obtain quantitative results on gain, saturation current, etc., it was necessary to know the cavity impedances. From a perturbation measurement an accurate value of R/Q was obtained. The result was R/Q = 57 ohms. A conventional measurement of Q , by plotting a Q-circle, yielded the result Q = 130. The shunt impedance of the cavity was then determined yielding R = Q(R/Q) = 7400 ohms.

The driving source was a 1 milliwatt 1 kc/s square-wave modulated signal generator. When it became necessary to drive the input cavity at large signals, this signal generator was fed into a traveling wave tube amplifier capable of delivering 1 watt maximum output.

Incident power to the input cavity was measured, using a directional coupler and rf wattmeter. The actual power absorbed by the buncher was obtained from the knowledge of the reflection coefficient in the input line as determined by a standing wave detector. Then from the knowledge of the rf power input and the cavity shunt impedance, the rf voltage at the buncher could be computed.

Similarly, from the knowledge of the loaded and unloaded Q of the output cavity, the total power supplied to the output gap could be calculated in terms of the measured power reaching the external load.

The beam coupling coefficient M is given in terms of the dc gap transit angle $d = \beta_e \ell$ where ℓ is the gap width. This distance ℓ between the grids constituting the gap was measured, yielding the result $\ell = 0.040"$. It follows then that $M = \sin(d/2)/(d/2)$ has the value $M = 0.9$, for a beam velocity corresponding to 500 v and frequency of 2890 Mc/s . The output cavity was heavily overcoupled and had a coupling coefficient $\beta = Q_0/Q_{ext}$ equal to 5. The rf beam current at the output cavity was then calculated in terms of the known measured quantities by using the expression

$$\left(\frac{I}{I_0}\right)^2 = \frac{2(1+\beta)^2}{M^2 R \beta I_0^2} \cdot P_L \quad ,$$

where P_L denotes the power to the external load, and I_0 is the dc beam current. It was found unnecessary to make measurements for different values of the beam current, since the effect of beam loading on the output cavity was negligible. In the final part of the experimental work, to be described later, attention was concentrated upon the possibility of harmonic generation. A new input cavity was designed and built to operate in L-band, and to be used as the buncher. The fundamental operating frequency was chosen to be 1770 Mc/s and the output cavity was tuned to twice this frequency.

c. Electron Beam

(1). Focusing and Interception Problems

It was found difficult to achieve perfect focusing of the electron beam along the axis of the tube. It was in trying to fulfill this idealized requirement, with the arc off and no magnetic field, that trouble was first encountered.

Nevertheless, after proper voltage adjustments, it was possible, with no plasma, to determine that the beam was reasonably focusing in the helix portion of the tube by visual observation of the luminosity it produced along its path.

The dc behavior of the electron beam in this region is controlled by the accelerating voltage impressed on the input gap and the dc voltages applied to the helix and output grids, respectively. With the plasma on, the beam could not be seen. We rely, in this case, on the positive ion neutralization due to the plasma ions which should improve the beam focus somewhat. The dc beam current reaching the output region can be considered as a measure of the degree of this improvement.

The beam transmission to the collector was measured to be of the order of 30%. Interception by the focusing grid near the cathode and the two pair of grids which form the gaps, besides collisions with neutral molecules, are responsible for this relatively poor transmission.

(2). Electron Beam Parameters

For the reasons discussed above, an accurate measurement of the diameter of the electron beam is not possible. We assumed in the calculations made that the beam diameter in the interaction path is approximately the diameter of the cathode button.

The beam current is partially controlled by applying to the focussing grid positive (or negative) voltages with respect to the cathode. Unfortunately, it was found difficult to maintain a constant beam current, as measured at the cathode, over a wide range of beam voltages. Arcing between the gun electrodes, due to ions in the gun region, often occurred, therefore limiting the operation of the beam gun. Moreover, the beam current was shown to vary as much as 20%, as the arc current was varied in the course of the experiment. Positive ion bombardment of the emitting surface could not be avoided.

By recording the magnitudes of the dc collector current for different plasma currents, and by comparison with the readings at the collector when only the plasma is on, the actual beam collector current is recorded. In the present experiments, the electron beam voltage ranges from 100 to 500 volts. Values of beam cathode currents of 1 ma and 1.5 ma were convenient for our purposes. The beam plasma wave number β_{pb} for a beam voltage 500 v, and a beam current 1 ma, 3 mm diameter is such that: $\beta_{pb}a = 0.05$, where a is the beam radius. At a frequency of 2890 Mc/s and a beam velocity corresponding to 500 volts, the beam electronic wave number $\beta_e = \omega/u_0$ is such that $\beta_e a = 2$.

d. Plasma

(1). Characteristics of the Arc Discharge

The plasma used in these experiments consists of the positive column of a low pressure hot cathode mercury arc discharge. The theoretical calculations of beam interaction in earlier chapters assumed a completely quiescent ("cold") plasma with no collisions. To estimate the effects of departures from this ideal condition in later sections we shall need some values of the plasma temperature and collison frequency.

The vapor pressure of mercury at room temperature (26.8 C) is 2.1×10^{-3} mm Hg. The equivalent plasma electron temperature (T_e) is defined in terms of the random energy of electrons according to

$$\frac{1}{2} m \bar{v}_t^2 = \frac{3}{2} kT_e \quad , \tag{5.1}$$

where $\bar{v}_T$ is the average thermal velocity of the plasma electrons and k is the Boltzmann constant.

Boyd[15] reported measurement of this plasma electron temperature with a Langmuir probe. An average value of T_e = 36000 K was obtained in a tube of internal diameter equal to 1.04 cm. The straight part of our tube where the beam-plasma interaction takes place has an inside diameter of 0.9 cm. We may then assume this value of T_e as approximately correct for our case. A random energy for the plasma electrons of approximately 4.7 ev would correspond to this plasma temperature.

The collisionfrequency as calculated from the mean free path for collisions[14] of electrons with neutrals was approximately 37 Mc/s. Collision effects are therefore negligible for this value of the collision frequency at the modulation frequencies of 3000 Mc/s or 1800 Mc/s used in the experiments.

(2). Plasma Electron Density; Cavity Perturbation Measurements

The plasma electron density is easily calculated from the formula

$$f_p = \frac{1}{2\pi} \sqrt{\frac{ne^2}{m\epsilon_0}} \quad , \qquad (5.2)$$

where n designates the number of electrons/cm^3 , where f_p is the plasma frequency of the plasma, ϵ_0 is the permittivity of free space, e and m the charge and mass of the electron, respectively. At a plasma frequency of 3000 Mc/s, the plasma electron density turns out to be 1.12×10^{11} electrons/cm^3 . It is convenient for this purpose to consider the plasma as a charge-free region[15] exhibiting a frequency-dependent dielectric constant given by $\epsilon/\epsilon_0 = 1 - \omega_{pp}^2/\omega^2$, (when no magnetic field is present) and one can measure the dielectric constant by perturbing the resonant frequency of a cavity by introducing a plasma.

A split cylindrical cavity supporting a TM_{010} mode was designed for this purpose. Measurements were made of the change of resonant frequency of this mode when the plasma density was varied by means of the arc current. The frequency deviations allow us to calculate the average electron plasma density with the help of a perturbation formula.[16] Figure 7 is a plot of the square of plasma frequency against arc current, indicating approximately the expected linear dependence of the plotted variables.

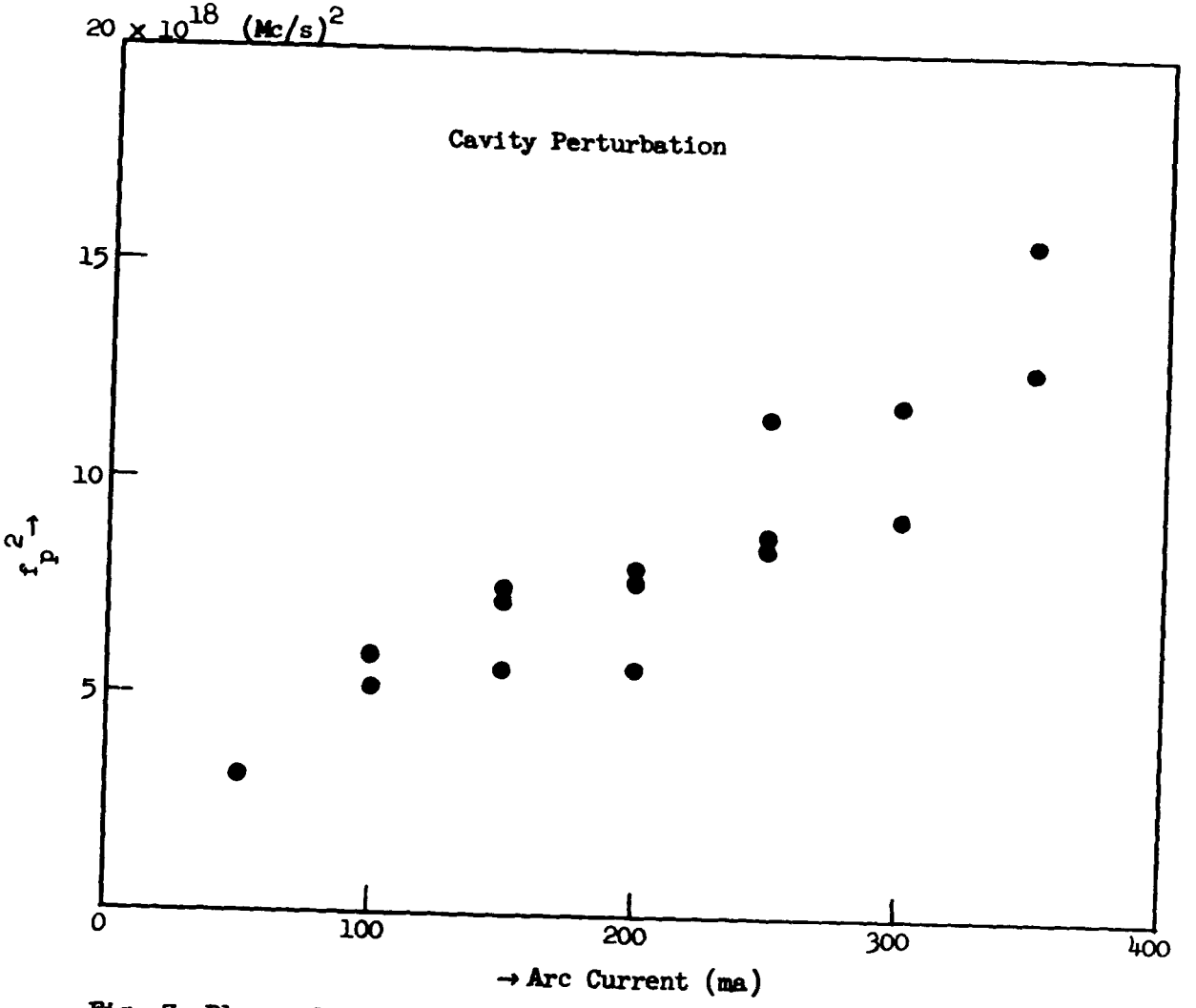

Fig. 7--Plasma frequency versus arc current; obtained by cavity perturbation measurements.

5.2 EXPERIMENTAL RESULTS; DISCUSSION

Power measurements were taken both at the input and output of the tube, according to the procedure outlined in the previous section. First, the electron beam was modulated with a low power signal and measurements were taken of the output power, for a fixed input, as a function of the plasma density. The plasma density was changed by varying the arc current. Figure 8 is a plot of the output power versus arc current with a low-level input signal (input power 1 mwatt). By comparing this curve with the data showing the plasma frequency dependence on arc current (Fig. 7), one can see that at the operating frequency of 2890 Mc/s, the maximum output signal appears near the expected value for resonance (i.e., $f \sim f_p$). Although no net gain was observed, it may be seen that this maximum output corresponds to a gain due to the plasma of approximately 5.5 db. With the same dc conditions for the electron beam (beam velocity and beam current unchanged), this experiment was repeated with a larger driving power (20 mwatts) which was the order of power necessary to cause rf saturation of the beam. A plot of the output power as a function of arc current is given in Fig. 9. It is seen that the saturation power is about 10 db above the low-level power, for an increase in drive of 13 db, and so the saturation "gain" is 3 db below the small-signal gain. Similar data taken with the same beam velocity and modulation frequency, and 20 milliwatts rf input power, but with a beam current of 1.5 ma instead of 1 ma, are plotted in Fig. 10. For this value of input power, the gain due to the plasma is 7.5 db at an arc current of approximately 220 ma, which corresponds to an average plasma density such that the resonance condition is nearly satisfied. It is interesting to notice in these curves that, as we might expect from the theory, for values of the arc current above that for maximum gain, the output signal falls less rapidly as current is changed than it does for arc currents below this value. The broad shape of the curves might be explained as a consequence of inhomogeneity in plasma density and as a result of the poor focusing of the beam. As pointed out before, the electron beam was not as well focused along the axis of the plasma column as would be desirable.

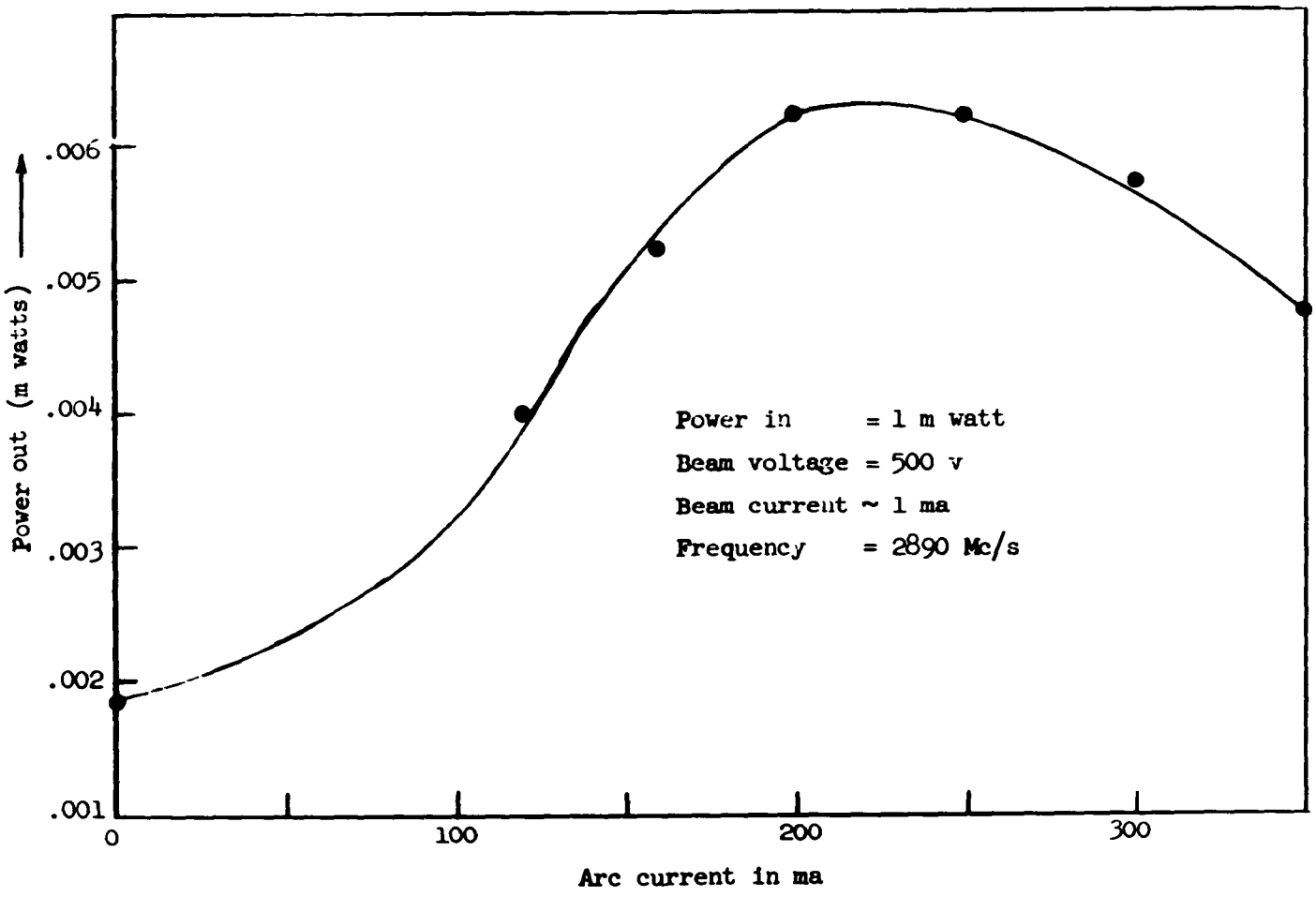

Fig. 8--Output power versus arc current.

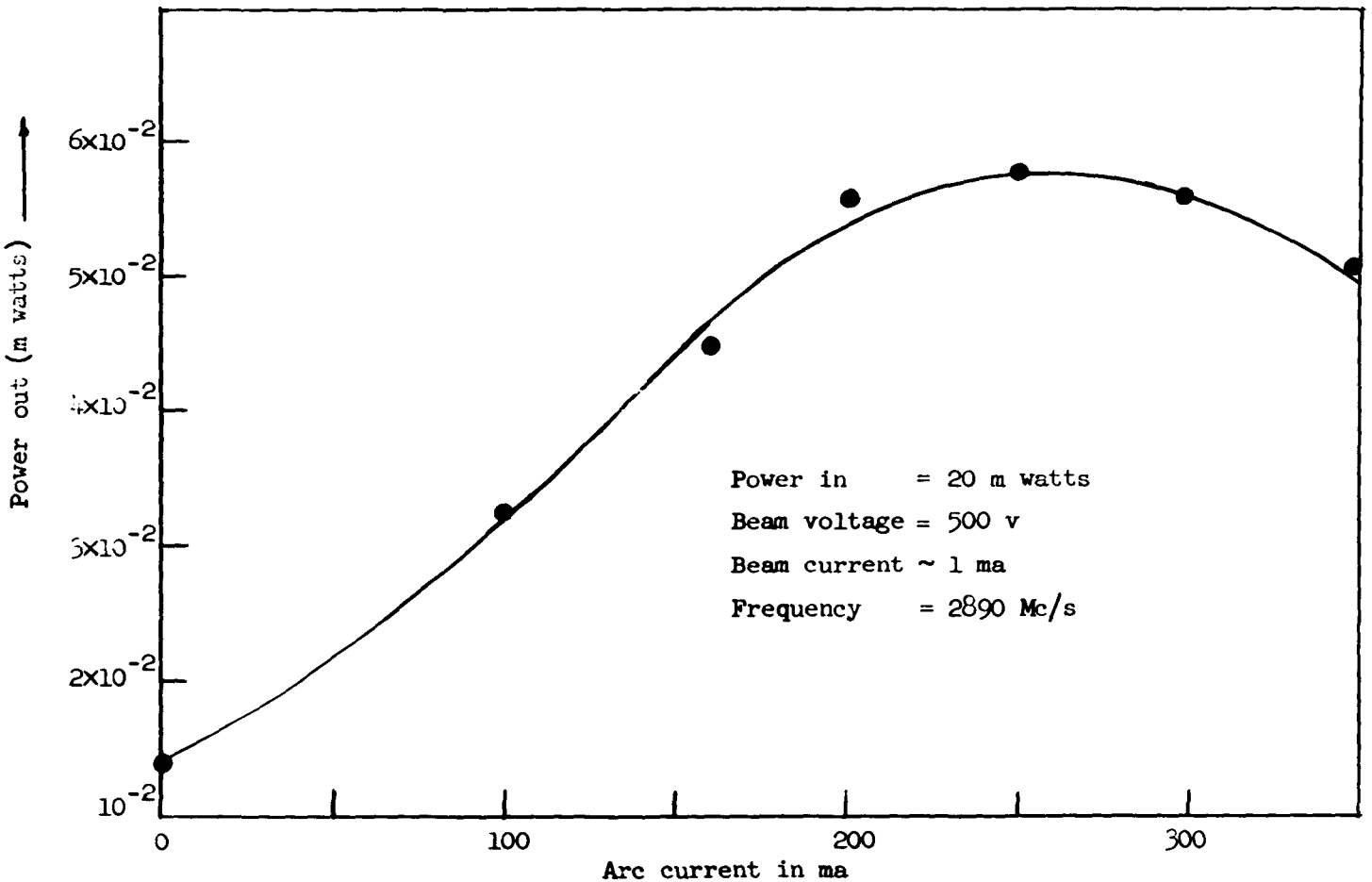

Fig. 9--Output power versus arc current for input saturation power.

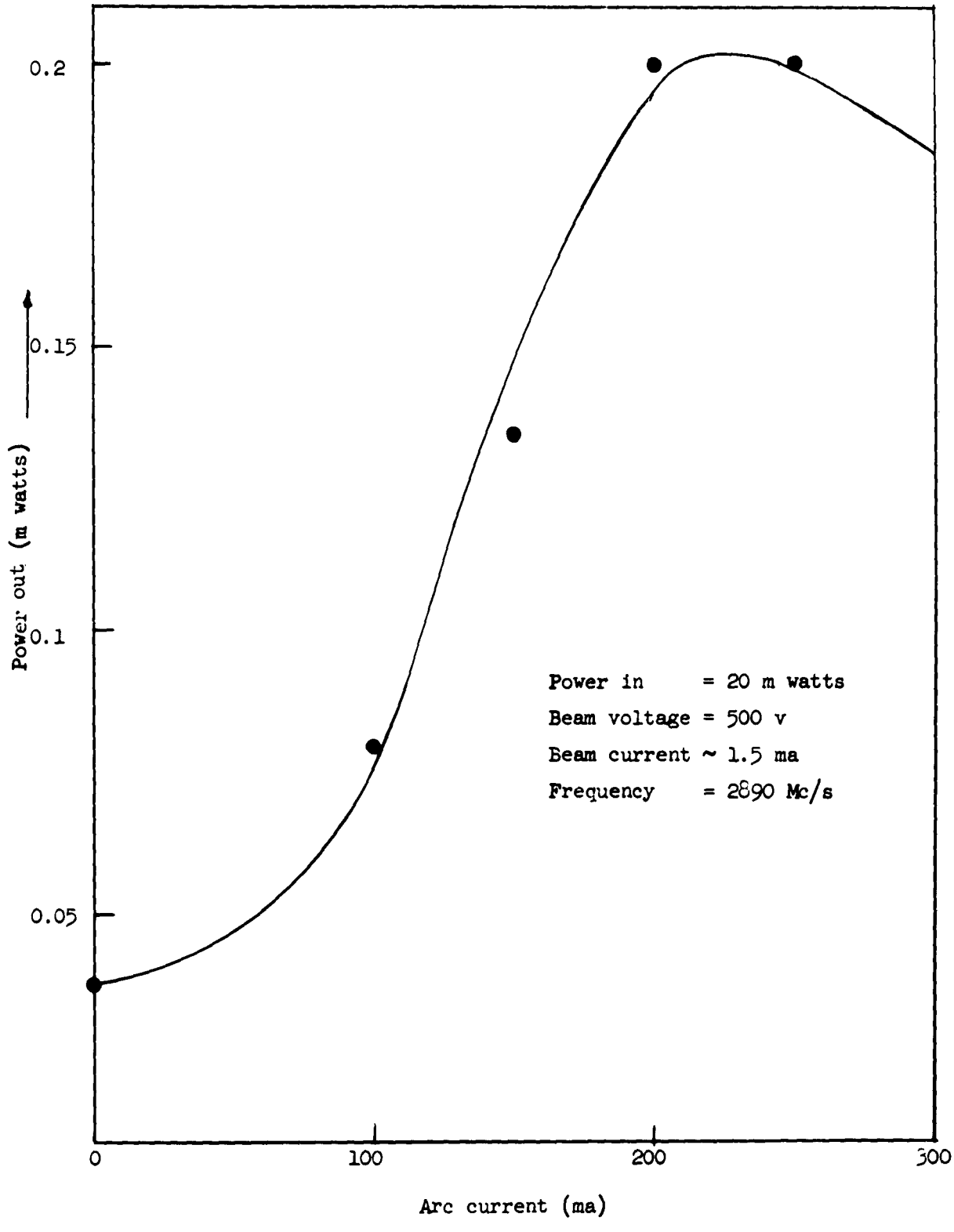

Fig. 10--Output power versus input power for different values of arc currents (beam current ~ 1.5 ma).

The interaction process may take place there at different distances from the axis of the plasma, which is not uniform over its cross section. Nonuniformity in the plasma, i.e., only its length, was presumably one of the main effects contributing to the small values of gain which were measured. Actually, it was observed that the plasma did not completely fill the glass tube along the path of the electron beam, from input to output cavity. Regions near the cavities were found to be free of plasma. Under these circumstances, the electron beam leaves the plasma region and drifts in a plasma-free space with a length of approximately 2 cm, before entering the output cavity. This corresponds to a length $\beta_p z = .7$, and such a drift region may reduce the gain and maximum rf current.

An appreciable reduction in the output levels would also be expected by virtue of thermal effects and collisions in the plasma, which we shall discuss below. However, the calculations will show that at maximum these effects cannot completely account for the low gain and it is probable that the nonuniformity of the plasma is the principal source of gain reduction.

There are several interesting aspects to the measurements of the output power versus input power which are plotted in Figs. 11 and 12. These measurements were taken successively at different arc currents whose values correspond, respectively, to the conditions at which the modulation frequency is

(a) below the plasma frequency

(b) near the plasma frequency

(c) above the plasma frequency.

Power measurements with only the electron beam, in the absence of plasma, are also included. It is important to note, from these curves, the significant increase in the saturation output power when the plasma is on.

The measurements given in Figs. 11 and 12 are replotted in Figs. 13 and 14 in terms of the output current versus input voltage. In these graphs, the dc beam current given is that based on collector current rather than total emitted current.

It is known that the simple first-order bunching theory due to Webster predicts for a two-cavity klystron that

$$I_1 = 2I_0 J_1(X) \quad , \tag{5.3}$$

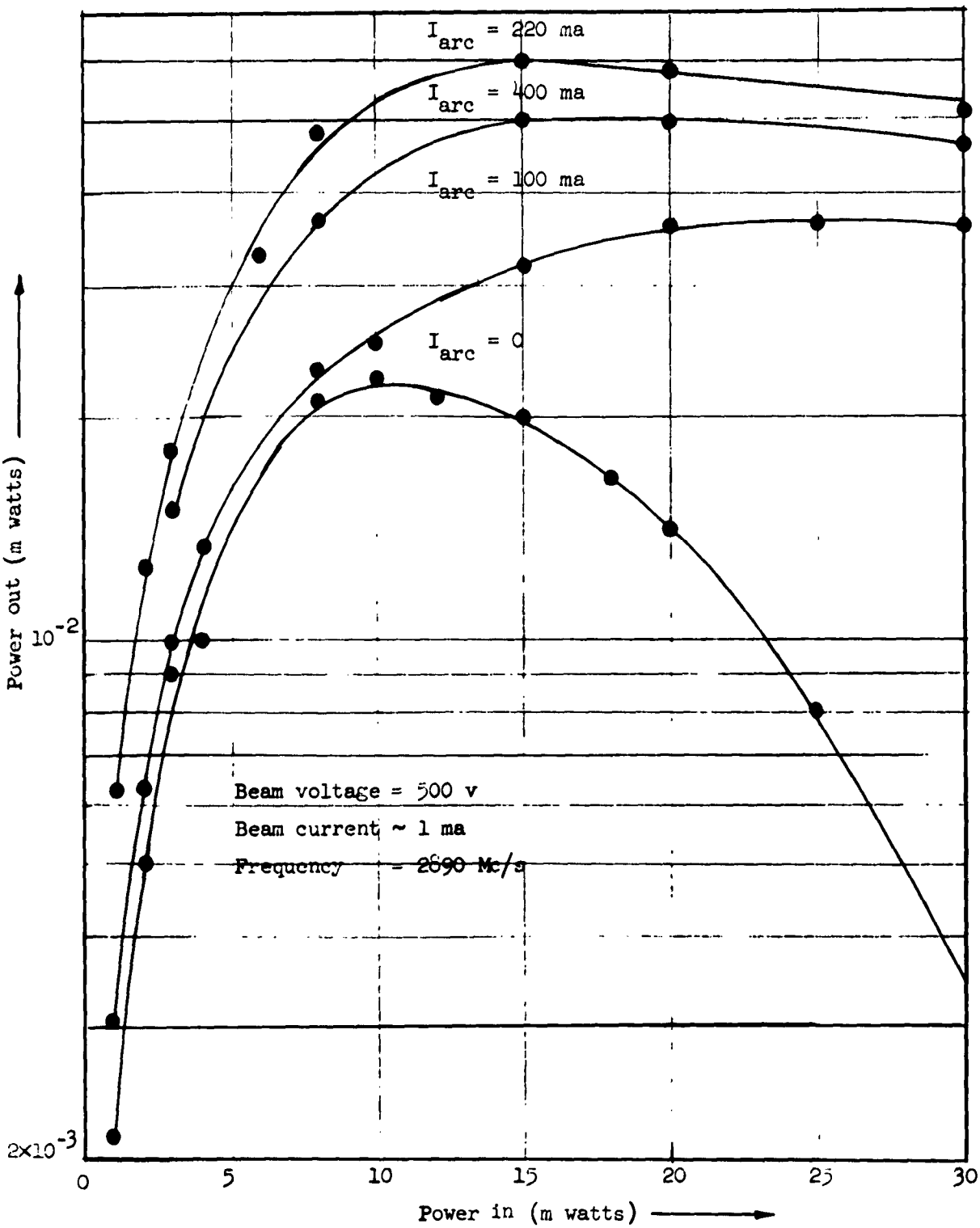

Fig. 11--Output power versus input power for different values of arc current (beam current ~ 1 ma).

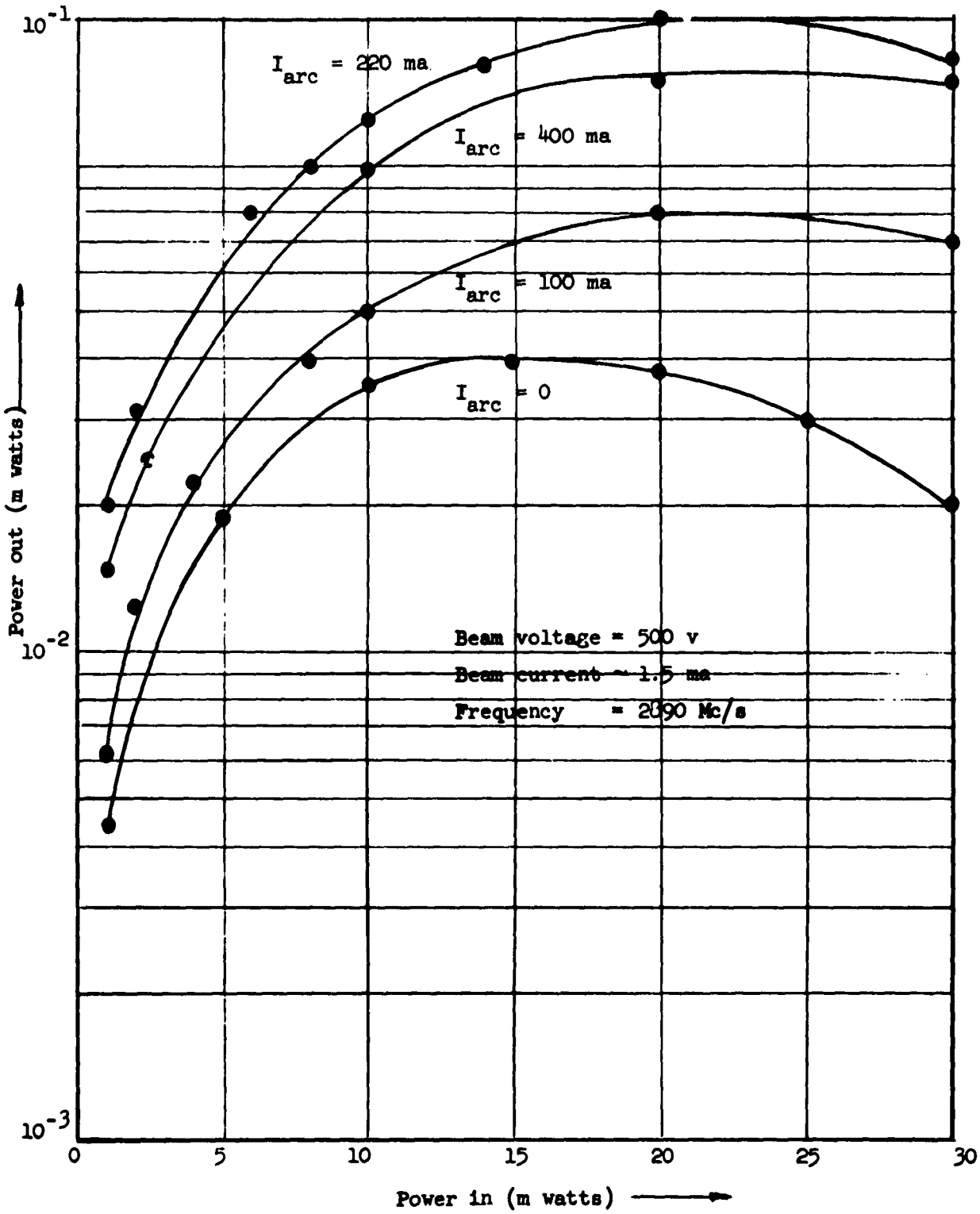

Fig. 12--Output power versus input power for different values of arc current (beam current ~ 1.5 ma).

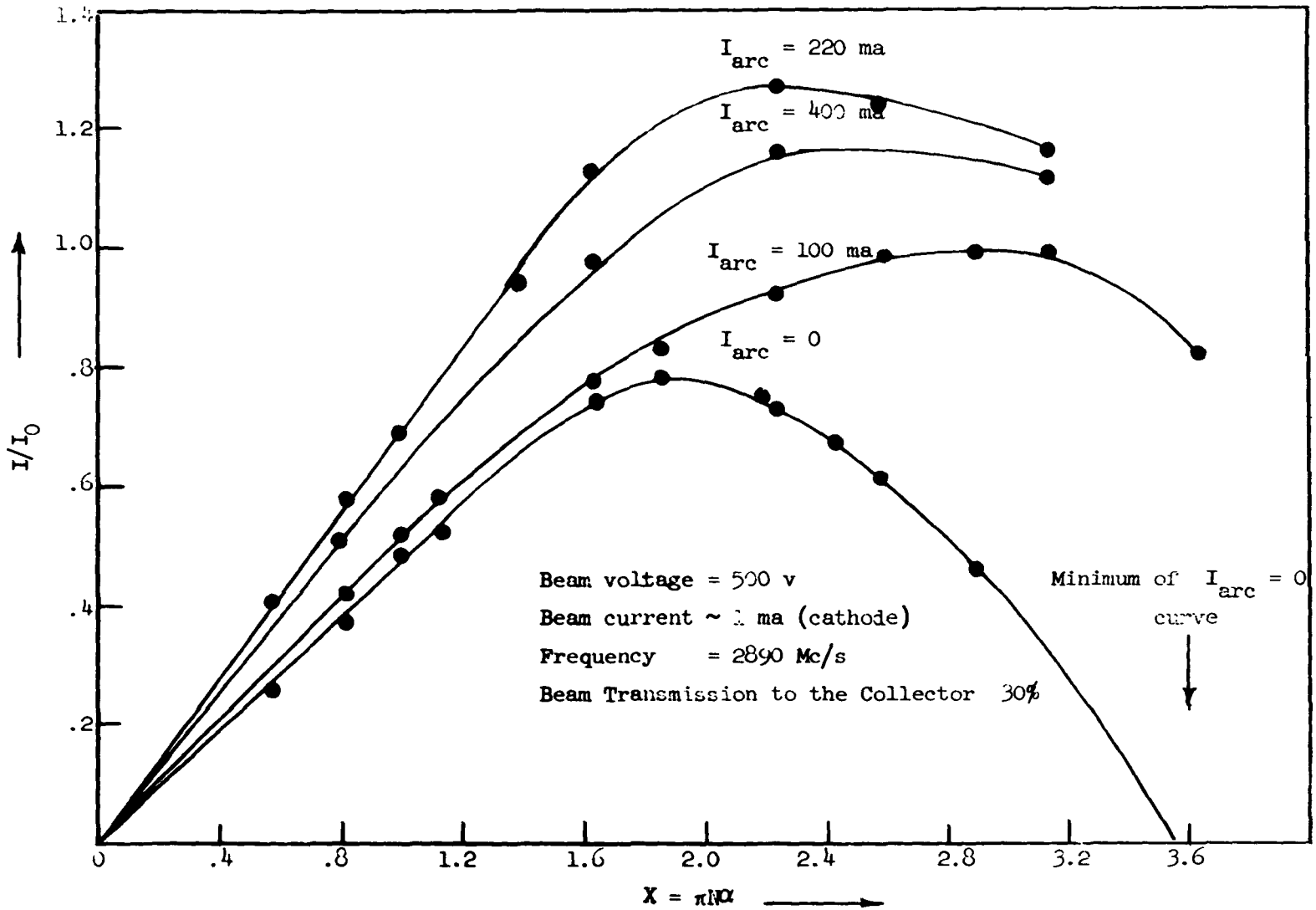

Fig. 13--Fundamental component of the current versus the bunching parameter (beam current ~ 1 ma).

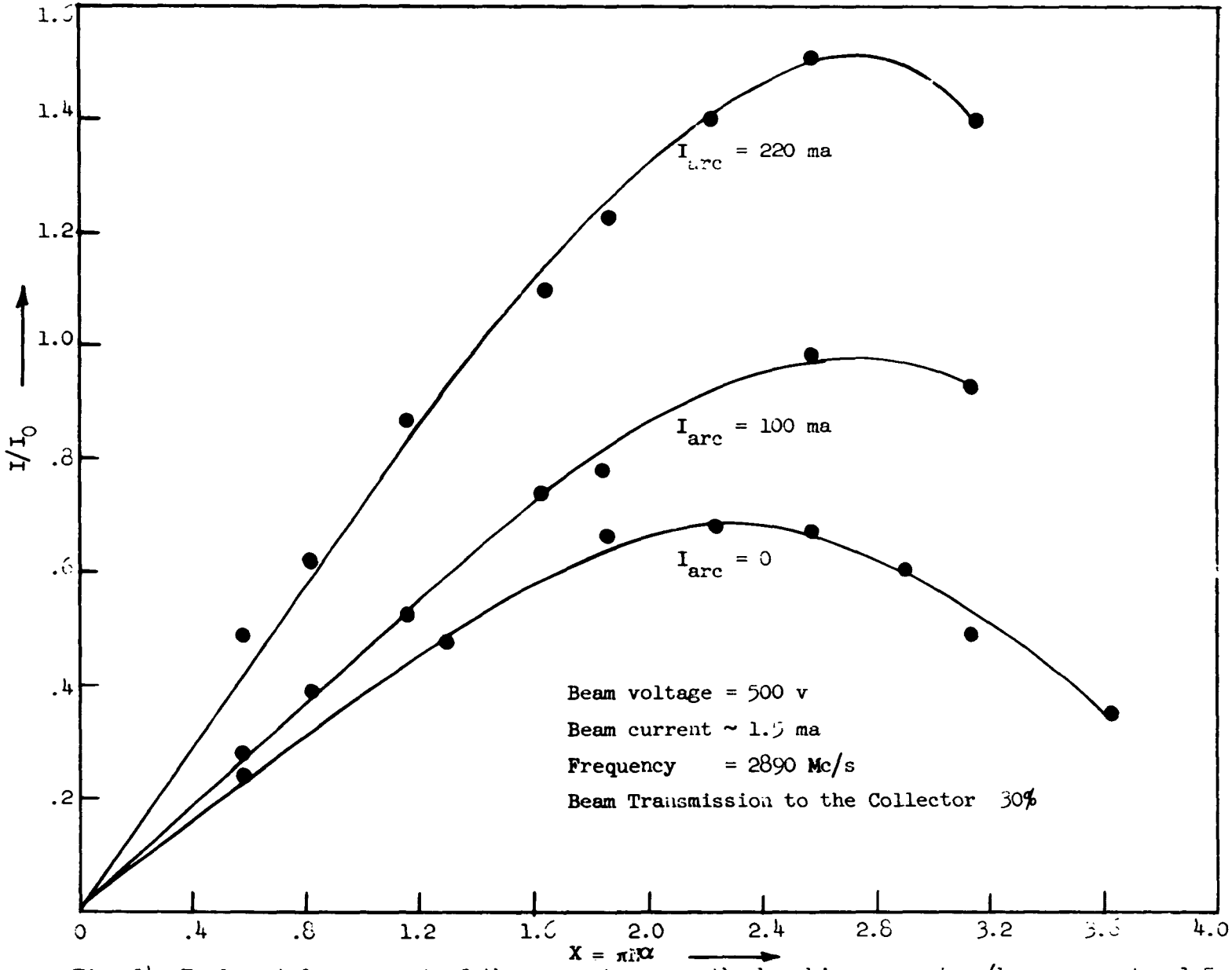

Fig. 14--Fundamental component of the current versus the bunching parameter (beam current ~ 1.5 ma).

where

I_1 = rf beam current

I_0 = dc beam current

$X = \pi N\alpha$ = bunching parameter ,

derived for a beam of infinite extent, without any consideration of space-charge effects.

From the observed output currents, with no arc present, it may be seen that the maximum value of the rf current is approximately $0.8\ I_0$, at a value of the parameter approximately 1.9; this value for X is indeed near the theoretical value, 1.84, for which the maximum of $J_1(X)$ would be expected to occur. The fact that the observed value of the maximum current is below 1.16, as it should be in the simple formula, would indicate the effect of the space-charge debunching of the electron bear which drifts along a tube of length L such that $\beta_{pb}L > \pi/2$. However, it should also be noted that the observed minimum of the current is at a value of the bunching parameter $X(X = 3.6)$, very close to the value of the argument of the Bessel function J_1 which corresponds to a zero of this function $(X = 3.83)$.

The discrepancy observed at small signal levels between the theoretical values for the current as given by the Bessel function dependence and the corresponding experimental values may also be accounted for by the finite-beam space-charge effects.

When the argument of the Bessel function is small, according to the Ramo single-mode approximation, the expression for current in a finite beam is simply

$$\frac{I_1}{I_0} = \frac{V_1}{2V_0}\ \frac{\omega}{\omega_{qb}} \sin \frac{\omega_{qb} z}{v_0} \quad . \tag{5.4}$$

In the above equation ω_{qb} represents the "effective" or "reduced" plasma frequency of the beam.

A similar expression applies to the case of a beam passing through a plasma with the reduction factor being due to the presence of the plasma. To make any comparison with experiments for this case (beam-plasma), we must first justify an approximation made in Chapter III. In considering the nonsolenoidal waves the assumption was made that $h/\beta_e \ll 1$. This obviously

is not true at $\omega = \omega_{pp}$ where the simple theory gives an infinite value for this ratio. The assumption can be justified even for this value of ω if one considers the effects of thermal velocities of the plasma electrons. The effect of these thermal velocities has been calculated for a plasma-beam system of infinite extent but the calculations are applicable to the nonsolenoidal waves of a finite system, since the difficulties with h/β_e arise in the same form for both cases.

For the electron beam and the plasma, both of infinite extent, it has been shown [Chapter III, Eq. (3.127)] that the fundamental component of the current is given by the expression

$$\frac{I_1}{I_0} = \frac{V_1 M^2}{2V_0} \frac{\omega\sqrt{\epsilon_1}}{\omega_{pb}} \sin \frac{\omega_{pb} z}{u_0 \sqrt{\epsilon_1}} \quad . \tag{5.5}$$

Comparing the above two expressions, (5.4) and (5.5), the analogy at small signals, between the finite-beam case and the infinite beam-plasma case, is apparent. The correspondence is made, as in Chapter IV, between the plasma frequency reduction factor $p = \omega_{qb}/\omega_{pb}$ in one case and $\left|1/\sqrt{\epsilon_1}\right|$ in the beam-plasma case.

However, while p is always less than unity, as already stated, the factor $\left|1/\sqrt{\epsilon_1}\right|$ could be allowed theoretically to assume values greater than unity, to become imaginary when $\omega < \omega_{pp}$, and even to be infinite, at $\omega = \omega_{pp}$, in a lossless, uniform plasma. The ideal situation of a lossless plasma is not encountered in practice. In our present experiment, it may be shown that with the inclusion of thermal effects,[1] for the typical beam parameters used here, this factor turns out to be greater than unity but not infinite at the plasma resonance frequency.

The dispersion relation for the infinite beam in a plasma has been solved numerically by taking into account the thermal motion of the plasma electrons and collisions (see ref. 14). At $\omega = \omega_{pp}$ it was found that, neglecting collisions,

$$\frac{h}{\beta_e} = \sqrt{R \frac{\omega_{pb}^2}{\omega_{pp}^2}} \quad , \tag{5.6}$$

[1] It can be shown that collision effects are much smaller.

where R denotes the ratio of the beam electron energy to the average random energy of the plasma electrons, i.e.,

$$R = \frac{\frac{1}{2} m u_0^2}{\frac{3}{2} kT} \quad . \tag{5.7}$$

Assuming a 500 volt electron beam, and $T_e = 36000^\circ$ K, we have $R \sim 100$. For a beam current of 1 ma, we have at $\omega = \omega_{pp}$, for a frequency equal to 3 kMc/s:

$$\left(\frac{\omega_{pb}}{\omega_{pp}}\right)^2 = 6 \times 10^{-4} \quad .$$

It follows then that

$$\frac{h}{\beta_e} \sim 0.1 \quad ,$$

which justify the approximations made ($h/\beta_e < 1$) in the analysis of the problem studied in Chapter III. The nonsolenoidal solutions were shown in that chapter to yield the following expression for the volume beam current:

$$\frac{I_v}{I_0} = \frac{\alpha M^2}{2} \frac{\beta_e}{h_1} \sin (hz) + \cdots \quad ,$$

applicable for $\omega < \omega_{pp}$, which should be compared with Eq. (5.5). When ω approaches ω_{pp} , by using the quantities calculated above, we have

$$\frac{\beta_e}{h} \sim 10 \quad , \qquad h \sim 1.3 \text{ nepers/cm} \quad .$$

Under these conditions, the growth constant for these nonsolenoidal currents is

$$\alpha_{n.s.} = 8.68\ h_1 = 8.68 \times 1.3 = 11.2 \text{ db/cm} \quad .$$

The solenoidal currents which are associated with purely surface wave propagation have also been investigated in Chapter III, since they also constitute

part of the excitation produced by grid coupling to the electron beam. However, as was shown before, these waves would lead to rates of growth which, as compared to the nonsolenoidal waves, are reduced by a factor F due to the finiteness of the system. This factor was calculated as a function of the ratio of the plasma and electron beam diameters, and also of $\beta_e a$, with the assumption that $h/\beta_e < 1$. This reduction factor is obtained from the curves plotted in Fig. 2. In our case, we shall assume that we may take account of thermal velocity in the same way as for the infinite plasma and still use the same reduction F to estimate the gain of the finite system. Therefore, by assuming $b/a = 3$, $\beta_e a = 2$, we have

$$F \equiv 0.6 \quad .$$

It follows therefore that the growth constant, for these solenoidal currents, at the plasma resonance frequency, should be

$$g_{s_1} = Fh_1 = 0.6 \times 1.3 = 0.78 \text{ nepers/cm} \quad ,$$

or

$$g_{s_1} = 6.9 \text{ db/cm} \quad .$$

These theoretical results indicate that there are no difficulties due to infinities in the gain characteristic. It should be pointed out, however, that the small signal gain calculated here for both kinds of waves is much larger than actually measured. As previously stated this discrepancy is probably due to inhomogeneities in the plasma and, in particular, the existence of a short plasma-free region just preceding the output cavity could affect the small signal gain greatly. Additional evidence for this is shown by the small decrease in gain for increase in plasma frequency above resonance (400 ma, ac current, see Figs. 11, 12). For a homogeneous plasma density the difference between 250 ma and 400 ma should be much greater.

a. Saturation Effects.

Under large signal saturated conditions, with crossing trajectory, a space-charge wave theory is never valid, and one can only consider the experimental results.

An investigation of the experimental curves shows that, near resonance, the rf output currents reached maximum values around 1.3 I_0 and 1.5 I_0, which respectively correspond to total beam cathode currents of 1 ma and 1.5 ma. The curves were calculated on the basis of the dc beam current reaching the collector which was found to be about 30 % of the total beam current. These values for the rf currents should be compared with the maximum theoretical value for the electron beam in a drift tube, in the absence of plasma. As was shown before, in theory the fundamental component of the beam current, with no plasma, has a maximum for $I_1/I_0 = 1.16$.

The reasons for the increase in the ratio, I/I_0, in the presence of the plasma as compared to this ratio in the absence of the plasma can be understood by considering the nature of the interaction mechanism between the electron beam and the plasma at frequencies where gain occurs. As can be seen from the theory, for $\omega < \omega_{pp}$ the plasma exhibits a negative dielectric constant and in its response to the current in the electron beam behaves like an inductive medium. For this condition $\omega < \omega_{pp}$ the modulated beam is continuously passing through an inductive medium. It is known from the theory of multi-cavity klystrons that if the cavities close to the output end are inductively detuned then the resultant modulation produced by these cavities is such as to distort the bunching in the electron beam in a way so as to produce larger rf currents than if one had merely a beam drifting through a drift tube.(or through cavities tuned to resonance). This is known theoretically and experimentally, and it has been well established that detuning (as is usually the case) the second to last cavity in a klystron will increase the efficiency by increasing the saturated value of the rf current, beyond what is possible with a series of cavities all tuned to resonance. Presumably, the same phenomena occurs in the case described here in the plasma region near the output cavity. In this region the rf current in the beam produces fields in the plasma such as to produce better bunching than if the medium were either not present or not inductive. The increase in the rf current measured here indicated this phenomena is taking place.

The reasons for the discrepancy in the ratio of rf to dc for the two values of dc current, shown in the figures, is not easily understood and may be due to experimental inaccuracy, e.g., discrepancies between beam current measured at the collector and the true current effective in the interaction.

b. Second Harmonic Experiments.

Experiments similar to the ones described above for measuring second harmonic currents were performed by using a different pair of cavities appropriate for detection of second-harmonic signals. The input cavity was tuned at 1770 Mc/s and the output cavity at twice this frequency. Measurements of output power at second harmonic versus arc current are plotted in Fig. 15. The observed peaks at values of arc current around 90 ma and 290 ma are found to correspond to the conditions that the input frequency ω is $\omega \sim \omega_p$ and $\omega \sim \omega_p/2$, respectively, at a modulation frequency equal to 1770 Mc/s.

Figure 16 shows results of input and output measurements, indicating a maximum output power for the second harmonics at $\omega \sim \omega_p/2$. In the analysis made in a previous chapter, for infinite beam-plasma, it may be seen that maximum values for the second harmonic output should be expected for $\omega = \omega_p$ and $\omega = \omega_p/2$. The experiment confirmed the theory by revealing that, for a fixed input frequency, these maxima occur at a subharmonic of the plasma frequency $(\omega_p/2)$ and also at the plasma frequency ω_p.

The experimental data were also plotted in a normalized fashion, similar to the plots of Figs. 14 and 15, so that they could be compared directly with the results obtained previously for the fundamental components.

The plot shown in Fig. 17 of the second harmonic current at the output cavity with respect to twice the bunching parameter X, calculated at 2890 Mc/s, was derived from the observed curves of input power versus output power. The low R/Q's of the input and output cavities used limited the power levels obtainable. Nevertheless, one can see the significant effect due to the plasma when comparison is made with the situation where only the electron beam is present. The saturated output current is shown to increase by a factor of approximately two when the arc current is changed from zero (no plasma) to $I_{arc} = 290$ ma $(\omega \sim \omega_p/2)$. The fundamental components were not measured at the same time since it was not possible to tune the output cavity to a frequency as low as 1770 Mc/s. However, we may make some comparison between the relative magnitudes of fundamental components of current and second harmonic by considering some of the experimental curves that were taken at 2890 Mc/s. For the latter in the saturation region (input power of 30 mw, for instance), the maximum value of a fundamental component of current was approximately $1.3\ I_0$, whereas in the same range of frequency, the maximum value of current as a second harmonic component was about $0.2\ I_0$.

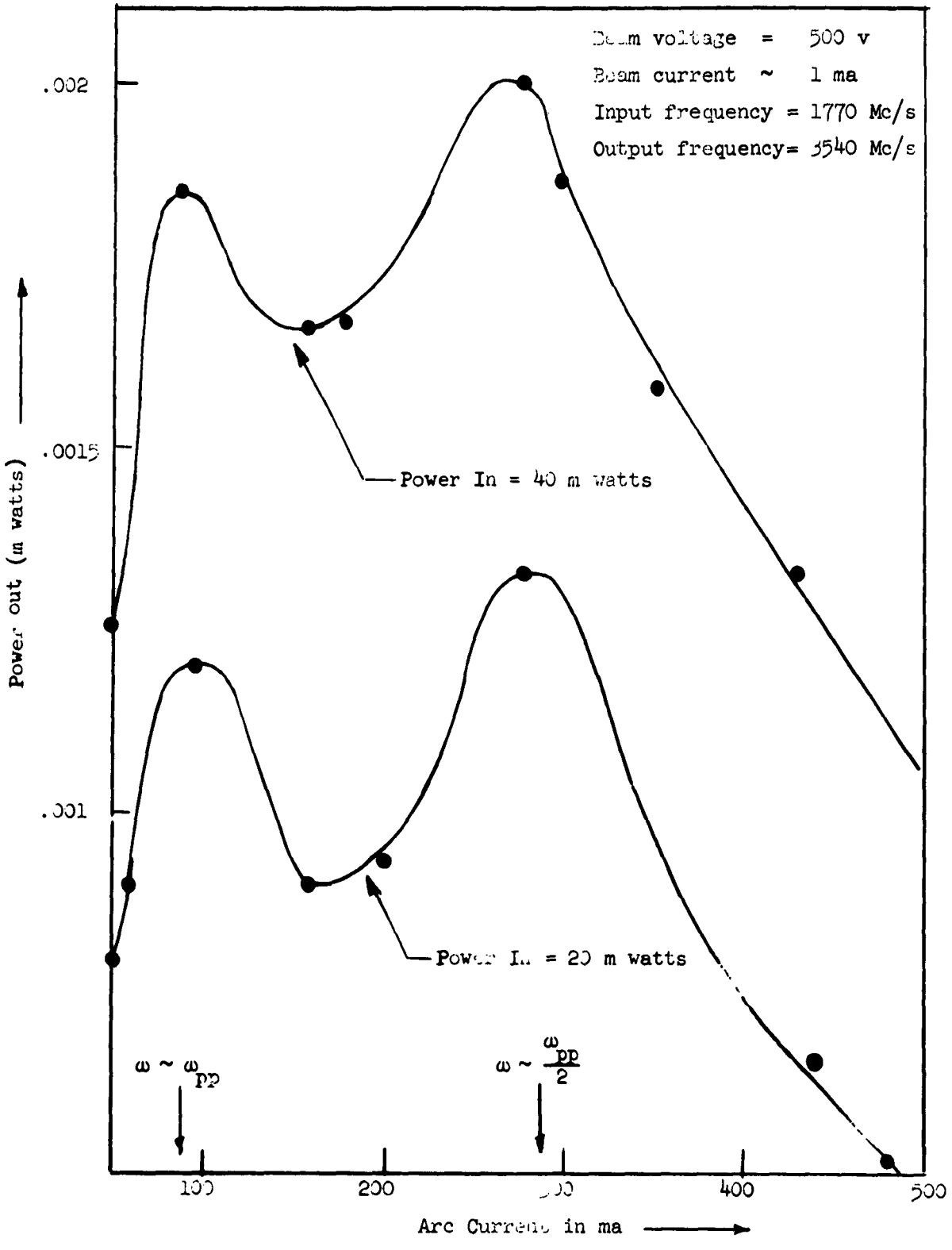

Fig. 15--Output power at second harmonic versus arc current.

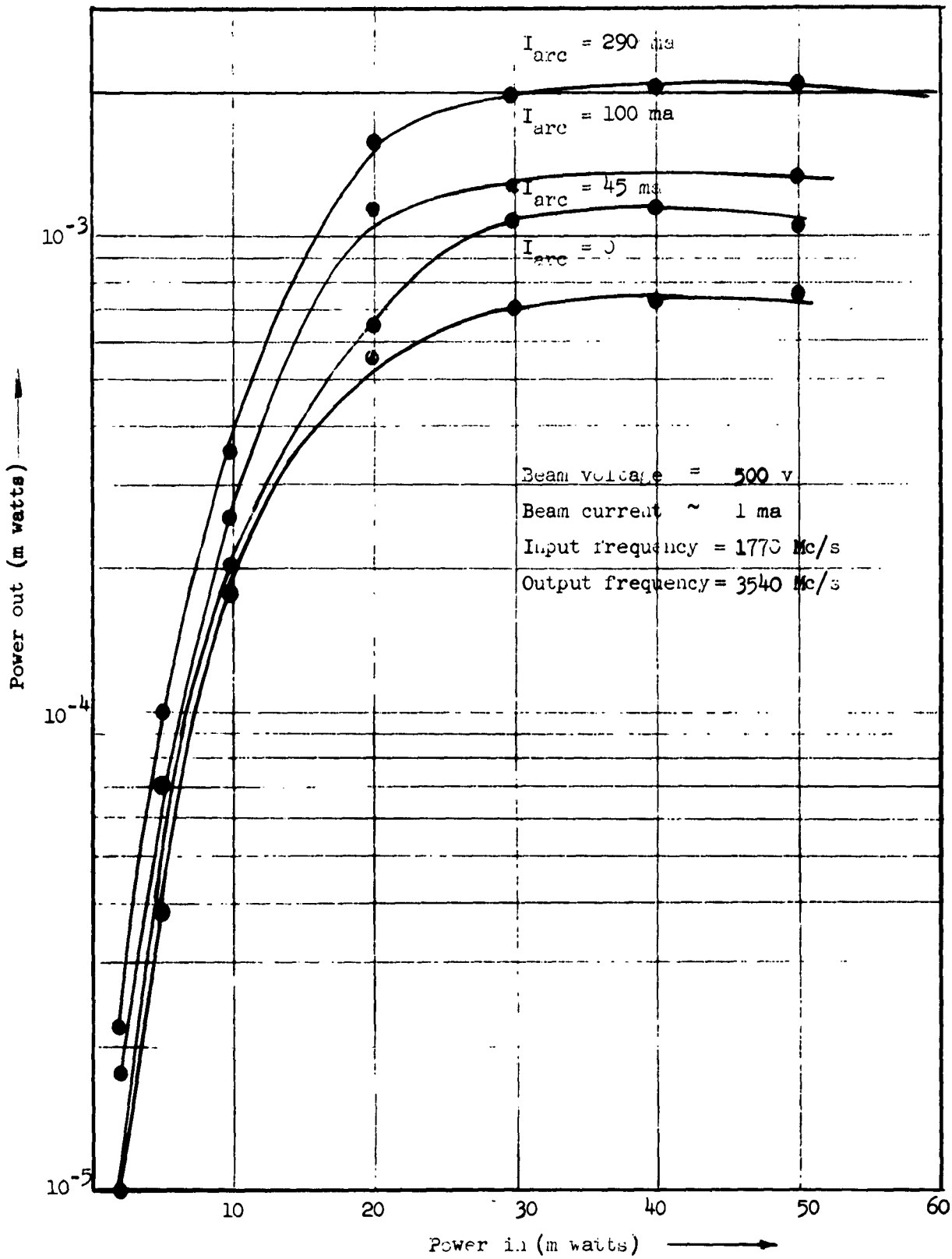

Fig. 16--Output power at second harmonic versus input power.

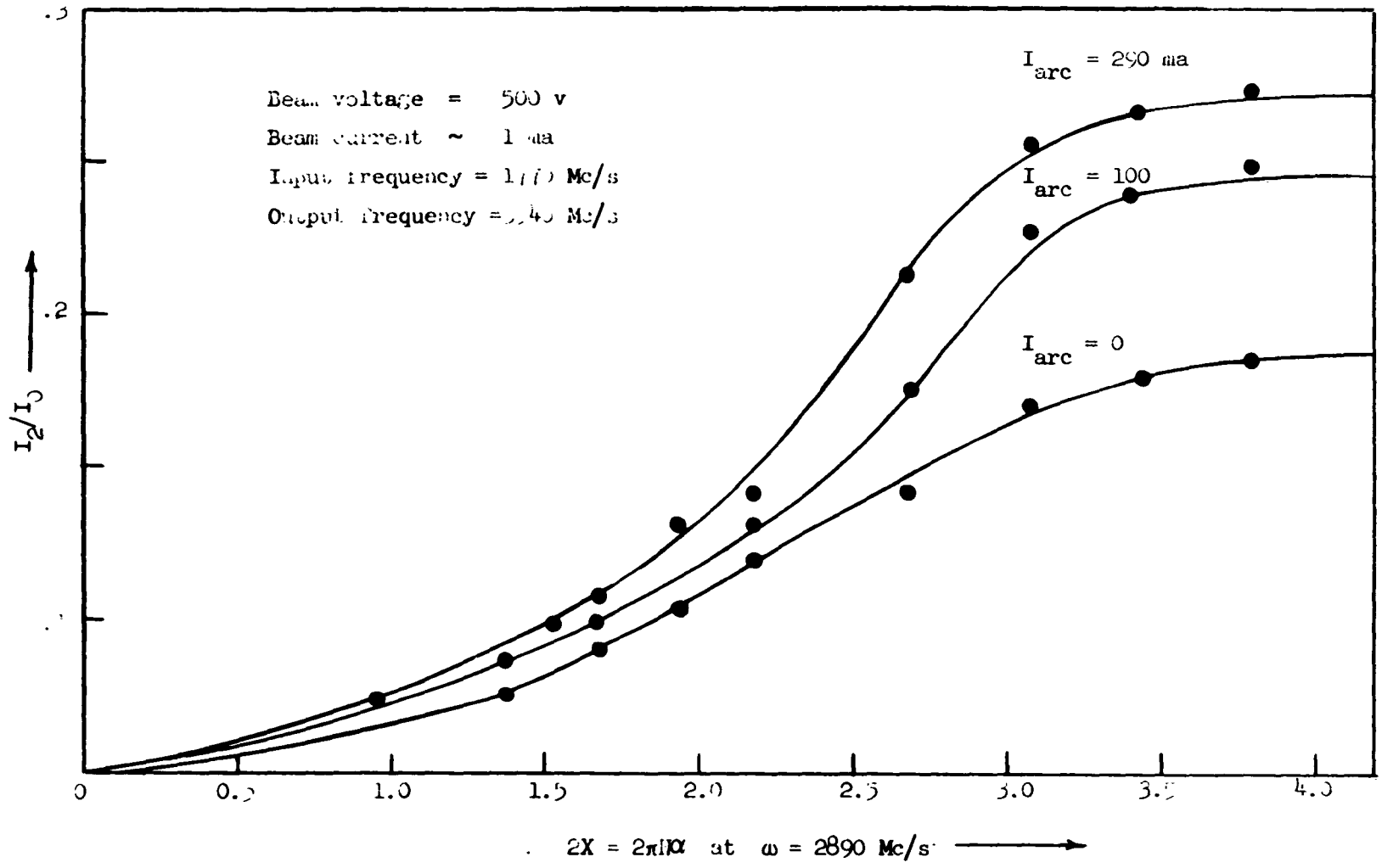

Fig. 17--Second harmonic component of the current versus $2X = 2\pi N\alpha$ (calculated at 2890 Mc/s).

5.3 SUMMARY AND CONCLUSIONS

The experimental data described in this chapter agree qualitatively with the predictions of the theory. We found that the gain measured between two cavities was not appreciably affected by the presence of a plasma until the plasma density reached a value approximately equal to the modulating frequency. For this condition, an increase in gain was noticed although numerically this gain due to the plasma was considerably less than would be indicated by the theory (even with thermal velocities in the plasma). However, there were imperfections in the plasma column, principally inhomogeneities, and an actual short region preceding the output cavity which was free of plasma, all of which would tend to drastically reduce the expected gain.

The interesting feature of the small signal performance however was that, at plasma densities corresponding to higher plasma frequencies than the modulating frequency, one still showed gain as compared to a no plasma case. In agreement with the qualitative prediction of the theory, there was a marked asymmetry in the gain shown for densities lower than plasma frequency as compared to above plasma frequency.

Possibly the most interesting feature of the experimental results was the saturation current measured in the presence of a plasma with the plasma frequency approximately equal to the modulating frequency. Under these circumstances there was a marked increase in the saturation current, as compared to the no plasma or low density plasma cases. Typical numbers for the ratio of rf current to the dc current ranged from 1.3 to 1.5 in the case where the plasma frequency was approximately equal to the modulating frequency, whereas this ratio was about 0.8 for the no plasma case. This behavior is attributed to the distorted bunching effects of an inductive medium acting on an electron beam and should have interesting implications for the use of the plasma direction in an actual operating device. Measurements of the harmonic content of an electron beam passing through a plasma showed, as expected, marked effects when the plasma frequency was approximately equal to the modulating frequency or twice the modulating frequency. These results may have implications for using a plasma device as a frequency multiplier.

APPENDIX A

ELECTRON BEAM IN A PLASMA; DIELECTRIC WALLS

The theoretical model which was considered in Chapter III does not completely apply to our experimental tube. In this tube, there are no conducting walls surrounding the plasma column. Dielectric walls (glass) should be assumed instead.

In this appendix a brief discussion is given which shows that the presence of metallic walls is not relevant to the validity of the conclusions stated in Chapter III concerning the fields vanishing in the region outside the beam. Refer to Fig. 1, and assume that in the dielectric region (region III), the longitudinal electric fields vary as

$$E_{z_{III}} = CH_0^{(2)}(\beta r) \quad .$$

As before, in region II, we have

$$E_{z_{II}} = A_2 I_0(\beta r) + B_2 K_0(\beta r) \quad .$$

The boundary conditions at $r = a$ are

$$E_{z_I}(a) = E_{z_{II}}(a) \tag{A.1}$$

and

$$\left.\frac{\partial E_{z_{II}}}{\partial r}\right|_{r=a} = 0 \quad , \tag{A.2}$$

which results from Eq. (3.52), by assuming nonsolenoidal solutions (propagation constants $\beta = \beta_e \pm h$) inside the beam region.

At $r = b$ (plasma-dielectric), we have

$$E_{z_{II}} = E_{z_{III}} \quad . \tag{A.3}$$

It is apparent that $A_2 = B_2 = C = 0$ is a solution of the system of equations represented by (A-1), (A-2), (A-3). This solution is compatible with the nonsolenoidal fields assumed inside the beam. It is known, from the analysis in Chapter III with a metallic boundary, that these nonsolenoidal solutions in region I are determined without any effects imposed by the region outside the beam. The treatment of this appendix merely shows formally that the same holds for an unbounded dielectric region outside the plasma.

APPENDIX B

CALCULATION OF THE TOTAL VOLUME CURRENT

To calculate the volume current density, we consider the separate contributions of the electron beam and plasma, and in both cases we take into account the nonsolenoidal and solenoidal solutions for the fields.

1. Electron Beam

a. Nonsolenoidal component of the beam current density.

We have:

$$\frac{(i_{zb})_{n.s.}}{i_0} = \frac{i_{zb}^{(1)}}{i_0} \cdot e^{-jhz} + \frac{i_{zb}^{(2)}}{i_0} \cdot e^{jhz}$$

$$= \frac{(i_{zb}^{(1)} + i_{zb}^{(2)})}{i_0} \cos(hz) - j\left(\frac{(i_{zb}^{(1)} - i_{zb}^{(2)})}{i_0}\right)\sin(hz) \quad .$$

But, we know

$$\frac{i_{zb}^{(1)} + i_{zb}^{(2)}}{i_0} = \frac{\rho_b^{(1)} + \rho_b^{(2)}}{\rho_{0b}} + \frac{v_{zb}^{(1)} + v_{zb}^{(2)}}{u_0}$$

and

$$\frac{i_{zb}^{(1)} - i_{zb}^{(2)}}{i_0} = \frac{\rho_b^{(1)} - \rho_b^{(2)}}{\rho_{0b}} + \frac{v_{zb}^{(1)} - v_{zb}^{(2)}}{u_0} \quad .$$

Substituting Eqs. (3.119) and (3.120) into the two above equations yields the following expressions:

$$\frac{i_{zb}^{(1)} + i_{zb}^{(2)}}{i_0} = -\frac{\alpha M}{2}\left\{\frac{I_0(\beta_e r)}{I_0(\beta_e a)} - 0\left(\frac{\Delta}{\beta_e}\right)^2\right\} \quad ,$$

and

$$\frac{i_{zb}^{(1)} - i_{zb}^{(2)}}{i_0} = -\frac{\alpha M}{2}\left(\frac{\beta_e}{h}\right)\left\{1 - \frac{I_0(\beta_e r)}{I_0(\beta_e a)} + 0\left(\frac{\Delta}{\beta_e}\right)^2\right\} \quad .$$

Therefore, it follows

$$\frac{(i_{zb})_{n.s.}}{i_0} = -\frac{\alpha M}{2}\left\{\frac{I_0(\beta_e r)}{I_0(\beta_e a)}\cos(hz) - j\left(\frac{\beta_e}{h}\right)\sin(hz)\left(1 - \frac{I_0(\beta_e r)}{I_0(\beta_e a)}\right) + \ldots\right\} .$$

b. Solenoidal components of the beam current density.

We have

$$\frac{i_{zb}^{(3)}}{i_0} = -\left(1 + \frac{\beta_e}{F_3 h}\right)\cdot\frac{V_I^{(3)}}{2V_0}$$

$$\frac{i_{zb}^{(4)}}{i_0} = -\left(1 - \frac{\beta_e}{F_4 h}\right)\cdot\frac{V_I^{(4)}}{2V_0} \quad .$$

It is known that

$$\frac{(i_{zb})_{s.}}{i_0} = \frac{i_{zb}^{(3)}}{i_0}\cdot e^{-jF_3 hz} + \frac{i_{zb}^{(4)}}{i_0}\cdot e^{jF_4 hz} \quad .$$

Therefore, we have

$$\frac{(i_{zb})_{s.}}{i_0} = -\left(1 + \frac{\beta_e}{F_3 h}\right)\frac{V_I^{(3)}}{2V_0}\cdot e^{-jF_3 hz} - \left(1 - \frac{\beta_e}{F_4 h}\right)\frac{V_I^{(4)}}{2V_0} e^{jF_4 hz} \quad .$$

It had been shown before [Eq. (3.95)] that

$$hF_3 = \Delta + \frac{\delta}{2}$$

and

$$hF_4 = \Delta - \frac{\delta}{2} \quad .$$

By using these relations, we have

$$\frac{(i_{zb})_{s.}}{i_0} = e^{-j\frac{\delta}{2}z} \cdot \left\{ \cos(\Delta z) \left[\left(\frac{V_I^{(3)} + V_I^{(4)}}{2V_0} \right) + \frac{\beta_e}{2hV_0} \left(\frac{V_I^{(3)}}{F_3} - \frac{V_I^{(4)}}{F_4} \right) \right] \right.$$

$$\left. - j \sin(\Delta z) \left[\left(\frac{V_I^{(3)} - V_I^{(4)}}{2V_0} \right) + \frac{\beta_e}{2hV_0} \left(\frac{V_I^{(3)}}{F_3} + \frac{V_I^{(4)}}{F_4} \right) \right] \right\} \quad . \quad \text{(B.2)}$$

On the other hand, by using Eqs. (3.105) and (3.117), the following expression is obtained:

$$\frac{V_I^{(3)} + V_I^{(4)}}{2V_0} = - \left(\frac{V_I^{(1)} + V_I^{(2)}}{2V_0} \right)$$

$$= - \frac{\alpha M}{2} \left(\frac{\Delta}{\beta_e} \right)^2 \left\{ \beta_e \frac{\partial}{\partial \beta_e} \left(\frac{I_0(\beta_e r)}{I_0(\beta_e a)} \right) + 0 \left(\frac{\Delta}{\beta_e} \right)^2 \right\} \quad ,$$

and from Eqs. (3.110) and (3.116) we obtain

$$\frac{\beta_e}{2\Delta V_0} (V_I^{(3)} - V_I^{(4)}) = - \frac{\alpha M}{2} \left\{ \frac{I_0(\beta_e r)}{I_0(\beta_e a)} + 0 \left(\frac{\Delta}{\beta_e} \right)^2 \right\} \quad .$$

Substituting the latter two expressions into Eq. (B.2), we obtain

$$\frac{(i_{zb})_{s.}}{i_0} = \frac{\alpha M}{2} e^{-j\frac{\delta}{2}z} \cdot \left\{ \frac{I_0(\beta_e r)}{I_0(\beta_e a)} \cdot \cos(\Delta z) \right.$$

$$\left. - j \left(\frac{\Delta}{\beta_e} \right) \sin(\Delta z) \cdot \left[\frac{\beta_e}{2} \cdot \frac{\partial}{\partial \beta_e} \left(\frac{I_0(\beta_e r)}{I_0(\beta_e a)} \right) + \frac{I_0(\beta_e r)}{I_0(\beta_e a)} + \ldots \right] \right\} \cdot \quad \text{(B.3)}$$

Finally, the total electron beam current density is given by the sum of the right-hand sides of Eqs. (B.1) and (B.3), that is,

$$\frac{i_{zb}}{i_0} = \frac{(i_{zb})_{n.s.}}{i_0} + \frac{(i_{zb})_{s.}}{i_0}$$

$$= \frac{\alpha M}{2}\left\{ j\left(\frac{\beta_e}{h}\right)\sin(hz) + \left[e^{-j\frac{\delta}{2}z}\cdot\cos(\Delta z) - \cos(hz)\right]\cdot\frac{I_0(\beta_e r)}{I_0(\beta_e a)} + \ldots \right\} .$$

The total volume current, at the output grids, $(z = L)$, is calculated by averaging over the cross-section of the beam the quantity (i_{zb}/i_0) and by multiplying the result by the beam coupling coefficient M. We have

$$\frac{I_{vb}}{I_0} = \frac{\alpha M^2}{2}\cdot\left\{ j\left(\frac{\beta_e}{h}\right)\sin(hL) + \left[e^{-j\frac{\delta}{2}L}\cdot\cos(\Delta L) - \cos(hL)\right]\cdot\frac{2I_1(\beta_e a)}{(\beta_e a)I_0(\beta_e a)} + \ldots \right\} .$$

Figure 4 shows

$$\frac{2I_1(\beta_e a)}{(\beta_e a)I_0(\beta_e a)}$$

as a function of $(\beta_e a)$.

2. Plasma Electrons (in Region I)

The nonsolenoidal component of the plasma current density is

$$\frac{(i_{zp})_{n.s.}}{i_0} = \frac{i_{zp}^{(1)}}{i_0} e^{-jhz} + \frac{i_{zp}^{(2)}}{i_0} e^{jhz}$$

$$= \frac{(i_{zp}^{(1)} + i_{zp}^{(2)})}{i_0}\cdot\cos(hz) - j\sin(hz)\left(\frac{i_{zp}^{(1)} - i_{zp}^{(2)}}{i_0}\right) .$$

But, it is known that the linearized longitudinal plasma current densities are

$$i_{zp}^{(1)} = \rho_{0p} \cdot v_{zp}^{(1)}$$

$$i_{zp}^{(2)} = \rho_{0p} \cdot v_{zp}^{(2)} \quad .$$

Then, it follows that

$$\frac{i_{zp}^{(1)} + i_{zp}^{(2)}}{i_0} = \left(\frac{\rho_{0p}}{\rho_{0b}}\right)\left(\frac{v_{zp}^{(1)} + v_{zp}^{(2)}}{u_0}\right) \quad ,$$

and

$$\frac{i_{zp}^{(1)} - i_{zp}^{(2)}}{i_0} = \left(\frac{\rho_{0p}}{\rho_{0b}}\right)\left(\frac{v_{zp}^{(1)} - v_{zp}^{(2)}}{u_0}\right) \quad .$$

By substituting Eq..(3.112) into the two above equations, we get

$$\frac{i_{zp}^{(1)} + i_{zp}^{(2)}}{i_0} = -\left(\frac{\omega_{pp}}{\omega_{pb}}\right)^2 \cdot \frac{\alpha h M}{2\beta_e} \cdot \left\{1 - \frac{I_0(\beta_e r)}{I_0(\beta_e a)} + 0\left(\frac{\Delta}{\beta_e}\right)^2\right\} \quad ,$$

$$\frac{i_{zp}^{(1)} - i_{zp}^{(2)}}{i_0} = \left(\frac{\omega_{pp}}{\omega_{pb}}\right)^2 \cdot \frac{\alpha M}{2}\left(\frac{\Delta}{\beta_e}\right)^2 \left\{\beta_e \cdot \frac{\partial}{\partial \beta_e} \cdot \left(\frac{I_0(\beta_e r)}{I_0(\beta_e a)}\right) + 0\left(\frac{\Delta}{\beta_e}\right)^2\right\} \quad .$$

Therefore, it follows that

$$\frac{(i_{zp})_{n.s.}}{i_0} = -\frac{\alpha M}{2}\left(\frac{\omega_{pp}}{\omega_{pb}}\right)^2 \cdot \left\{\left(\frac{h}{\beta_e}\right)\left(1 - \frac{I_0(\beta_e r)}{I_0(\beta_e a)}\right) \cdot \cos(hz) + \ldots\right\} \quad .$$

For solenoidal component of the plasma current density, we have

$$\frac{(i_{zp})_{s.}}{i_0} = \frac{i_{zp}^{(3)}}{i_0} \cdot e^{-jF_3 hz} + \frac{i_{zp}^{(4)}}{i_0} e^{jF_4 hz} \quad .$$

But we know [Eqs. (3.65)] that

$$\frac{i_{zp}^{(3)}}{i_0} = \left(\frac{\omega_{pp}}{\omega_{pb}}\right)^2 \cdot \left(1 + \frac{F_3 h}{\beta_e}\right) \cdot \frac{V_I^{(3)}}{2V_0}$$

and

$$\frac{i_{zp}^{(4)}}{i_0} = \left(\frac{\omega_{pp}}{\omega_{pb}}\right)^2 \cdot \left(1 - \frac{F_4 h}{\beta_e}\right) \cdot \frac{V_I^{(4)}}{2V_0} \quad .$$

By using the expressions derived in the text for these potentials, $V_I^{(3)}$ and $V_I^{(4)}$ [Eqs. (3.110)], the solenoidal part of the plasma volume current density turns out to be given by the following expression:

$$\frac{(i_{zp})_{s.}}{i_0} = j\,\frac{\alpha M}{2}\left(\frac{\omega_{pp}}{\omega_{pb}}\right)^2 \frac{\Delta}{\beta_e} \cdot \left(\frac{I_0(\beta_e r)}{I_0(\beta_e a)}\right) \cdot \sin(\Delta z)\, e^{-j\frac{\delta}{2}z} \quad .$$

The total plasma volume current density, at any point in the plasma-beam interaction region, distant z from the input grids $(0 < z < L)$, is therefore

$$\frac{I_{vp}}{I_0} = \frac{(i_{zp})_{n.s.}}{i_0} + \frac{(i_{zp})_{s.}}{i_0}$$

$$= -\frac{\alpha M}{2}\left(\frac{\omega_{pp}}{\omega_{pb}}\right)^2 \cdot \left\{ \left(\frac{h}{\beta_e}\right)\left(1 - \frac{2I_1(\beta_e a)}{(\beta_e a) I_0(\beta_e a)}\right) \cdot \cos(hz) \right.$$

$$\left. - j\left(\frac{\Delta}{\beta_e}\right) e^{-j\frac{\delta}{2}z} \cdot \left(\frac{2I_1(\beta_e a)}{(\beta_e a) I_0(\beta_e a)}\right) \cdot \sin(\Delta z) + \ldots \right\} \quad .$$

APPENDIX C

CALCULATION OF THE SURFACE CURRENTS

To calculate the surface currents per unit of circumference, at $r = a$, we have to determine the surface currents originated by the electrons of the beam in the two propagating waves modes. We have, then, nonsolenoidal surface currents, which are given by

$$\frac{i_{sb}^{(1)}}{i_0} = \sigma_b^{(1)} \cdot \frac{u_0}{i_0} = \frac{1}{h^2} \frac{d}{dr} \left(\frac{V_I^{(1)}}{2V_0} \right)_{r=a}$$

and (C.1)

$$\frac{i_{sb}^{(2)}}{i_0} = \sigma_b^{(2)} \cdot \frac{u_0}{i_0} = \frac{1}{h^2} \frac{d}{dr} \left(\frac{V_I^{(2)}}{2V_0} \right)_{r=a} .$$

From the condition that $(\Delta a)^{(1,2)}$ must vanish at $z = 0$, we obtain

$$\frac{(i_{sb})_{n.s.}}{i_0} = \frac{i_{sb}^{(1)}}{i_0} (e^{-jhz} - 1) + \frac{i_{sb}^{(2)}}{i_0} (e^{jhz} - 1) .$$

It follows, from Eqs. (C.1) and (3.118), that the right-hand side of the above equation can be written as

$$\frac{(i_{sb})_{n.s.}}{i_0} = \frac{\alpha M}{2} \left(\frac{\Delta}{\beta_e} \right)^2 \cdot \left\{ \left(\frac{\Delta}{\beta_e} \right)^2 \cdot \frac{\partial}{\partial \beta_e} \left(\frac{I_1(\beta_e a)}{I_0(\beta_e a)} \right) \cdot [\cos(hz) - 1] \right.$$

$$\left. - j \left(\frac{h}{\beta_e} \right) \sin(hz) \frac{I_1(\beta_e a)}{(\beta_e a) I_0(\beta_e a)} + \ldots \right\} . \qquad (C.2)$$

For the solenoidal components, we have

$$\frac{i_{sb}^{(3)}}{i_0} = \frac{1}{F_3^2 h^2} \cdot \frac{d}{dr} \left(\frac{V_I^{(3)}}{2V_0} \right)_{r=a} \simeq \left(\frac{\beta_e}{\Delta} \right)^2 \frac{1}{\beta_e^2} \cdot \frac{d}{dr} \left(\frac{V_I^{(3)}}{2V_0} \right)_{r=a} ,$$

and

$$\frac{i_{sb}^{(4)}}{i_0} = \frac{1}{F_4^2 h^2} \cdot \frac{d}{dr}\left(\frac{V_I^{(4)}}{2V_0}\right)_{r=a} \simeq \left(\frac{\beta_e}{\Delta}\right)^2 \cdot \frac{1}{\beta_e^2} \cdot \frac{d}{dr}\left(\frac{V_I^{(4)}}{2V_0}\right)_{r=a} .$$

At $z = 0$, we must have $(\Delta a)^{(3,4)} = 0$, from which we obtain

$$\frac{(i_{sb})_{s.}}{i_0} = \frac{i_{sb}^{(3)}}{i_0} \cdot \left(e^{-jF_3 hz} - 1\right) + \frac{i_{sb}^{(4)}}{i_0}\left(e^{jF_4 hz}\right)$$

$$= \frac{\alpha M}{2} e^{-j\frac{\xi}{2}z} \cdot \left\{\left[e^{j\frac{\xi}{2}z} - \cos(\Delta z)\right] \cdot \frac{\partial}{\partial\beta_e}\left(\frac{I_1(\beta_e a)}{I_0(\beta_e a)}\right)\right.$$

$$\left. + j\left(\frac{\beta_e}{\Delta}\right)\sin(\Delta z) \cdot \frac{I_1(\beta_e a)}{(\beta_e a) I_0(\beta_e a)} + \ldots\right\} . \qquad (C.3)$$

Therefore, from Eqs. (C.2) and (C.3), the total surface current density, at $r = a$ due to the electrons of the beam, is

$$\frac{i_{sb}}{i_0} = \frac{\alpha M}{2}\left\{\frac{I_1(\beta_e a)}{\beta_e I_0(\beta_e a)} \cdot \left[-j\beta_e \frac{\sin(hz)}{h} + j\beta_e \frac{\sin(\Delta z)}{\Delta} e^{-j\frac{\delta}{2}z}\right]\right.$$

$$\left. + \frac{\partial}{\partial\beta_e}\left(\frac{I_1(\beta_e a)}{I_0(\beta_e a)}\right)\left[\left(\frac{\Delta}{h}\right)^2 [\cos(hz) - 1] + [1 - e^{-j\frac{\xi}{2}z} \cdot \cos(\Delta z)]\right] + \ldots\right\} .$$

The total surface current, at $z = L$ (output grids), is determined by averaging the surface current density over the cross-section of the beam and multiplying the result by the beam coupling coefficient M.

The result is

$$\frac{I_{sb}}{I_0} = \frac{\alpha M^2}{2}\left\{\frac{2I_1(\beta_e a)}{\beta_e I_0(\beta_e a)} \cdot j\beta_e \left[\frac{\sin(\Delta z)}{\Delta} e^{-j\frac{\xi}{2}z} - \frac{\sin(hz)}{h}\right]\right.$$

$$\left. + \frac{\partial}{\partial \beta_e}\left(\frac{2I_1(\beta_e a)}{I_0(\beta_e a)}\right)\left[\left(\frac{\Delta}{h}\right)^2 [\cos(hz) - 1] + [1 - e^{-j\frac{\xi}{2}z} \cdot \cos(\Delta z)] + \ldots\right]\right\} \quad . \tag{C.4}$$

APPENDIX D

CALCULATION FOR $\partial/\partial t\ (i_{b_2}^+)$

In this appendix, we will go through some purely mathematical manipulations which would lead to an expression for $\partial/\partial t\ (i_{b,2}^+)$ in terms of the fundamental and second-harmonic components of the electric field. From Eq. (4.35), we have

$$\left(\frac{\partial}{\partial t}\ i_{b_2}^+\right)_{(I)} = \left(\frac{\partial}{\partial t} + u_0 \frac{\partial}{\partial z}\right)\left(\frac{1}{2}\rho_{b_1}^+ \cdot v_{b_1}^+\right) - \frac{\rho_{0b}}{2} v_{b_1}^+ \cdot \frac{\partial}{\partial z} v_{b_1}^+ \quad .$$

It can be shown, however, from Eq (4.15), that

$$\frac{\rho_{0b}}{2} v_{b_1}^+ \cdot \frac{\partial}{\partial z} v_{b_1}^+ = \frac{\epsilon_1^2 u_0^2}{\rho_{0b}} \left\{ \frac{\beta_e^2}{2}\left(D_1^+ \frac{\partial}{\partial z} D_1^+ + D_1^- \frac{\partial}{\partial z} D_1^-\right) - \frac{h_1^2}{2} D_1^+ \frac{\partial}{\partial z} D_1^+ \right.$$

$$\left. - j\frac{\beta_e}{2}\left(\frac{\partial}{\partial z} D_1^+ \frac{\partial}{\partial z} D_1^-\right) + (h_1^2 - \beta_e^2)(D_1^+ \cdot D_1^-) \right\} \quad ,$$

and from Eqs. (4.13) and (4.15), the following expression results:

$$u_0 \frac{\partial}{\partial z}\left(\frac{1}{2} v_{b_1}^+ \rho_{b_1}^+\right) = + \frac{\epsilon_1^2 u_0^2}{\rho_{0b}} \left\{ j\frac{\beta_e}{2}\left(3\frac{\partial}{\partial z} D_1^+ \cdot \frac{\partial}{\partial z} D_1^- - D_1^- \frac{\partial^2}{\partial z^2} D_1^+\right) \right.$$

$$\left. + (h_1^2 - \beta_e^2)\, D_1^+ \cdot \frac{\partial}{\partial z} D_1^+ \right\} \quad .$$

From the same equations (4.13) and (4.15), we obtain

$$\frac{\partial}{\partial t}\left(\frac{1}{2}\rho_{b_1}^+ v_{b_1}^+\right) = - \frac{\epsilon_1^2 u_0^2}{\rho_{0b}} \left\{ j\beta_e \frac{\partial}{\partial z} D_1^+ \cdot \frac{\partial}{\partial z} D_1^- - \frac{\beta_e^2}{2}\left(D_1^- \frac{\partial}{\partial z} D_1^- + D_1^+ \frac{\partial}{\partial z} D_1^+\right) \right\} \quad .$$

It follows, therefore, that

$$\left(\frac{\partial}{\partial t} i_{b_2}^{+}\right)_{(I)} = -\frac{\epsilon_1^2 u_0^2}{2\rho_{0b}} \left\{-3h_1^2 D_1^{+} \frac{\partial D_1}{\partial z} + 2j\beta_e \left(D_1^{-} \frac{\partial^2}{\partial z^2} D_1^{+} - \frac{\partial}{\partial z} D_1^{+} \cdot \frac{\partial}{\partial z} D_1^{-}\right)\right.$$

$$\left. + 2\beta_e^2 \left(D_1^{+} \frac{\partial}{\partial z} D_1^{+} - D_1^{-} \frac{\partial}{\partial z} D_1^{-}\right)\right\} \quad .$$

To calculate $(\partial/\partial t)(i_{b_2}^{+})_{(II)}$ we make use of Eq. (4.34) whose partial time derivative is

$$2u_0 \frac{\partial}{\partial t} \rho_{b_2}^{+} = 2u_0 \epsilon_2 \frac{\partial^2}{\partial t \partial z} D_2^{+} + \frac{2u_0 \rho_{0p}}{4\omega^2} \cdot \frac{\partial^2}{\partial t \partial z} \left(\frac{1}{2} v_{p_1}^{+} \frac{\partial}{\partial z} v_{p_1}^{+}\right)$$

$$- \frac{u_0}{2\omega^2} \frac{\partial^3}{\partial t^2 \partial_z} \left(\frac{1}{2} v_{p_1}^{+} \rho_{p_1}^{+}\right) \quad .$$

From Eq. (4.11) we derive the result

$$\frac{1}{2} v_{p_1}^{+} \frac{\partial}{\partial z} v_{p_1}^{+} = -\frac{\omega_{pp}^4}{2\omega^2 \rho_{0p}^2} D_1^{-} \cdot \frac{\partial}{\partial z} D_1^{-} \quad ,$$

and

$$\frac{\partial}{\partial z} \left(\frac{1}{2} v_{p_1}^{+} \frac{\partial}{\partial z} v_{p_1}^{+}\right) = -\frac{\omega_{pp}^4}{2\omega^2 \rho_{0p}^2} \left\{\left(\frac{\partial}{\partial z} D_1^{-}\right)^2 + D_1^{-} \cdot \frac{\partial^2}{\partial z^2} D_1^{-}\right\} \quad ,$$

from which we obtain

$$\frac{\partial^2}{\partial t \partial z} \left(\frac{1}{2} v_{p_1}^{+} \frac{\partial}{\partial z} v_{p_1}^{+}\right) = -\frac{\omega_{pp}^4}{2\omega \rho_{0p}^2} \left\{2j \frac{\partial D_1^{+}}{\partial z} \cdot \frac{\partial D_1^{-}}{\partial z} + j\left(D_1^{+} \frac{\partial^2 D_1^{-}}{\partial z^2} + D_1^{-} \frac{\partial^2 D_1^{+}}{\partial z^2}\right)\right\} .$$

From Eqs. (4.11) and (4.14) we obtain

$$\frac{1}{2} v_{p_1}^{+} \rho_{p_1}^{+} = - \frac{j\omega}{2 \rho_{Op}} \cdot \left(\frac{\omega_{pp}}{\omega}\right)^4 \cdot D_1^- \frac{\partial D_1^+}{\partial z} \quad ,$$

from which we derive the result

$$\frac{-u_0}{2\omega^2} \frac{\partial^3}{\partial t^2 \partial z} \left(\frac{1}{2} \rho_{p_1}^{+} v_{p_1}^{+}\right) = - \frac{\omega_{pp}^4 u_0}{2\omega \rho_{Op}} \left\{ 2j \frac{\partial D_1^+}{\partial z} \cdot \frac{\partial}{\partial z} D_1^- + j \left(D_1^- \frac{\partial^2 D_1^+}{\partial z^2} + D_1^+ \frac{\partial^2 D_1^-}{\partial z^2} \right) \right\} .$$

It follows, then, that

$$\left(\frac{\partial}{\partial t} i_{b_2}^{+}\right)_{(II)} = \omega_{pb}^2 D_2^+ + 4j\omega u_0 \epsilon_2 \frac{\partial D_2^-}{\partial z} + u_0^2 \epsilon_2 \frac{\partial^2 D_2^+}{\partial z^2} - \frac{\omega_{pp}^4 u_0^2}{4\omega^4 \rho_{Op}}$$

$$\left\{ - 3j\beta_e \frac{\partial D_1^+}{\partial z} \cdot \frac{\partial D_1^-}{\partial z} + j\beta_e \left(2D_1^+ \cdot \frac{\partial^2 D_1^-}{\partial z^2} + D_1^- \frac{\partial^2 D_1^+}{\partial z^2} \right) \right.$$

$$\left. + 2(\beta_e^2 - h_1^2) \left(D_1^+ \frac{\partial}{\partial z} D_1^+ + 2D_1^- \frac{\partial}{\partial z} D_1^- \right) \right\} .$$

APPENDIX E

DERIVATION OF THE PARTICULAR SOLUTION OF THE DIFFERENTIAL EQUATION (4.43)

The inhomogeneous term of the differential equation can be written in the following form:

$$e^{2j\lambda}\left\{-\frac{3i_0}{4u_0^2\epsilon_2}\cdot\frac{\omega_{pb}}{\sqrt{\epsilon_1}}\left(1+\frac{2\mu}{3}\right)\left(\frac{\alpha M}{2}\right)^2\cdot\sin 2h_1 z\right.$$

$$\left.+\,j\,\frac{3i_0\omega}{2u_0^2\epsilon_2}\left(1+\frac{2\mu}{3}\right)\left(\frac{\alpha M}{2}\right)^2\sin^2 h_1 z-\frac{2ji_0\omega}{2u_0^2\epsilon_2}\left(1+\frac{3\mu}{4}\right)\left(\frac{\alpha M}{2}\right)^2\right\}$$

$$+\,e^{-2j\lambda}\cdot\left\{-\frac{3i_0}{4u_0^2\epsilon_2}\cdot\frac{\omega_{pb}}{\sqrt{\epsilon_1}}\left(1+\frac{2\mu}{3}\right)\left(\frac{\alpha M}{2}\right)^2\sin 2h_1 z\right.$$

$$\left.-\,j\,\frac{3i_0\omega}{2u_0^2\epsilon_2}\left(1+\frac{2\mu}{3}\right)\left(\frac{\alpha M}{2}\right)^2\sin^2 h_1 z+\frac{2ji_0\omega}{2u_0^2\epsilon_2}\left(1+\frac{3\mu}{4}\right)\left(\frac{\alpha M}{2}\right)^2\right\}\quad .$$

Consider the part in the above expression, which corresponds to the phase-factor $e^{2j\lambda}$, where $\lambda=\omega t-\beta_e z$. We have

$$\left(\frac{\alpha M}{2}\right)^2\left\{-\frac{3}{8}\,j\,\frac{i_0}{u_0\epsilon_2}\left(1+\frac{2\mu}{3}\right)\left[\left(\beta_e-h_1\right)e^{2jh_1 z}+\left(\beta_e+h_1\right)e^{-2jh_1 z}-2\beta_e\right]\right.$$

$$\left.-\,j\,\frac{i_0\beta_e}{u_0\epsilon_2}\left(1+\frac{3\mu}{4}\right)\right\}e^{2j\lambda}\quad .$$

The complementary function is written

$$D_2(z,t)=\left(A_2e^{jh_2 z}+B_2e^{-jh_2 z}\right)\cdot e^{2j\lambda}\quad ,$$

where A_2 and B_2 are arbitrary constants.

According to the method of variation of parameters to determine a particular integral for the differential equation, we assume that A_2 and B_2 are functions of z, which should now be looked upon as two new dependent variables.

The following condition is imposed on $A_2(z)$ and $B_2(z)$:

$$\frac{dA_2(z)}{dz} e^{jh_2 z} + \frac{dB_2(z)}{dz} e^{-jh_2 z} = 0 \quad .$$

From this system of equations,

$$\frac{dA_2(z)}{dz} e^{jh_2 z} + \frac{dB_2(z)}{dz} e^{-jh_2 z} = 0$$

$$j(h_2 - 2\beta_e) \frac{dA_2}{dz} e^{jh_2 z} - j(h_2 + 2\beta_e) \frac{dB_2}{dz} e^{-jh_2 z} = \text{Inhomogeneous Term} \quad ,$$

dA_2/dz and dB_2/dz are determined. We can then find expressions for A_2 and B_2 by direct integration.

The results are

$$A_2 e^{jh_2 z} = \left(\frac{\alpha M}{2}\right)^2 \frac{1}{2jh_2} \left\{ - \frac{3i_0\beta_e}{4u_0\epsilon_2 h_2} \left(1 + \frac{2\mu}{3}\right) \left[1 + \frac{\cos 2h_1 z}{4\xi^2 - 1} + j \frac{2\xi \cdot \sin 2h_1 z}{4\xi^2 - 1} \right] \right.$$

$$\left. + \frac{3i_0 h_1}{4u_0\epsilon_2 h_2} \left(1 + \frac{2\mu}{3}\right) \left[\frac{2\xi \cdot \cos 2h_1 z}{4\xi^2 - 1} + j \frac{\sinh_2 z}{4\xi^2 - 1} \right] + \frac{i_0\beta_e}{\epsilon_2 u_0 h_2} \left(1 + \frac{3\mu}{4}\right) \right\} \quad ,$$

and

$$B_2 e^{jh_2 z} = \left(\frac{\alpha M}{2}\right)^2 \frac{1}{2jh_2} \left\{ - \frac{3i_0\beta_e}{4u_0\epsilon_2 h_2} \left(1 + \frac{2\mu}{3}\right) \left[1 + \frac{\cos 2h_1 z}{4\xi^2 - 1} - 2j \frac{\xi \cdot \sin 2h_1 z}{4\xi^2 - 1} \right] \right.$$

$$\left. + \frac{3i_0 h_1}{4u_0\epsilon_2 h_2} \left(1 + \frac{2\mu}{3}\right) \left[- \frac{2\xi \cos 2h_1 z}{4\xi^2 - 1} + j \frac{\sin h_2 z}{4\xi^2 - 1} \right] + \frac{i_0\beta_e}{\epsilon_2 u_0 h_2} \left(1 + \frac{3\mu}{4}\right) \right\} \quad .$$

It follows then that the particular integral corresponding to that part of the inhomogeneous term with the phase factor $e^{2j\lambda}$ is

$$\left(A_2 e^{jh_2 z} + B_2 e^{-jh_2 z}\right) e^{2j\lambda} = \left(\frac{\alpha M}{2}\right)^2 \frac{i_0 \omega}{4j\omega_{pb}^2}\left[(1+\mu)\right.$$

$$\left. - \frac{3(1+\frac{2\mu}{3})}{4\xi^2 - 1} \cdot \cos 2h_1 z + 3j\left(\frac{h_1}{\beta_e}\right)\frac{(1+\frac{2\mu}{3})}{4\xi^2 - 1} \sinh_2 z\right] e^{2j\lambda} \quad .$$

The complete particular solution to (4.43) is obtained by adding the above result to its complex conjugate, resulting in

$$\left(\frac{\alpha M}{2}\right)^2 \cdot \frac{i_0 \omega}{2\omega_{pb}^2}\left\{\left[(1+\mu) - \frac{3(1+\frac{2\mu}{3})}{4\xi^2 - 1} \cdot \cos 2h_1 z\right] \sin 2\lambda\right.$$

$$\left. + \frac{3h_1}{\beta_e}\frac{(1+\frac{2\mu}{3})}{4\xi^2 - 1} \sin h_2 z \cos 2\lambda\right\} \quad .$$

APPENDIX F

DERIVATION OF SECOND HARMONIC VELOCITIES

The second harmonic velocity is calculated from

$$v^+_{b_2} = \frac{1}{\rho_{0b}} \left(i^+_{b_2} - u_0 \rho^+_{b_2} - \frac{1}{2} v^+_{b_1} \rho^+_{b_1} \right) . \qquad (F.1)$$

We know that

$$- \frac{\partial}{\partial t} \rho^+_{p_2} = \frac{\partial}{\partial z} i^+_{p_2} \quad , \qquad (F.2)$$

and

$$i^+_{p_2} = (\epsilon_2 - 1) \frac{\partial D^+_2}{\partial t} - P \quad , \qquad (F.3) \text{ , (Eq. 4.52)}$$

where P is defined as being given by

$$P = \frac{3}{4} \frac{i_0}{\omega \epsilon_1} \left(\frac{\omega_{pp}}{\omega} \right)^2 \left(\frac{\alpha M}{2} \right)^2 \left\{ 2 \sin^2 h_1 z \cdot \sin 2(\omega t - \beta_e z) \right.$$

$$\left. + \left(\frac{h_1}{\beta_e} \right) \sin 2h_1 z \cdot \cos 2(\omega t - \beta_e z) \right\} .$$

From Eqs. (F.2) and (F.3), the following expression is obtained for $\rho^+_{p_2}$:

$$\rho^+_{p_2} = (1 - \epsilon_2) \frac{\partial D^+_2}{\partial z} - \frac{1}{4\omega^2} \frac{\partial^2 P}{\partial t \partial z} \quad , \qquad (F.4)$$

since we have

$$\rho^+_{b_2} + \rho^+_{p_2} = \frac{\partial D^+_2}{\partial z} \quad .$$

It follows, from (F.4), that

$$\rho_{b_2}^{+} = \frac{\partial D_2^{+}}{\partial z} - \rho_{p_2}^{+} = \epsilon_2 \frac{\partial D_2^{+}}{\partial z} + \frac{1}{4\omega^2} \cdot \frac{\partial^2 P}{\partial t \partial z} \quad .$$

By using the expression for P, we have

$$u_0 \rho_{b_2}^{+} = u_0 \epsilon_2 \frac{\partial D_2^{+}}{\partial z} + \frac{3}{4} \frac{i_0}{\omega \epsilon_1} \left(\frac{\omega_{pp}}{\omega}\right)^2 \left(\frac{\alpha M}{2}\right)^2 \left[2 \sin^2 h_1 z \cdot \sin 2(\omega t - \beta_e z) \right.$$

$$\left. + 2\left(\frac{h_1}{\beta_e}\right) \sin 2h_1 z \cdot \cos 2(\omega t - \beta_e z) - \left(\frac{h_1}{\beta_e}\right)^2 \cdot \cos 2h_1 z \cdot \sin 2(\omega t - \beta_e z) \right] .$$

It results in

$$i_{b_2}^{+} - u_0 \rho_{b_2}^{+} = - \epsilon_2 \frac{\partial D_2^{+}}{\partial t} - u_0 \epsilon_2 \frac{\partial D_2^{+}}{\partial z}$$

$$+ \frac{3}{4} \frac{i_0}{\omega \epsilon_1} \left(\frac{\omega_{pp}}{\omega}\right)^2 \left(\frac{\alpha M}{2}\right)^2 \left\{ -\left(\frac{h_1}{\beta_e}\right) \sin 2h_1 z \cdot \cos 2(\omega t - \beta_e z) \right.$$

$$\left. + \left(\frac{h_1}{\beta_e}\right)^2 \cdot \cos 2h_1 z \cdot \sin 2(\omega t - \beta_e z) \right\} \quad , \qquad \text{(F.5)}$$

where use was made of the expression for $i_{b_2}^{+}$ [Eq. (4.53)]. From Eqs. (4.24) and (4.25), we have

$$\frac{1}{2} v_{b_1}^{+} \rho_{b_1}^{+} = - 2 i_0 \left(\frac{\alpha M}{2}\right)^2 \cdot \left[\cos^2 h_1 z \cdot \cos^2(\omega t - \beta_e z) \right.$$

$$\left. + \frac{1}{4}\left(\frac{\beta_e}{h_1}\right) \sin 2h_1 z \cdot \sin 2(\omega t - \beta_e z) \right] \quad .$$

By substituting this above expression and (F.5) in (F.1), we obtain

$$v_{b_2}^{+} = - u_0 \frac{\omega\sqrt{\epsilon_2}}{2\omega_{pb}} \left(\frac{\alpha M}{2}\right)^2 \left\{ \left[\frac{6\xi(1 + \frac{2\mu}{3})}{4\xi^2 - 1} - \frac{1}{\xi} \right] \sin 2h_1 z \cdot \sin 2(\omega t - \beta_e z) \right.$$

$$- \frac{4(1 - \xi^2) + \mu(3 - 4\xi^2)}{4\xi^2 - 1} \sin h_2 z \cdot \sin 2(\omega t - \beta_e z)$$

$$+ \left(\frac{h_1}{\beta_e}\right) \frac{3(1 + \frac{2\mu}{3})}{4\xi^2 - 1} \cdot \cos h_2 z \cdot \cos 2(\omega t - \beta_e z) - 2\left(\frac{h_2}{\beta_e}\right) \cdot \cos^2 h_1 z \cdot \cos^2 (\omega t - \beta_e z)$$

$$\left. + \frac{3}{2} \frac{\mu}{\xi} \left[\sin 2h_1 z \cdot \cos 2(\omega t - \beta_e z) - \left(\frac{h_1}{\beta_e}\right) \cos 2h_1 z \cdot \sin 2(\omega t - \beta_e z) \right] \right\} \quad .$$

LIST OF REFERENCES

1. D. Bohm, E. P. Gross, Phys. Rev. 75, 1851 (1949); also 75, 1864 (1949); and 79, 992 (1950).
2. G. D. Boyd, L. M. Field, R. W. Gould, "Excitation of Plasma Oscillations and Growing Plasma Waves," Phys. Rev. 109, 1393-94 (Feb. 1958).
3. E. V. Bogdanov, V. J. Kislov, Z. S. Tchernov, "Interaction Between an Electron Stream and a Plasma," Symposium on Millimeter Wave Generation, Brooklin Polytechnic Institute, 57-72 (1959).
4. M. A. Allen, G. S. Kino, "Interaction of an Electron Beam with a Fully Ionized Plasma," Phys. Rev. Letters 6, 163-165 (Feb. 1961).
5. W. C. Hahn, "Small-Signal Theory of Velocity-Modulated Tubes," G. E. Rev. 42, 258-270 (1939).
6. E. Feenberg, "Notes on Velocity Modulation," Sperry Gyroscope Co., Inc. (1945).
7. O. Buneman, "Plasma Dynamics," (unpublished notes) Stanford University (1961).
8. D. L. Bobroff, "Independent Space Variables for Small-Signal Electron Beam Analysis," IRE Trans. on Electron Devices ED-6, 68 (Jan. 1959).
9. M. Chodorow, C. Susskind, "Fundamentals of Microwave Tubes," (unpublished notes) Stanford University.
10. R. Warnecke, P. Guenard, Les Tubes á Commande de Modulation de Vitesse, (1951).
11. G. M. Brauch, T. G. Mihrau, "Plasma Frequency Reduction Factors in Electron Beams," IRE Trans. on Electron Devices, ED-2, 3-11 (April 1955).
12. F. Paschke, "On the Nonlinear Behavior of Electron-Beam Devices," RCA Review, Vol. XVIII, No. 2 (June 1957); also "Generation of Second Harmonic in a Velocity-Modulated Electron Beam of Finite Diameter," RCA Review, Vol. XIX, No. 4 (Dec. 1958); and "Nonlinear Theory of a Velocity-Modulated Electron Beam with Finite Diameter," RCA Review, Vol. XXI, No. 1 (March 1960).
13. A. W. Beck, Space-Charge Waves and Slow Electromagnetic Waves, (Pergamon Press, New York, 1958).
14. G. D. Boyd, "Experiments on the Interaction of a Modulated Electron Beam with a Plasma," Technical Report No. 11, Electron Tube and Microwave Laboratory, California Institute of Technology (May 1959).

15. A. W. Trivelpiece, "Slow Wave Propagation in Plasma Waveguides," Technical Report No. 7, Electron Tube and Microwave Laboratory, California Institute of Technology (May 1958).

16. S. J. Buchsbaum, L. Mower, S. C. Brown, "Interaction between Cold Plasmas and Guided Electromagnetic Waves," The Physics of Fluids 3, No. 3 (Sept.-Oct. 1960).

DISTRIBUTION LIST

CONTRACT AF 19(604)-1930

Code	Organization	No. of Copies
AF 5	AFMTC(AFMTC Tech Library - MU - 135) Patrick AFB, Florida	1
AF 18	AUL Maxwell AFB, Alabama	1
AF 43	ASD (ASAPRD-Dist) Wright-Patterson AFB, Ohio	1
AF 91	AFOSR (SRGL) Washington 25, D. C.	1
AF 124	RADC (RAYLD) Griffiss AFB, New York ATTN: Documents Library	1
AF 139	AF Missile Development Center (MDGRT) Holloman AFB, New Mexico	1
AF 318	ARL (Technical Library) Building 450 Wright-Patterson AFB, Ohio	1
AF 5	Commanding General USASRDL Ft. Monmouth, New Jersey ATTN: Tech. Doc. Ctr. SIGRA/SL-ADT	1
Ar 9	Department of the Army Office of the Chief Signal Officer Washington 25, D. C. SIGRD-4a-2	1
Ar 50	Commanding Officer ATTN: ORDTL-012 Diamond Ordnance Fuze Laboratories Washington 25, D. C.	1
Ar 67	Army Rocket and Guided Missile Agency Redstone Arsenal, Alabama ATTN: ORDXR-OTL, Technical Library	1
G 2	ASTIA (TIPAA) Arlington Hall Station Arlington 12, Virginia	10
G 68	National Aeronautics and Space Agency 1520 H. Street, N. W. Washington 25, D. C. ATTN: Library	1

Code	Organization	No. of Copies
G 109	Director Langley Research Center National Aeronautics and Space Administration Langley Field, Virginia	1
M 6	AFCRL, OAR (CRIPA-Stop 39) L. G. Hanscom Field Bedford, Massachusetts	10
M 78	AFCRL, OAR (CRT, Dr. A. M. Gerlach) L. G. Hanscom Field Bedford, Massachusetts	1
N 1	Director, Avionics Division (AV) Bureau of Aeronautics Department of the Navy Washington 25, D. C.	2
N 29	Director (Code 2027) U. S. Naval Research Laboratory Washington 25, D. C.	2
I 292	Director, USAF Project RAND The Rand Corporation 1700 Main Street, Santa Monica, Calif. Thru: A. F. Liaison Office	1
AF 127	Boston Office-Patents and Royalties Division (Hq AFLC) Building 133, 424 Trapelo Road Waltham 54, Massachusetts	1
AF 253	Technical Information Office European Office, Aerospace Research Shell Building, 47 Cantersteen Brussels, Belgium	1
Ar 107	U. S. Army Aviation Human Research Unit U. S. Continental Army Command P. O. Box 438, Fort Rucker, Alabama ATTN: Maj. Arne H. Eliasson	1
G 8	Library Boulder Laboratories National Bureau of Standards Boulder, Colorado	2
M 63	Institute of the Aerospace Sciences, Inc. 2 East 64th Street New York 21, New York ATTN: Librarian	1

Code	Organization	No. of Copies
N 73	Office of Naval Research Branch Office, London Navy 100, Box 39 F. P. O. New York, N. Y.	10
U 32	Massachusetts Institute of Technology Research Laboratory of Electronics Building 26, Room 327, Cambridge 39, Massachusetts ATTN: John H. Hewitt	1
U 431	Alderman Library University of Virginia Charlottesville, Virginia	1
	Dr. Glen Wade, Spencer Laboratories Burlington, Massachusetts	1
	Mr. Charles Turner 585 Kenton Road, Kenton, Harrow Middlesex, England	1
	Electronics Laboratories General Electric Company Electronics Park Syracuse, New York ATTN: Mr. Henry Grimm	1
	Dr. Yen, Department of Electrical Engineering University of Toronto Toronto 5, Ontario, Canada	1
	Matthew A. Allen Microwave Associates, Inc. Burlington, Massachusetts	1
AF 247	WADD (WCLKTR) Wright-Patterson AFB, Ohio	1
AF 329	Hq. ARDC (RDR-62) Reference 4619-Ca Andrews AFB, Washington 25, D. C.	2
Ar 103	Commanding Officer U. S. Army Signal Research and Development Lab. Fort Monmouth, New Jersey ATTN: SIGFM/EL-PRG	1
G 112	Oak Ridge National Laboratory P. O. Box X Oak Ridge, Tennessee ATTN: Central Research Laboratory	1

Code	Organization	No. of Copies
I 774	Lenkurt Electric Company, Inc. 1105 Country Road San Carlos, California ATTN: D. Mawdsley, Mail Stop 85	1
I 775	Radio Research Laboratories Kokubunki, P. O. Tokyo, Japan	1
I 925	Hughes Aircraft Company P. O. Box 278 Newport Beach, California ATTN: Miss Eileen D. Andjulis Assistant Librarian	1
I 943	General Telephone and Electronics Laboratories, Inc. 1015 Corporation Way Palo Alto, California ATTN: Librarian	1
I 944	Bomac Laboratories, Inc. Salem Road Beverly, Massachusetts ATTN: Mr. Arthur McCoubrey, Manager Research and Development	1
I 954	S.F.D. Laboratories, Inc. 800 Rahway Avenue Union, New Jersey ATTN: R. Ullrich, Librarian	1
I 988	Institute of Defense Analysis Research and Engineering Support Division 1825 Connecticut Avenue, N. W. Washington 9, D. C. ATTN: Technical Information Office	1
U 10	Cornell University School of Electrical Engineering Ithaca, New York ATTN: Prof. G. C. Dalman	1
U 238	University of Southern California University Park Los Angeles 7, California ATTN: Z. A. Kaprielian Associate Professor of Electrical Engineering	1
U 290	Dr. A. L. Cullen Department of Electrical Engineering University of Sheffield Sheffield 1, England	1

Code	Organization	No. of Copies
U 358	University of Arizona Tucson 25, Arizona ATTN: Prof. Donald C. Stinson Department of Electrical Engineering	1
U 359	The University of British Columbia Department of Electrical Engineering Vancouver 8, B. C. Canada ATTN: G. B. Walker Microwave Laboratory	1
U 391	University of Illinois Electrical Engineering Research Laboratory Urbana, Illinois ATTN: Professor P. D. Coleman Ultramicrowave Group	1
U 430	Chalmers University of Technology Gibraltargaton 5 G Gothenburg, Sweden ATTN: Mr. H. Wilhelmsson Research Laboratory of Electronics	1
G 70	Advisory Group on Electron Devices (AGED) Office of the Director of Defense Res and Eng. 346 Broadway, 8th Floor New York 13, New York	2
N 160	U. S. Naval Research Laboratory Washington 25, D. C. ATTN: Mr. F. J. Liberatore, Code 7420	1
I 13	Bell Telephone Laboratories, Inc. Whippany Laboratory Whippany, New Jersey ATTN: Technical Information Library	2
I 53	Hughes Aircraft Company Florence Avenue and Teale Street Culver City, Calif. ATTN: Documents Section Research and Development Library	1
I 96	Sandia Corporation Sandia Base, P. O. Box 5800 Albuquerque, New Mexico ATTN: Mrs. B. R. Allen, Librarian	1
I 237	Technical Library G. E. TWT Product Section 601 California Avenue Palo Alto, California ATTN: Verna Van Velzer, Librarian	1

Code	Organization	No. of Copies
I 260	Sylvania Elec. Prod. Inc. Electronic Defense Laboratory P. O. Box 205, Mountain View, Calif. ATTN: Library	1
I 266	ITT Federal Laboratories Technical Library 500 Washington Avenue Nutley 10, New Jersey	1
I 297	Sperry Gyroscope Company Division of Sperry Rand Corporation Great Neck, N. Y. ATTN: Mrs. Florence W. Turnbull Engineering Librarian	1
I 305	General Electric Company Power Tube Dept. Electronic Components Division Building 269, Room 205 One River Road Schenectady 5, New York	1
I 306	General Telephone and Electronics Laboratories, Inc. Bayside Laboratories Bayside 6, New York ATTN: Mr. D. Lazare Manager, Project Adm.	1
I 309	Litton Industries, Inc. 960 Industrial Road San Carlos, California ATTN: Document Custodian, Engr. Dept.	1
I 310	Varian Associates 611 Hansen Way Palo Alto, California ATTN: Dr. Richard B. Nelson	1
I 312	STL Technical Library Document Acquisitions Space Technology Laboratories, Inc. P. O. Box 95001 Los Angeles 45, California	1
I 366	Radio Corporation of America Defense Electronic Products Camden, New Jersey ATTN: Mr. S. Schach, Building 10-5 Standards Engineering, Section 577	1

Code	Organization	No. of Copies
I 367	Stanford Research Institute Document Center Menlo Park, California ATTN: Acquisitions	1
I 370	General Telephone and Electronics Labs., Inc. Bayside, New York ATTN: Dr. T. G. Polanyi, Head Thermionics Branch	1
I 382	RCA Laboratories David Sarnoff Research Center Princeton, New Jersey ATTN: Dr. Harwick Johnson	1
I 384	Bell Telephone Laboratories Murray Hill Laboratory Murray Hill, New Jersey ATTN: Dr. J. R. Pierce	2
I 435	General Electric Company P. O. Box 1088 Schenectady, New York ATTN: Mr. E. D. McArthur, Manager Superpower Microwave Tube Laboratory	1
I 450	Bell Telephone Laboratories Murray Hill, New Jersey ATTN: J. W. Fitzwilliam, Director Electron Tube Development	1
I 547	The Rand Corporation 1700 Main Street Santa Monica, California ATTN: Technical Librarian	1
I 562	Philips Laboratories A Division of North American Philips Co.,Inc. Irvington on Hudson, New York ATTN: William P. Arnett Security Officer	1
I 577	Raytheon Manufacturing Company 520 Winter Street Waltham, Massachusetts ATTN: Mr. O. T. Fundingsland	1
I 594	Research Technology Associates, Inc. 100 Ladge Drive Electronic Park at Avon Avon, Massachusetts ATTN: J. Babakian	1

Code	Organization	No. of Copies
I 595	Gianninni Research Santa Ana, California ATTN: J. K. Hagele Technical Librarian	1
I 666	Ramo-Wooldridge A Division of Thompson Ramo-Wooldridge Inc. 8433 Fallbrook Avenue Canoga Park, California ATTN: Technical Information Services	1
I 756	Varian Associates 611 Hansen Way Palo Alto, California ATTN: Mr. C. W. McClelland Technical Publications Manager	1
I 759	Stanford Research Institute Menlo Park, California ATTN: Mr. C. J. Cook	1
I 760	General Atomic, Div. of General Dynamics Corp. P. O. Box 608, San Diego, California ATTN: Mr. M. Rosenbluth	1
I 761	Linfield Research Institute McMinnville, Oregon ATTN: Dr. W. P. Dyke, Director	1
I 762	Columbia Radiation Laboratory 538 West 120th Street New York 27, New York	1
I 763	Sperry Gyroscope Company Engineering Library Mail Station C-39 Great Neck, Long Island, New York	1
I 764	Watkins-Johnson Company 3333 Hillview Avenue Palo Alto, California ATTN: Dr. H. R. Johnson	1
I 765	Westinghouse Electric Corporation Friendship International Airport Box 746, Baltimore 3, Maryland ATTN: G. Ross Kilgore, Manager Applied Research Department Baltimore Laboratory	1
I 766	Services Electronic Research Laboratories Baldock, Herts, England ATTN: Dr. Boot	1

Code	Organization	No. of Copies
I 767	Standard Telephone Laboratories Harlow, Essex, England ATTN: Dr. E. A. Ash	1
I 768	Eitel-McCullough, Inc. 798 San Mateo Avenue San Bruno, California ATTN: Librarian	1
I 769	Hewlett-Packard Company 275 Page Mill Road Palo Alto, California	1
I 770	Hughes Aircraft Company Research and Development Laboratories Culver City, California ATTN: L. M. Field	1
I 999	Raytheon Company Box 171, Wayland, Mass. ATTN: E. Rolfe	1
I 771	Advanced Kinetics Inc. P. O. Box 1803 Newport Beach, California ATTN: Dr. R. Waniek	1
I 772	RCA Laboratories Princeton, New Jersey ATTN: Harwell Johnson	1
I 944	Bomac Laboratories, Inc. 8 Salem Road Beverly, Massachusetts ATTN: Dr. Arthur McCoubrey, Manager Research and Development	1
U 2	California Institute of Technology Jet Propulsion Laboratory Pasadena 4, California ATTN: Documents Library	1
U 21	The Johns Hopkins University Radiation Laboratory 1315 St. Paul Street Baltimore 2, Maryland ATTN: Librarian	1
U 22	The Johns Hopkins University Department of Physics Homewood Campus Baltimore 18, Maryland ATTN: Dr. Donald E. Kerr	1

Code	Organization	No. of Copies
U 26	Massachusetts Institute of Technology Lincoln Laboratory P. O. Box 73 Lexington 73, Massachusetts ATTN: Mary A. Granese, Librarian	1
U 40	New York University Department of Physics College of Arts and Sciences Washington Square, New York 3, New York ATTN: Professor J. H. Rohrbaugh	1
U 42	The Ohio State University 2024 Neil Avenue Columbus 10, Ohio ATTN: Prof. E. M. Boone Department of Electrical Engineering	1
U 59	Library Georgia Technology Research Institute, Engineering Experiment Station 722 Cherry Street, N. W. Atlanta, Georgia ATTN: Mrs. J. H. Crosland, Librarian	1
U 79	University of Michigan Engineering Research Institute Radiation Laboratory ATTN: Prof. K. M. Siegel 912 N. Main Street Ann Arbor, Michigan	1
U 100	University of California Electronics Research Lab. 332 Cory Hall, Berkeley 4, Calif. ATTN: J. R. Whinnery	1
U 102	Harvard University Technical Reports Collection Gordon McKay Library 303A Pierce Hall Oxford Street Cambridge 38, Massachusetts ATTN: Librarian	1
U 107	University of Michigan Electronic Defense Group Engineering Research Institute Ann Arbor, Michigan ATTN: J. A. Boyd, Supervisor	1

Code	Organization	No. of Copies
U 114	University of California 390 Cory Hall Berkeley 4, Calif. ATTN: Dr. Charles Susskind	1
U 150	University of Washington Department of Electrical Engineering Seattle 5, Washington ATTN: Mr. A. E. Harrison	1
U 168	The George Washington University Department of Electrical Engineering School of Engineering Washington 6, D. C. ATTN: Dr. N. T. Grisamore, Exec. Officer	1 1
U 169	Illinois Institute of Technology 3301 S. Dearborn Street Chicago 16, Illinois ATTN: Dr. George I. Cohn	1
U 209	New York University College of Engineering 346 Broadway New York, New York ATTN: Mr. L. S. Schwartz, Research Division	1
U 228	University of Kansas Electrical Engineering Department Lawrence, Kansas ATTN: Dr. H. Unz	1
U 237	Polytechnic Institute of Brooklyn Microwave Research Institute 55 Johnson Street Brooklyn, New York ATTN: Dr. N. Marcuvitz	1
U 240	Illinois Institute of Technology Technology Center Department of Electrical Engineering Chicago 16, Illinois ATTN: Paul C. Yuen Electronics Research Laboratory	1
U 284	Dr. J. T. Senise Instituto Tecnologico de Aeronautica Sao Jose dos Campos Sao Paulo, Brazil	1

Code	Organization	No. of Copies
U 288	Polytechnic Institute of Brooklyn Microwave Research Institute 55 Johnson Street Brooklyn 1, New York	1
U 292	University of Maryland College Park, Maryland ATTN: Dr. J. M. Burgers	1
U 294	University of Illinois Electrical Engineering Research Laboratory Urbana, Illinois ATTN: Dr. A. A. Dougal	1
U 308	Brandeis University Waltham, Massachusetts ATTN: Dr. E. P. Gross	1
U 320	California Institute of Technology 1201 East California Street Pasadena, California ATTN: Prof. R. W. Gould	1
U 321	University of California Radiation Laboratory Livermore, California ATTN: N. Christofilos	1
U 322	University of California Radiation Laboratory Livermore, California ATTN: S. A. Colgate	1
U 323	University of California Radiation Laboratory Livermore, California ATTN: R. F. Post	1
U 324	Princeton University Princeton, New Jersey ATTN: L. Spitzer Project Matterhorn	1
U 325	Massachusetts Institute of Technology 77 Massachusetts Avenue Cambridge, Massachusetts ATTN: W. P. Allis	1
U 326	University of California Electrical Engineering Department Berkeley 4, California ATTN: Prof. J. R. Singer	1

Code	Organization	No. of Copies
U 327	University of California Radiation Laboratory Berkeley, California ATTN: Dr. R. K. Wakerling Information Division, Building 50, Room 128	1
U 328	University of Chicago Institute of Air Weapons Research Museum of Science and Industry Chicago 37, Illinois ATTN: Mrs. Norma Miller, Technical Librarian	1
U 329	University of Florida Department of Electrical Engineering Gainesville, Florida ATTN: Prof. W. E. Lear	1
U 330	University of Illinois Control Systems Laboratories Urbana, Illinois ATTN: Prof. Daniel Alpert	1
U 331	University of Illinois Department of Electrical Engineering Urbana, Illinois ATTN: Prof. L. Goldstein	1
U 332	University of Illinois Department of Physics Urbana, Illinois ATTN: Dr. John Bardeen	1
U 333	Johns Hopkins University Radiation Laboratory 1315 St. Paul Street Baltimore 2, Maryland ATTN: J. M. Minkowski	1
U 334	Iowa State University Physics Department Iowa City, Iowa ATTN: Professor Frank MacDonald	1
U 335	University of Colorado Department of Electrical Engineering Boulder, Colorado ATTN: Professor W. G. Worcester	1
U 337	McMurray College Department of Physics Abilene, Texas ATTN: Dr. Virgil E. Bottom	1

Code	Organization	No. of Copies
U 338	University of Michigan 3506 East Engineering Building Ann Arbor, Michigan ATTN: Electron Tube Laboratory	1
U 339	University of Minnesota Institute of Technology Department of Electrical Engineering Minneapolis, Minnesota ATTN: Prof. A. Van der Ziel	1
U 340	Ohio University College of Applied Science Athens, Ohio ATTN: D. B. Green	1
U 341	Oregon State College Department of Electrical Engineering Corvallis, Oregon ATTN: H. J. Oorthuys	1
U 342	Princeton University Department of Electrical Engineering Princeton, New Jersey	1
U 343	Purdue University Research Library Lafayette, Indiana ATTN: Electrical Engineering Department	1
U 344	Rensselaer Polytechnic Institute Office of the Librarian Troy, New York	1
U 345	Scientific Attache Swedish Embassy 2249 R Street, N. W. Washington 8, D. C.	1
U 346	Rutgers University Physics Department Newark 2, New Jersey ATTN: Dr. Charles Pine	1
U 347	University of Texas Military Physics Research Laboratory Box 8036, University Station Austin, Texas	1
U 348	University of Utah Electrical Engineering Department Salt Lake City, Utah ATTN: Richard W. Grow	1

Code	Organization	No. of Copies
U 350	University of Puerto Rico College of Agriculture and Mechanical Arts Mayaguez, Puerto Rico ATTN: Dr. Braulio Dueno	1
U 351	The Royal Institute of Technology Stockholm 70, Sweden ATTN: Dr. B. Agdur	1
U 352	Drexel Institute of Technology Department of Electrical Engineering Philadelphia 4, Pennsylvania ATTN: F. B. Haynes	1
U 353	Forsvarets Forskningsinstitutt Avdeling for Radar Bergen, Norway ATTN: WADD (WCOSR, Mr. Knutson) Wright-Patterson AFB, Ohio	1
U 354	Massachusetts Institute of Technology Research Laboratory of Electronics Cambridge 39, Mass. ATTN: L. D. Smullin	1
U 355	Massachusetts Institute of Technology Research Laboratory of Electronics Cambridge 39, Mass. ATTN: S. C. Brown	1
U 356	University of Chicago Midway Laboratories 6220 S. Drexel Avenue Chicago, Illinois ATTN: P. J. Dickerman	1
U 436	University of Mississippi University, Mississippi ATTN: Mr. Thomas Tullos	1
	Hq. AFCRL, Office of Aerospace Research (CRRC) L. G. Hanscom Field, Bedford, Mass.	4